Testing Procedures for Long Life Heavy Duty Stabilized Bases

Technical Report 0-6812-1

Cooperative Research Program

CENTER FOR TRANSPORTATION INFRASTRUCTURE SYSTEMS
THE UNIVERSITY OF TEXAS AT EL PASO
EL PASO, TX 79968
https://www.utep.edu/engineering/ctis/

in cooperation with the
Federal Highway Administration and the
Texas Department of Transportation

TECHNICAL REPORT STANDARD TITLE PAGE

1. Report No.	2. Government Accession No.	3. Recipient's Catalog No.
FHWA/TX-20/0-6812-1		

4. Title and Subtitle	5. Report Date
Testing Procedures for Long Life Heavy Duty Stabilized Bases	July 2016; Published June 2020
	6. Performing Organization Code
7. Author(s)	8. Performing Organization Report No.
Reza Ashtiani and Jose Tarin	0-6812-1
9. Performing Organization Name and Address	10. Work Unit No.
Center for Transportation Infrastructure Systems The University of Texas at El Paso El Paso, Texas79968-0516	11. Contract or Grant No. 0-6812
12. Sponsoring Agency Name and Address	13. Type of Report and Period Covered
Texas Department of Transportation Research and Technology Implementation Office P.O. Box 5080 Austin, Texas78763-5080	Technical Report March 2014 –August 31, 2016
	14. Sponsoring Agency Code

15. Supplementary Notes

Project performed in cooperation with the Texas Department of Transportation. Project title: Updated Testing Procedures for Long Life Heavy Duty Stabilized Bases

16. Abstract

Fatigue cracking is one of the major types of distresses observed in pavement structures due to repeated traffic loads. The new mechanistic pavement design protocols, such as TxME, require modulus of rupture of the materials as input to the fatigue performance models. This report discusses the practical and theoretical issues associated with traditional third point bending beam fatigue test and provides an alternative method for the determination of the tensile strength of the stabilized materials in the laboratory. To achieve the objective of the project, a full factorial laboratory experiment design consisted of four aggregates sources with distinct lithology, four stabilizer contents, and two conditioning/curing procedures were incorporated in the experiment matrix. The stabilized systems were subjected to unconfined compressive strength test, submaximal test at different strength ratios, static and dynamic indirect tension tests, free-free resonant column tests and dielectric tests, to better understand the mechanical behavior of materials in the laboratory. Moisture susceptibility tests were also incorporated in the study to monitor the degradation of the material properties with moisture intrusion in stabilized systems. A multi-dimensional aggregate feature database was developed based on 570 fabricated laboratory specimens in this research. The trend analysis of the laboratory data revealed the capability of the new laboratory procedure to provide an efficient and repeatable measure of the tensile strength of stabilized materials subjected to high number of load cycles in the laboratory.

17. Key Words	18. Distribution Statement
Stabilization, Aggregate Base layer, Fatigue, Pavement Design	No restrictions. This document is available to the public through the National Technical Information Service, 5285 Port Royal Road, Springfield, Virginia22161, www.ntis.gov

19. Security Classif. (of this report)	20. Security Classif. (of this page)	21. No. of Pages	22. Price
Unclassified	Unclassified	142	

Testing Procedures for Long Life Heavy Duty Stabilized Bases

by:

Reza Ashtiani, Ph.D.
and
Jose Tarin, BSCE

Research Project 0-6812

Conducted for
Texas Department of Transportation

Research Report 0-6812-1

Center for Transportation Infrastructure Systems
The University of Texas at El Paso
El Paso, TX 79968-051

DISCLAIMERS

The contents of this report reflect the view of the authors who are responsible for the facts and the accuracy of the data presented herein. The contents do not necessarily reflect the official views or policies of the Texas Department of Transportation or the Federal Highway Administration. This report does not constitute a standard, a specification or a regulation.

The material contained in this report is experimental in nature and is published for informational purposes only. Any discrepancies with official views or policies of the Texas Department of Transportation should be discussed with the appropriate Austin Division prior to implementation of the procedures or results.

NOT INTENDED FOR CONSTRUCTION, BIDDING, OR PERMIT PURPOSES

Reza Ashtiani, Ph.D.
Jose Tarin

ACKNOWLEDGEMENTS

The researchers and authors would like to express their gratitude to the Texas Department of Transportation for sponsoring this project. The professional advice, insights, and suggestions provided by TxDOT Professionals by the name of Messers. Kevin Pete, Mark McDaniel, Richard Izzo, Dr. Jimmy Si, and Andrew Holick are greatly appreciated.

The authors also gratefully acknowledge our material suppliers JOBE Material's Avispa Quarry in El Paso, Vulcan Material's Mico Quarry in Medina County, Smith Buster Quarry in Paris, and Frontera Reavis Pit in Hidalgo County for their service and reliability throughout the lifespan of this project.

Implementation Statement

This project was focused on identification, evaluation and validation of a practical laboratory testing protocol that can be implemented by TxDOT to characterize fatigue performance of the pavement structures with cement stabilized base layers.

The implementable products consist of a laboratory testing protocol in the TxDOT specification format for the estimation of the tensile strength of the materials in the laboratory. Appendix A presents the draft specification developed based on the finding of this research effort.

A workshop to disseminate the information on the specifics of the new testing protocol is developed in this project. This training document will be beneficial to inform TxDOT personnel and pavement design industry about the outcomes of the project.

TABLE OF CONTENTS

LIST OF FIGURES

LIST OF TABLES

Chapter 1. Literature Review

Introduction

Stabilization of granular materials is aimed to provide a robust structural platform to support surface layers in a multi-layer structural system. The primary role of the supporting layers is to reduce the stresses to a tolerable level for the subgrade soils, as well as to protect the subgrade from erosion. In addition to permanent deformation, fatigue cracking is one of the predominant types of pavement distresses often encountered in flexible pavements. For this reason, consideration of the fatigue performance due to repeated traffic loading in the process of mix and structural design is of prominent importance. The overall objective of providing the stabilized base under a flexible layer is to enhance the fatigue resistance of asphalt layers. Traditionally, horizontal tensile strain at the bottom of the flexible layer has been considered as the critical response that controls the design and the fatigue performance of pavement structures. The enhancement in fatigue performance can be attributed to the shift of neutral axis and therefore reduction of the critical tensile strain. Hence the fatigue resistance of stabilized layers under load applications plays the vital role in increasing the life of the pavement structure. Additionally, the presence of a robust stabilized layer underneath the flexible layer greatly enhances the compaction properties of the asphalt layer. Currently TxDOT does not have a practical fatigue test to characterize the crack resistance of stabilized layers. Specifications are required at the level of mixture selection and design to ensure the desired performance of pavements against fatigue cracking. The development and evaluation of valid fatigue tests suitable for Cement Stabilized Base (CTB) layer is considered an indispensable step to improve the performance of flexible pavements.

Considerable cases of premature pavement failures in Texas are attributed to cracking. To address this problem TxDOT, other states, and countries have implemented the use of stabilized layers to improve the cracking resistance of pavement structures. Typically, the strength properties of cement stabilized materials are characterized by Unconfined Compressive Strength (UCS) test, Modulus of Rupture (M_{rup}), and Resilient Modulus (M_r) tests. The aforementioned stiffness measures cannot differentiate the material cracking resistance under repeated loading. A laboratory mixture test to fully characterize the fatigue cracking susceptibility of cement stabilized bases is needed to identify the mixes that prone to develop fatigue cracking during service in the field. The objective of this literature search is to identify the current state of the practice testing protocols and analysis techniques used to mechanistically characterize the fatigue performance of cement stabilized layers. This information in turn was used to develop an all-inclusive experiment design for the laboratory characterization of CTBs subjected to repeated loading conditions.

Background

Fatigue cracking is one of the major types of distresses observed in pavement structures due to repeated traffic loads. Cracks can potentially initiate when the tensile stresses imposed by traffic loads exceeds the tensile strength of the flexible layer. Recent pavement design approaches incorporate mechanistic-empirical models to predict the fatigue performance of pavement structures. The rationale for the design of flexible pavements is to limit the tensile stresses developed in the bottom fiber of the CTB to a fraction of the tensile strength. This will ensure that the longevity of the stabilized layer, and to limit the initiation and propagation of cracks to the upper layer. Flintsch (2008) characterized the potential benefit of incorporation of chemically stabilized layers as shown in Figure 1.1. He rationalized that the improvements in the fatigue performance of the cement stabilized layers could be due to the fact that in CTB systems, the location of the neutral axis is typically lower than unbound systems. Considering the fact that bonded materials such as cement stabilized layers has an improved tensile stress distribution capacity than unbound particulate layers, the stabilized systems exhibit a more efficient orthogonal load distribution capacity compared to the unbound systems.

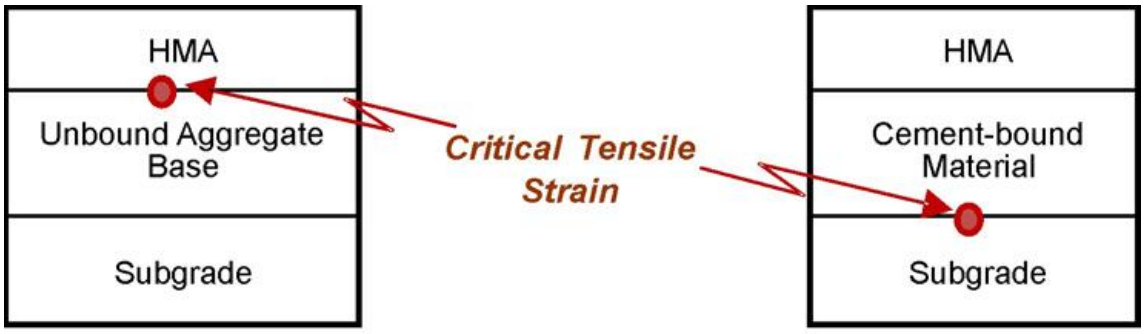

Figure 1.1 – Shift in Critical Strain Location from Traditional Flexible Pavement to Pavement with Cement-Treated Base (Flintsch et al. 2008)

Majumder et al. (1999) carried out flexural fatigue tests on 4 x 4 x 20 in (102 x 102 x 508 mm) beam specimens using a three-point loading system. The on-load and the off-load durations were 0.27 sec each. Load was applied until sudden and brittle failure was observed. The relations developed using fatigue life versus stress ratio was used as an input for the design of pavements. They also found that cement treated materials with laterite aggregates exhibit higher fatigue life as shown in Figure 1.2 when compared to mixes with gravel and dolerite aggregate types.

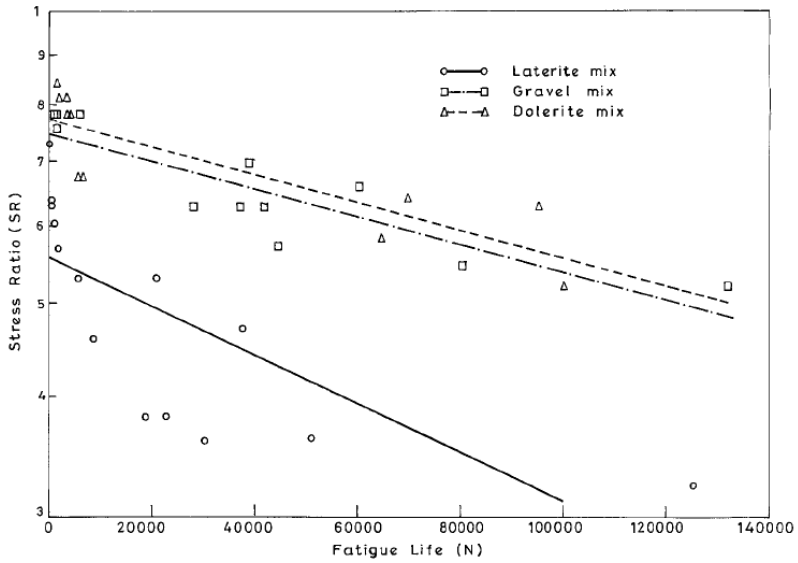

Figure 1.2 – **Fatigue life of cement treated mixes versus stress ratio (Majumder et al. 1999)**

Li et al. (1999) studied the performance and failure modes of asphalt pavements with soil-cement bases using an accelerated loading facility. Failure conditions for cracking were defined as 5 m/m^2 over 50 percent of the trafficked area and significant reduction in base course modulus. They found that the fatigue life of pavement structure was significantly improved by five to six times when a stone crack relief layer was placed between cement treated base and asphalt layer.

Mahasantipiya (2000) found that the modulus of cement treated bases varied significantly from laboratory to field cored specimens. He reported that these variations were manifested due to the difference in the environmental conditions between the laboratory and the field sections. The elastic layer analyses of the pavement structures with cement-treated base showed reduced stresses and strains at the bottom of the asphalt layer and the top of the subgrade when compared to pavement structures with traditional base and asphalt-treated base layers. Therefore, the researchers concluded that the life of pavement with cement-treated base layers was substantially longer when compared to traditional pavements.

Sobhan and Das (2007) assessed the durability of soil-cement mixtures against fatigue fracture. Flexural fatigue test with three-point loading was carried out at a frequency of 2 Hz on the specimen size of 6 x 6 x 30 in (152 x 152 x 762 mm) under constant sinusoidal load amplitude. They reported that the endurance limit for fatigue failure for the cement-stabilized specimens was up to 53% of its maximum strength indicating similar strength as other cementations materials. The damage ratio based on dissipated energy was used to characterize the fatigue performance of the cementations materials as shown in Figure 1.3. They also concluded that the rehabilitation strategy of the pavement structure could be devised using the damage ratio determined in the laboratory fatigue test.

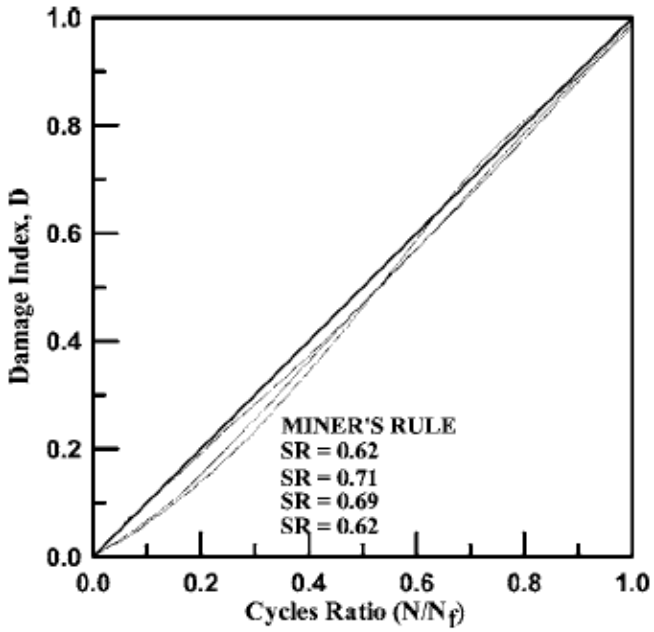

Figure 1.3 – Variation of Damage Index with Cycles Ratio (Majumder et al. 1999)

Khoury and Zaman (2007) studied the influence of different stabilizing materials on the durability of the mixes. Cement kiln dust, fly ash, and bed ash were selected as stabilizing binders. They found that the resilient modulus decreased with increased number of freeze thaw cycles. The distortion of composites during freezing and increased moisture content due to thawing were explained as the reasons for the decrease in the resilient modulus with freeze thaw cycles as shown in Figure 1.4.

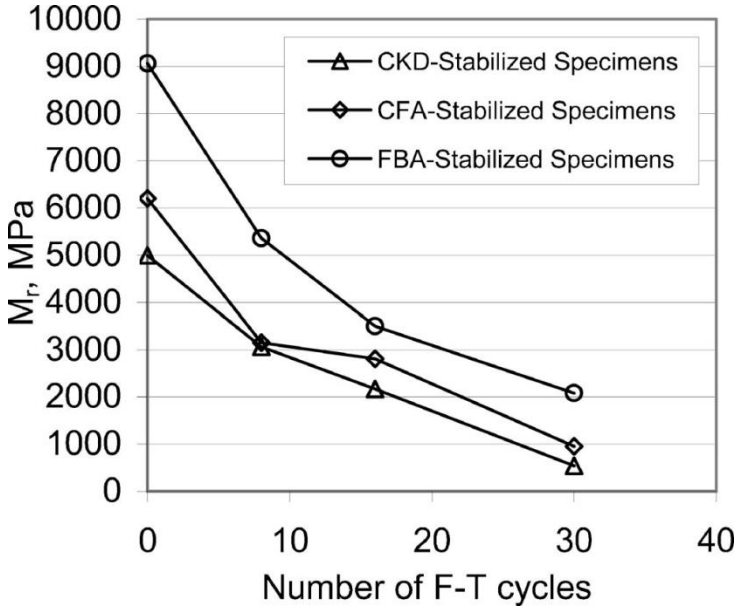

Figure 1.4 – Variation of Damage Index with Cycles Ratio (Majumder et al. 1999)

Midgley and Yeo (2008) explored the use of indirect tensile test as an alternative means to characterize the fatigue behavior of the cement-treated materials. They reported that gyratory compactor was suitable for the preparation of the laboratory indirect tensile samples. They also found that the indirect tensile test was more appropriate for testing less stiff materials (less than 5,000 MPa). Flintsch et al. (2008) found that the deflections in the pavement structure are significantly reduced as the stiffness of the base layer was increased. They also found that fatigue cracking in the asphalt layer was minimized due to the use of stabilized layers. However, findings were based on the pavement design models and not from a laboratory characterization of fatigue crack resistance.

Scullion et al. (2008) characterized the material properties of cement-treated soil bases to determine input values for a mechanistic-empirical pavement design analysis. The material properties used for design were the resilient modulus, modulus of rupture, and Poisson's ratio. They used three different methods to measure the resilient modulus in the laboratory; these included the seismic modulus test, dynamic modulus test, and the resilient modulus test. Results showed the resilient modulus as half of the value of the modulus measured using seismic-based devices. As shown in Figure 1.5, the authors reported that the frequency of loading has no significant effect on the modulus. They concluded that the soil cement acted as an elastic material. For this reason, they rationalized that the dynamic modulus is the same as the resilient modulus and can be used as an input. Table 1.1 shows the comparison of the three test methods. The seismic modulus test is the least expensive and fastest test to obtain a measure of the resilient modulus. The authors performed a case study on two different materials. The authors concluded that the seismic modulus can be considered as a reliable and repeatable alternative to traditional test procedures. The authors also developed a relationship between the unconfined compressive strength and the resilient modulus as well as with the modulus of rupture though this relationship was based on very limited data.

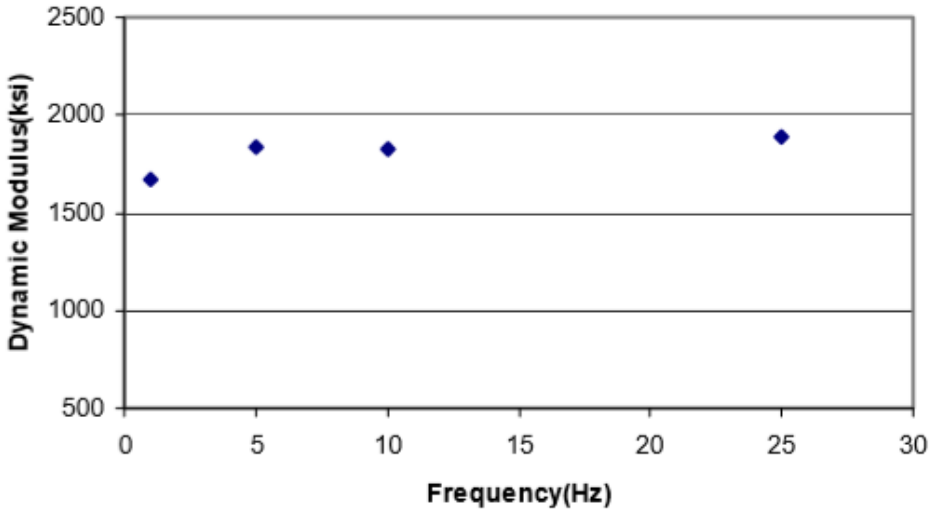

Figure 1.5 – Dynamic Moduli at different frequencies Scullion et al. (2008)

Table 1.1 – Comparison of Three Moduli Test Methods Scullion et al. (2008)

	Seismic Modulus Test	Dynamic Modulus Test	Resilient Modulus Test
Equipment Cost	$5,000	$40,000	$350,000
Testing Time	3 minutes	40 minutes	30 minutes
Sample Capping	No capping	Capping	Capping
Coefficient of Variation @ 28 day	7%	7%	10%

In a relevant study, Khalid (2000) used both the beam fatigue test and the diametrical test to compare five different bituminous materials. Khalid also provided a refined threshold of failure as the point below which the stiffness of the specimen was reduced by a specific amount from its initial value. Using that testing protocol, Khalid concluded that conducting the bending test at 20°C and 5 Hz would be equivalent to conducting the diametrical test at 12°C and 0.67 Hz for the range of binders used in the study. It can be seen from Figures 1.6 and 1.7 that at low strains fatigue lines assume similar relative position and the tensile fatigue test suggest lower fatigue lives for all of the materials tested (Khalid 2000).

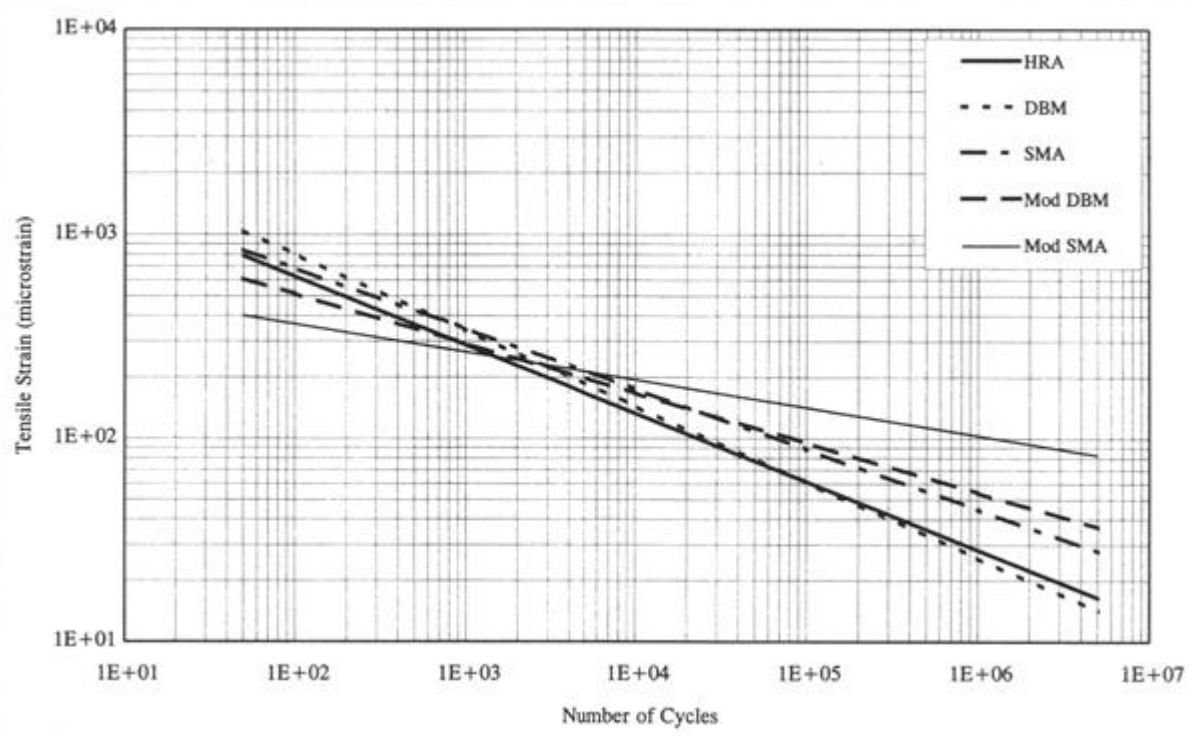

Figure 1.6 – Fatigue relationship for five mixtures from indirect tensile fatigue (Khalid 2000)

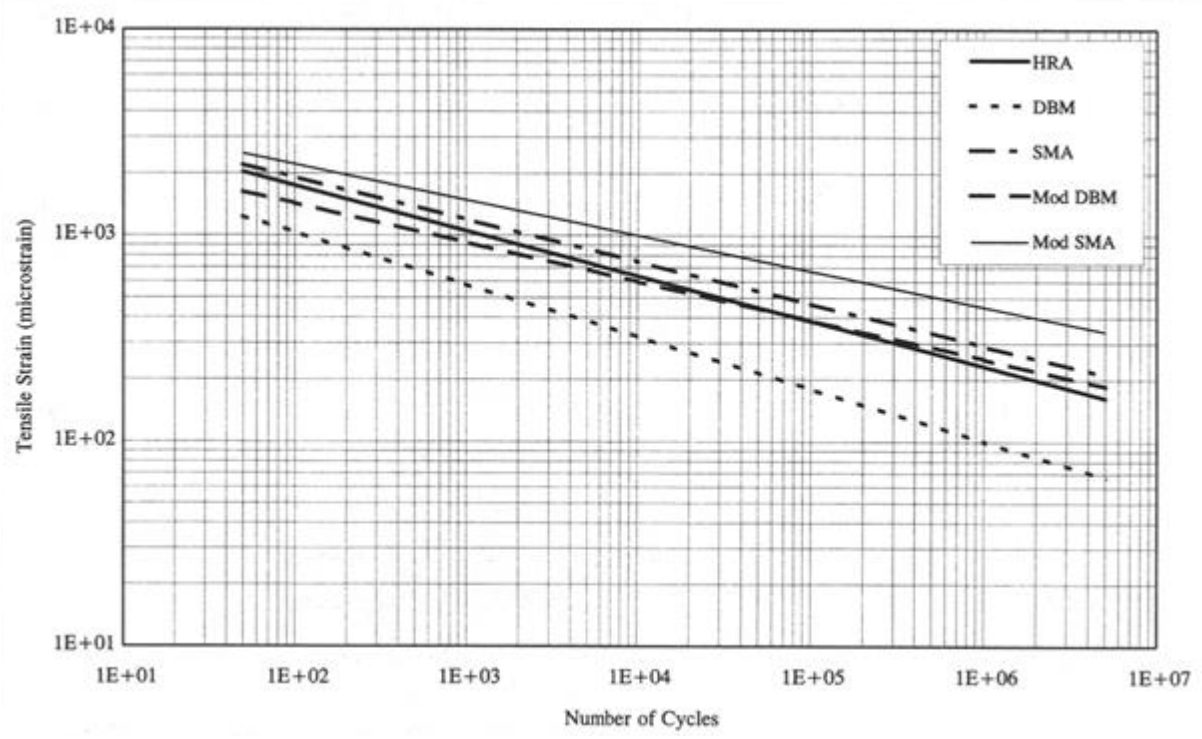

Figure 1.7 – Fatigue relationship for five mixtures from indirect tensile fatigue (Khalid 2000)

Kahild developed a typical pavement model to demonstrate the role of fatigue relationships and to validate the data found in the beam fatigue test and the diametrical fatigue test. The results of this model are shown in Table 1.2. From the results, Khalid concluded that the diametrical test was a desirable mix design and quality control tool. However, since the equivalency ratios between the beam and diametrical tests were very low, he concluded that the diametrical test was not suitable for use in pavement design.

Table 1.2 – Fatigue lives form flexural and diametrical fatigue tests and their equivalence ratios (Khalid 2000)

Mix Type	Maximum Tensile Strain (με)	Flexural Fatigue Life	Diametrical Fatigue Life	Equivalence Ratio (%)
HRA	210	1.57E-06	2553	0.2
DBM	212	5.38E-04	3538	7
SMA	203	6.21E-06	6055	0.1
Mod DBM	210	2.56E-06	3884	0.2
Mod SMA	204	9.87E-06	6952	0.04

Gnanendran and Piratheepan (2008) used the Indirect Diametric Tensile (IDT) test method as an alternative to the beam test for the characterization of the stiffness properties of lightly stabilized

materials. The stabilizing material used in their research was slag-lime because it does not create shrinkage cracking in the stabilized material. The IDT set up used a pair of LVDT and Perspex strips secured onto the test sample for better results, as shown in Figure 1.8. The modification was aimed at eliminating the underestimation of the horizontal deformations (restraining due to clamp supports) under vertical loading. The Static Stiffness Modulus (SSM) was determined from monotonic loading with a vertical deformation rate of 1mm/min and the Dynamic Stiffness Modulus (DSM) was determined from a series of cyclic loading test with a 3Hz frequency sinusoidal loading. The authors reported that SSM and DSM were not affected by the moisture content but did increase with binder content as shown in Figures 1.9 and 1.10.

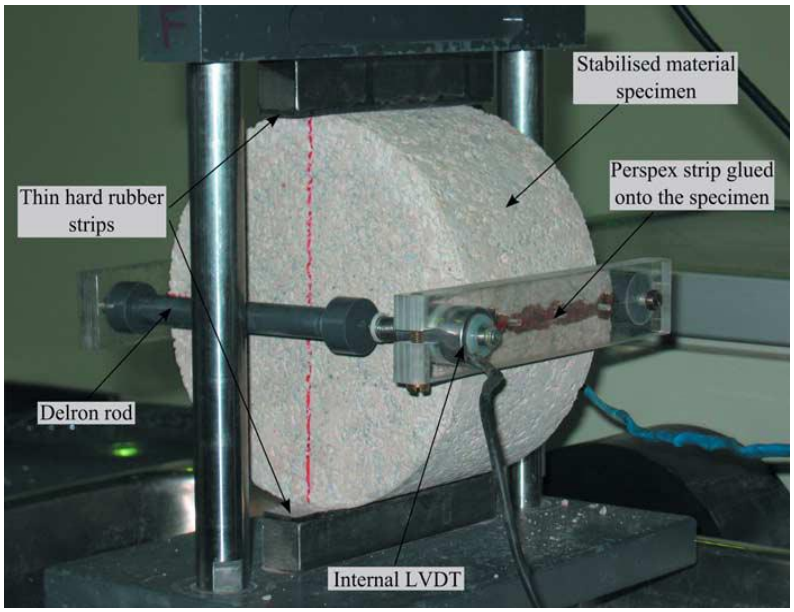

Figure 1.8 – Modifications for Horizontal Deformation Measurement (Gnanendran and Piratheepan, 2008)

The researchers performed fatigue tests on lightly stabilized cylindrical specimen using a stress-controlled cyclic load test, with a frequency of 3Hz of sinusoidal loading pattern. For that test, Gnanendran and Piratheepan (2008) defined fatigue by two methods: the stiffness reduction to 50% of its initial stiffness, and the energy ratio method. Based on the analysis of the laboratory data, the authors concluded that the two fatigue criteria produced similar relationship for lightly-stabilized granular materials with slag-lime. It was also concluded that the use of IDT testing was a reliable and repeatable means to characterize the stiffness properties of the lightly-stabilized materials in the laboratory. The researchers also developed several empirical relationships to correlate the fatigue performance and indirect tensile strength of lightly-stabilized materials based on monotonic IDT testing.

In a follow up study, Piratheepan et al. (2010) characterized lightly-stabilized materials using unconfined compressive testing and indirect tensile testing with internal displacement measurements. Based on the laboratory data, the authors developed relationships between the unconfined compressive strength and the tangent and secant moduli in the UCS test. The researchers also developed correlations between the unconfined compressive strength and the tensile strength from both monotonic and cyclic IDT testing. The authors concluded that the IDT strength is equal to 0.114 times the UCS value as supported by Figure 1.11. Based on the goodness of the fit, the authors reported that it is possible to estimate the IDT, SSM, and DSM of a lightly-stabilized material from the UCS value of that material. The authors commented on the practicality and ease of incorporation of the UCS in the experiment design to estimate the tensile properties of the stabilized mixes from its compressive behavior.

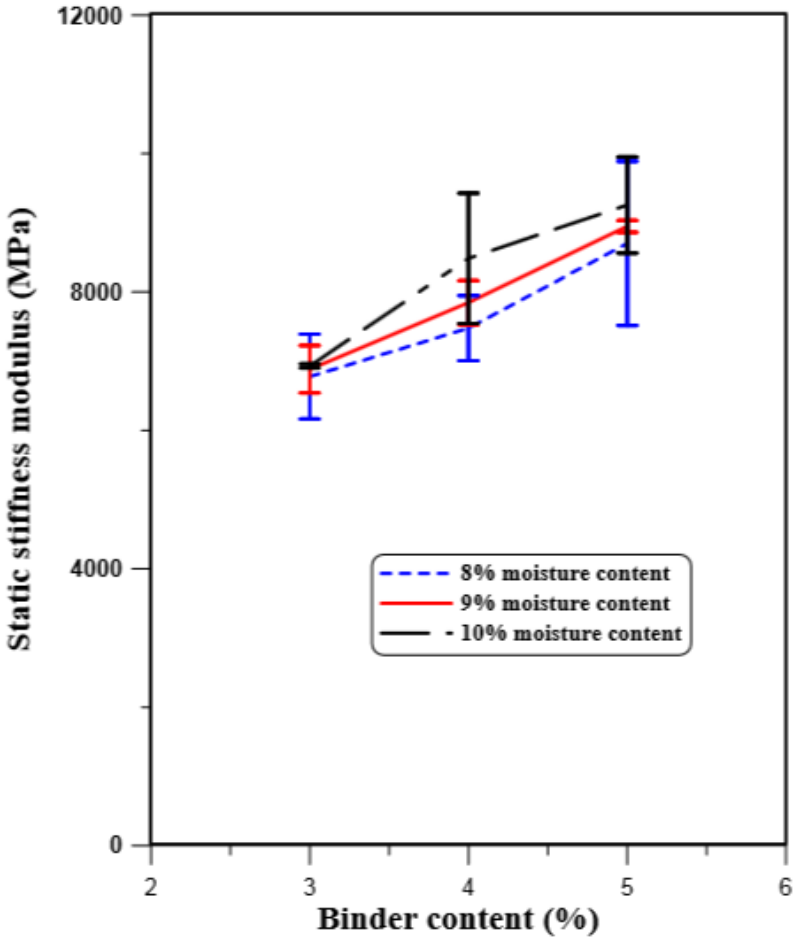

Figure 1.9 – Variation of static stiffness modulus versus content (Gnanendran and Piratheepan 2008)

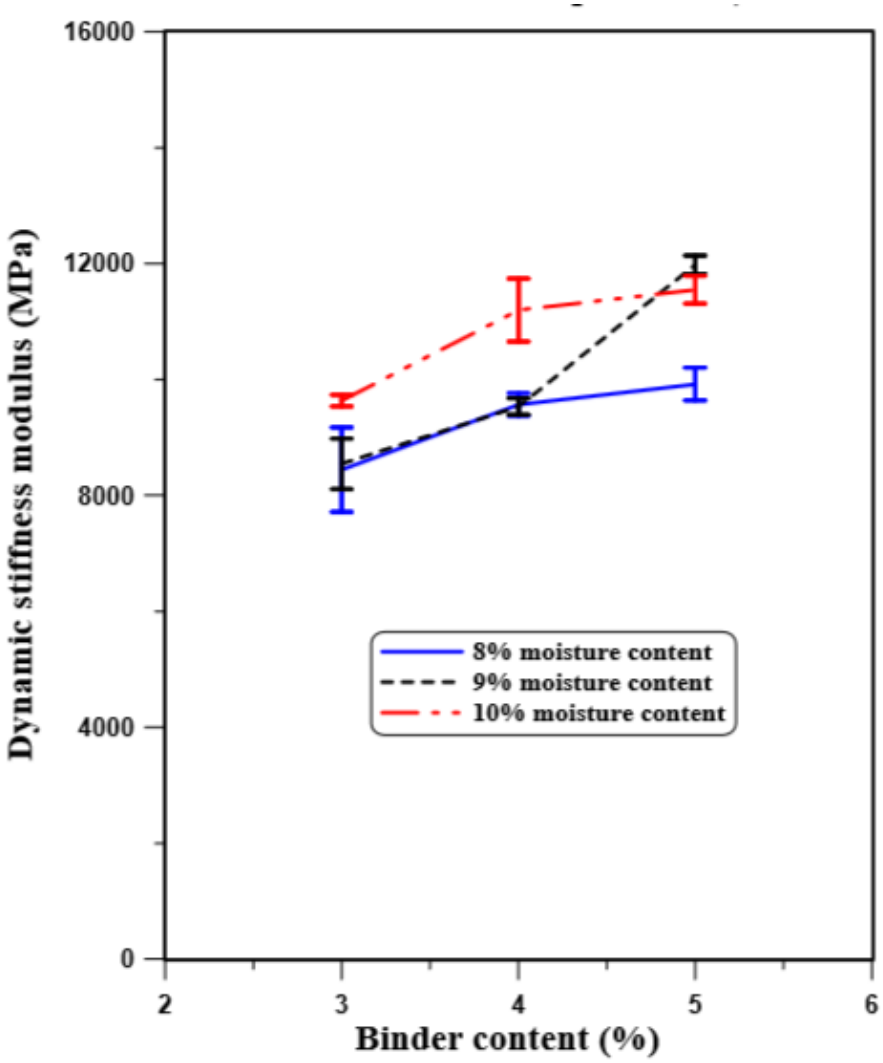

Figure 1.10 – Variation of dynamic stiffness modulus versus content (Gnanendran and Piratheepan 2008)

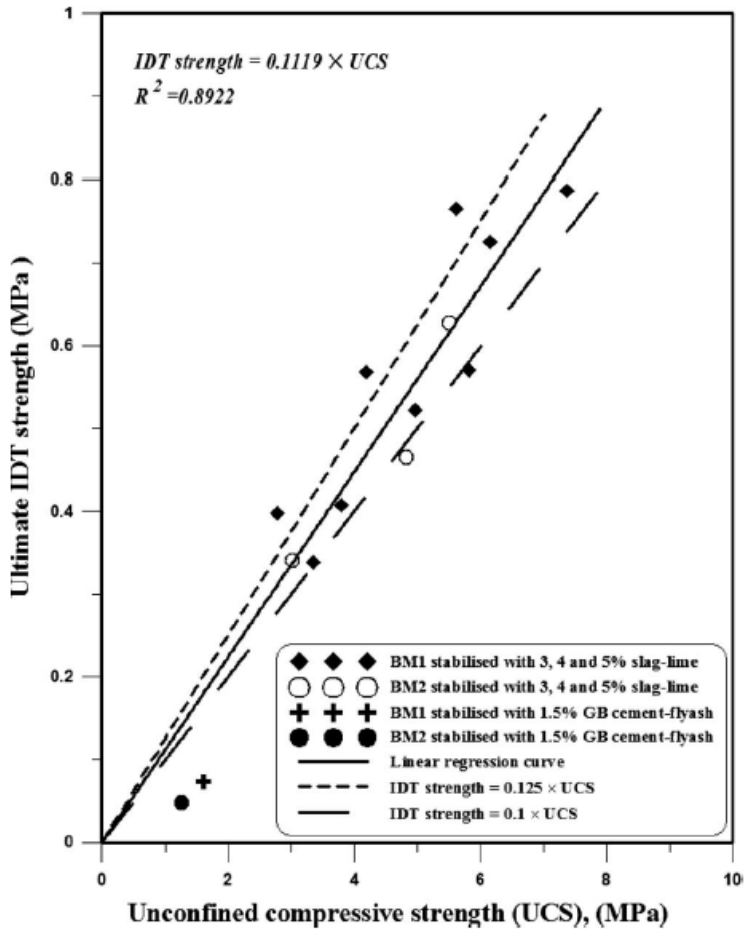

Figure 1.11 – Variation of ultimate IDT strength versus UCS (Piratheepan et al. 2010)

Yan et al. (2011) reported high variability in the fatigue life of cement-stabilized specimens subjected to similar stress states and cement contents. The authors attributed the high variability of the results to the low cement content, disintegration of the external granules, the variability in the strength of the specimens, and the loss of moisture during testing. They also reported that at lower cement contents, stress ratio was a determining factor that influenced the fatigue life of the laboratory specimen.

Puppala et al. (2011) reported that the resilient modulus estimations were less sensitive to the change in confining pressure for the cement-treated materials. He rationalized that this was due to the influence of the stiffening in the process of stabilization of the fabricated materials in the laboratory.

Arnold et al. (2012) developed a laboratory protocol for the estimation of the flexural strength, modulus and fatigue properties of stabilized materials using three-point loading test on prismatic specimens. The authors used a vibrating hammer to compact the laboratory specimens. A strain-controlled loading rate of 1 mm/min or 3.3 kN/min was recommended in their effort. The authors recommended minimum of 100 load cycles for the estimation of the modulus of a stabilized

specimen. Additionally, the researchers recommended at least 1 million load cycles or catastrophic failure of the specimen for the fatigue testing of the stabilized granular soils in the laboratory.

Papapcostas and Alderson (2013) tested different cementitious materials to determine the flexural strength, breaking strength, and flexural modulus. They concluded that cement content was most significantly correlated with the flexural strength followed by the moisture content and fine aggregate content. The materials tested included general purpose Portland Cement (PC), lateritic gravel, weathered granite, calcrete, ferricrete, and met greywacke. The test methods included the flexural test method, the flexural strength testing, and the flexural modulus testing. It can be noted that for the flexural beam test, a beam with dimensions of 100 mm high x 100 mm wide x 400 mm long was used for ease of handling. The test set up is shown in Figure 1.12.

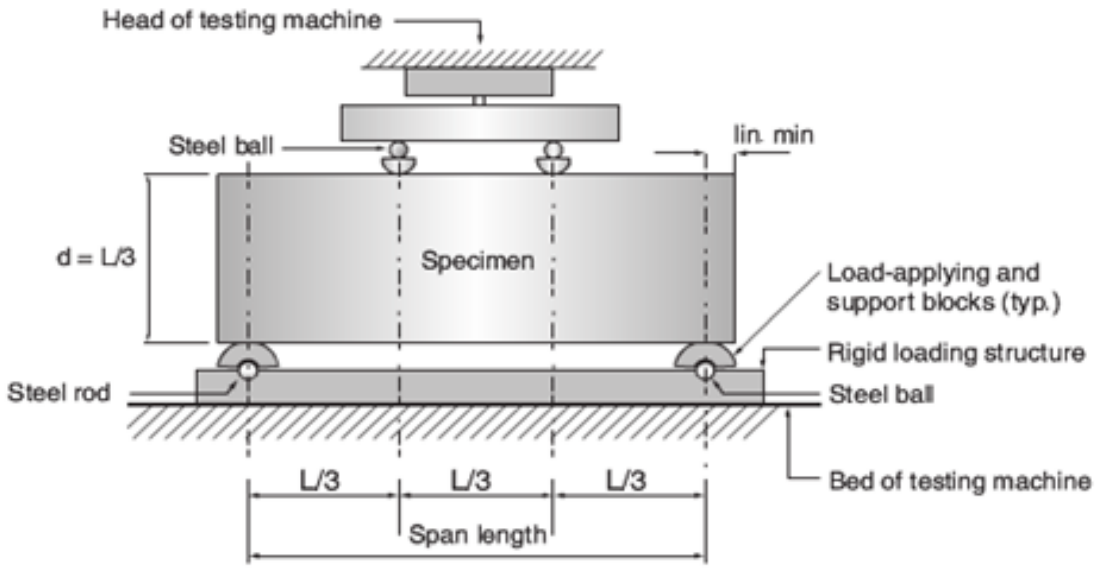

Figure 1.12 – Cross-sectional view of flexural beam testing apparatus (Papapcostas and Alderson 2013)

The researchers developed a model based on the laboratory-collected data to relate the material characteristics to the flexural strength and the breaking strength of the beams. They concluded that the cement content was the most significant feature and that no significant relationship between the breaking strain and material characteristic existed. They also reported that there was enough to conclude that a meaningful relationship between the unconfined compressive strength and the flexural modulus existed.

Molenaar and Pu (n.d.) researched to develop a field fatigue relationship for sand cement treated bases. Their relationship was based on the analysis of the SHRP-NL database, which contained data on pavements with sandy cement treated bases. The data included visual inspection, nondestructive testing in the field such as falling weight deflectometer, pavement structure, and

traffic for a period of 10 years. Based on the analyzed field data, the authors reported that the cracks were initiated at the bottom of the asphalt layer and propagated to the surface; therefore, the data could be used for the development of an in-situ fatigue model. To achieve this objective, the researchers initially calculated the magnitude of the tensile strain at the bottom of the cement treated base layer. A traffic analysis based on the available information was also performed. Equation 1.1 was developed to predict the fatigue life of cement treated bases.

$$logN = 8.5 - 0.034\mathcal{E} \quad (1.1)$$

N= allowable number of 100kN equivalent single axles

$\mathcal{E}$= tensile strain at the bottom of the cement treated base due to a 50kN falling weight deflectometer load (μm/m)

Mbaraga et al. (2013) studied the influence of the beam geometry and the particle size on the mechanical behavior of prismatic specimens. The cement-stabilized specimens were subjected to a displacement-controlled loading regime at a rate of 0.025 mm/second, on a four-point beam test, with a loading span of 300 mm and 450 mm. The stabilized materials were characterized based on their flexural strengths and elastic moduli. The deflections of the beams were measured using 20 mm LVDTs positioned at the mid-span of the beam. The study's main objectives were to analyze the influence of the beam geometry and particle size on the flexural strength and elastic modulus and to model the shear stress distribution throughout the prismatic specimen. The study was performed using crushed gravel rock at three varying cement contents, 2, 3, and 6%. The two aggregate particle sizes used included P_{max} 19.00 mm and P_{max}13.20 mm. The beam was loaded until fracture.

From Figure 1.13, it can be seen that the flexural strength of the beams increased with increase cement content. Beam with P_{max}19.00 mm and height of 50 mm had the lowest R^2 value. The authors reported that that behavior was due to the use of large aggregate particles in a small beam, which created localized zones of weakness (Mbaraga et al. 2013). They also concluded that at low cement contents, the presence of large aggregate particles in small beams had limited influence on the flexural strength. Figure 1.14 represents the elastic modulus vs. cement content in that study. The use of large aggregates in small beams would cause a reduction in the elastic modulus. The large aggregate influenced the material matrix and created zones of weakness. The authors rationalized that this was the underlying cause for the reduction of the flexural strength and elastic moduli of such specimens. The authors also reported that the beams with the highest span/depth ratio had lower maximum shear stresses compared to those with a lower span/depth ratio. The beam with the lowest shear maximum stress was the beam with a 50 mm depth and a span of 450 mm, a ratio of 9.

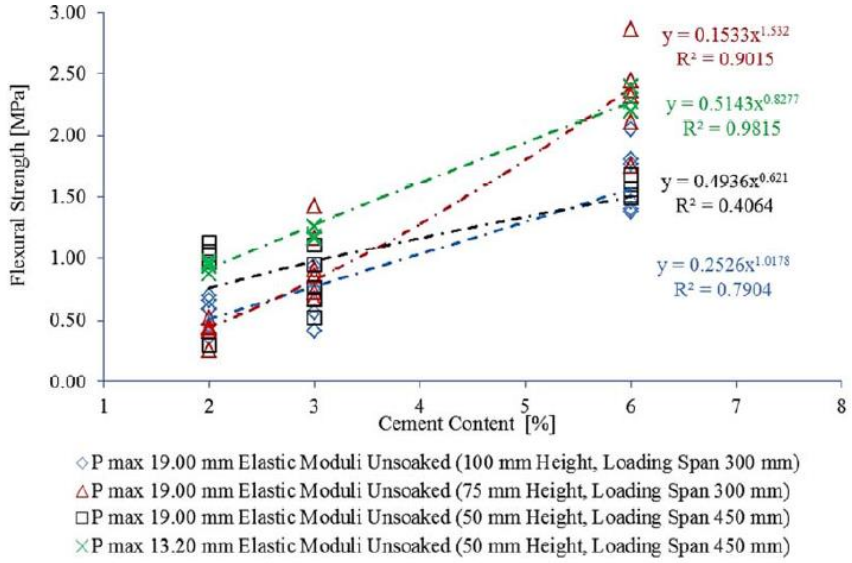

Figure 1.13 – Flexural strength versus cement content (Mbaraga et al. 2013)

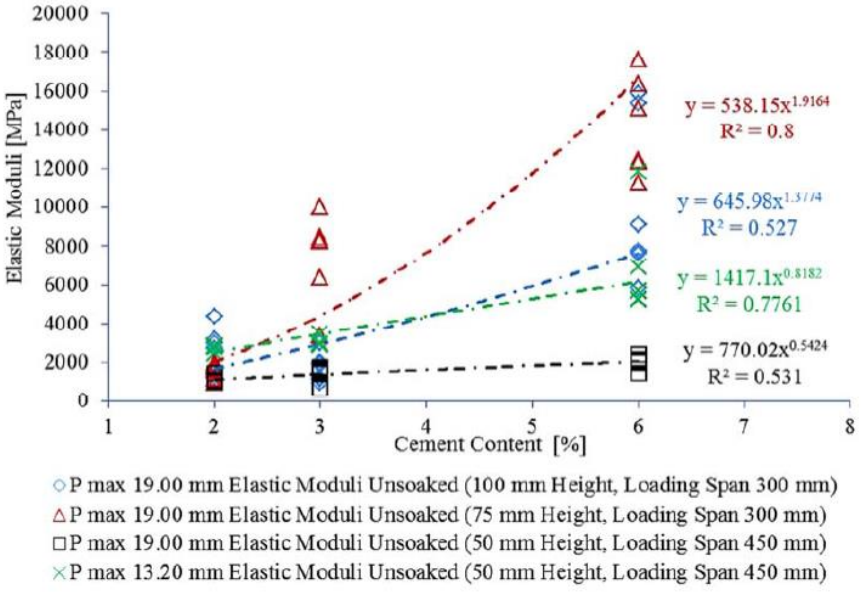

Figure 1.14 – Elastic moduli versus cement content (Mbaraga et al. 2013)

Based on the laboratory-analyzed data, the authors concluded that the use of large aggregate sizes in small beams resulted in the reduction of the flexural strength and elastic modulus. It was also reported that the increase in the beam depth at fixed loading span resulted in the decrease of the flexural strength and elastic modulus (Mbaraga et al. 2013). The authors recommended a smaller aggregate size of P_{max}20.00 mm to be used in beams with a height of less than 60 mm. A span/depth ratio of 9 and above should be used for a reduction and control of shear stresses developed under strain-controlled loading in the laboratory.

Paul and Gnanendran (2012) studied the characterization of lightly-stabilized granular base materials by the flexural beam test. In that study a monotonic load/displacement flexural beam test with an improved deflection measurement setup was used as shown in Figure 1.15. The two types of aggregates used were classified as well-graded sandy gravel with some fines under the Unified Soil Classification System (USCS). The binders chosen were general blend cement and fly ash because of their low shrinkage/cracking potential and for economic reasons. The aggregates were stabilized with 1% to 3% stabilizer contents. The dimensions of the specimens in this study were 76 mm height, 76 mm wide and 285 mm long. The authors reported that two of the samples containing 1% stabilizer content were damaged in the process of removal from the mold. A second attempt also resulted in failure.

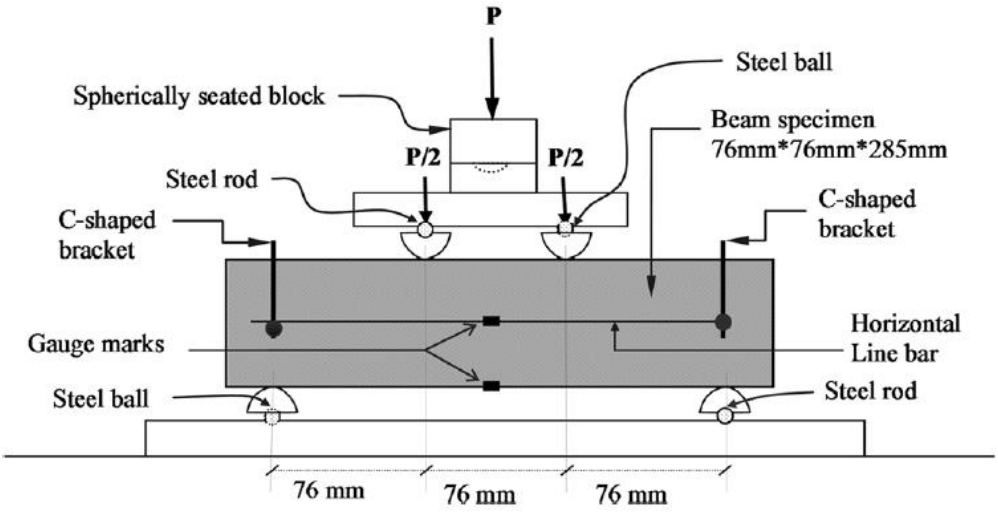

Figure 1.15 – Schematic diagram of flexural testing setup (Paul and Gnanendran 2012)

The test began with a displacement rate of 1.2 mm/min as per ASTM D1635 but the specimens failed within seconds, which suggested that such guidelines were not suitable for lightly-stabilized materials. The specimens were then tested at different loading rates. The results showed that loading rate significantly influenced the load deflection behavior of lightly-stabilized materials. Failure load and slope of the load-deformation curve increased with the increase in the imposed displacement rate (Paul and Gnanendran 2012). According to ASTM D1635, which requires constant fiber stress rate of 69 ±39 kPa/min for flexural testing of soils, the researchers adopted a rate of 0.5 mm/min for that study. The specimens were cured for 28 days and were then tested monotonically at a displacement rate of 0.5 mm/min. The results of the beams tested are reported in Table 1.3. Based on the results the authors concluded that the test setup was consistent and reliable. The authors noted that because of unavailability of equipment and required training of the operator, the test might not be very practical and therefore a relationship between the flexural strength and the stiffness modulus was created.

Table 1.3 – Flexural properties of lightly stabilized materials and comparison of variations in flexural testing (Paul and Gnanendran 2012)

		Flexural Strength M_R		Static Stiffness modulus E		Breaking strain ε_f	
Parent material	BC (%)	Mean (MPa)	CoV (%)	Mean (MPa)	CoV (%)	Mean (MPa)	CoV (%)
CLM	1.0	0.10	4.0	203	7.1	1020	16.7
	1.5	0.25	11.9	1620	7.8	270	12.3
	2.0	0.33	8.4	2040	12.1	216	8.3
	3.0	0.50	6.4	2507	5.7	214	15.2
QRM	1.0	0.10	-	159	-	1720	-
	1.5	0.63	1.4	2642	17.4	322	21.2
	2.0	0.85	8.1	4408	18.4	235	13.2
	3.0	1.17	6.7	5466	4.3	237	12.8

Zhou et al. (2010) characterized cement treated soils. The tests used for that study were the unconfined compressive strength, the free-free resonant column test to obtain the seismic modulus, and the flexural beam load test to determine the modulus of rupture. The cement-treated soil was tested at 2%, 3%, and 4% stabilizer content. Table 1.4 summarizes the results of the different tests performed.

Table 1.4 – Summary of all results (Zhou et al. 2010)

Cement Content (%)	Seismic Modulus (ksi)		7-day UCS (psi)	28-day MR (psi)
	Day 3	Day 7		
2% Cement - A	939.3	1011.3	316.7	67.5
2% Cement - B	964.8	1008.9	329.4	74.2
2% Cement - C	927.8	1089.4	306.1	75.8
3% Cement - A	982.7	1151.5	429.9	90.0
3% Cement - B	928.6	1095.6	440.6	93.3
3% Cement - C	942.7	1235.1	457.2	94.2
4% Cement - A	987.6	1239.2	586.0	117.5
4% Cement - B	963.2	1245.6	582.1	118.3
4% Cement - C	1012.5	1401.1	606.5	116.7

Burns and Tillman (2006) researched the influence of the fines content, cement content, mineralogy, and freeze-thaw cycles on the strength properties of the mixes characterized by the unconfined compressive strength tests for the Virginia Department of Transportation. The aggregates incorporated in the experiment design were mica, limestone, diabase, and granite.

These aggregates were tested with 3, 4, 5, and 6% cement contents by weight. The authors reported that the mineralogy of the aggregate materials significantly influenced the strength of the cement-treated specimen. As expected, an increase in the unconfined compressive strength was measured in the aggregates with greater cement content. Based on the laboratory results, the authors recommended a minimum of 250 psi (1.73 MPa) for 7-day unconfined compressive strength of cement-treated aggregates.

Paul and Gnanendran (2012) carried out a laboratory investigation to characterize lightly-stabilized granular base materials through UCS testing. Axial deformations were internally measured to obtain the stress-strain relationships to establish a mathematical model for predicting the experimental stress-strain behavior so that the stiffness modulus can be determined from the UCS value. A modified Ramberg-Osgood expression was found to be suitable to describe the nonlinear stress-strain curves.

The two materials tested were well-graded sandy gravels with some fines according to the Unified Soil Classification System (USCS). Slag lime and general-purpose cement with fly ash were used as stabilizers in their study. The samples had a diameter of 105 mm and a height of 115 mm. The fabricated specimens were capped with dental plaster so that the rough surfaces would not affect stress distribution. Figure 1.16 shows the UCS test set up.

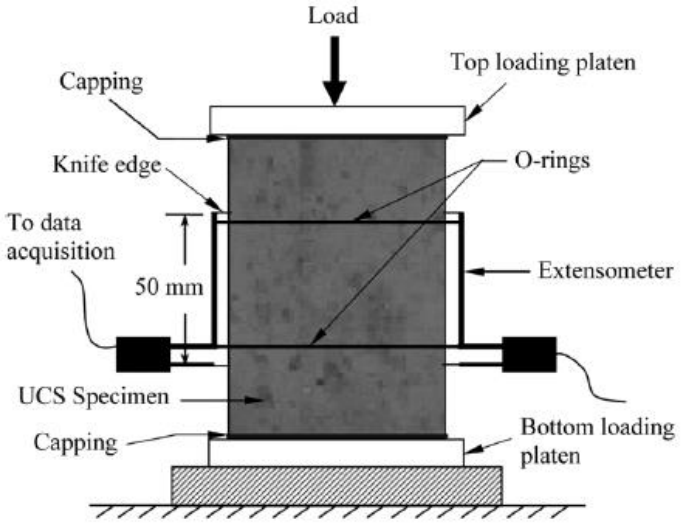

Figure 1.16 – Schematic Diagram of the Axial Deformation Measurement Setup (Paul and Gnanendran 2012)

Based on the Ramberg-Osgood expression modified by Hill and Rasmussen, a five-parameter stress-strain equation (1.2) was suggested for lightly stabilized granular material (Paul and Gnanendran 2012).

$$\bar{\varepsilon} = \frac{\bar{\sigma}}{E_{0.2}} + \bar{\varepsilon}_{up}\left(\frac{\bar{\sigma}}{\bar{\sigma}_u}\right)^m \quad for\ \sigma > \sigma_{0.2} \tag{1.2}$$

The authors reported that the UCS had an almost linear increase with the stabilizer content for the tested specimens. The secant modulus corresponding to the 0.2% proof stress (offset yield point) was suggested as the appropriate modulus of lightly-stabilized granular base materials for the purpose of pavement design. It should be noted that according to the study the findings were only applicable to the undamaged condition and a wider range of materials and binders should be used to validate the model.

Scullion et al. (2012) reported on the current state of practice and the specifications available for the Full Depth Reclamation (FDR). The authors pointed out that the major concerns were the amount of material needed and the time required to complete the test as it might take more than a month. The authors suggested looking into smaller test set ups that would take less time such as the Texas Gyratory Compactor and the IDT test. Three different materials form roads in Texas were tested and the UCS and the IDT strengths were compared. Limited number of field specimen presented in Figure 1.17 showed a meaningful correlation between the UCS as per Tex-120-E for 6 in. by 8in. samples and the IDT results of 2 in. by 4 in. samples.

The need of a faster and efficient test is also highlighted in Gaspard (2000) study. The authors performed a series of durability tests, which requires up to six weeks obtaining results.

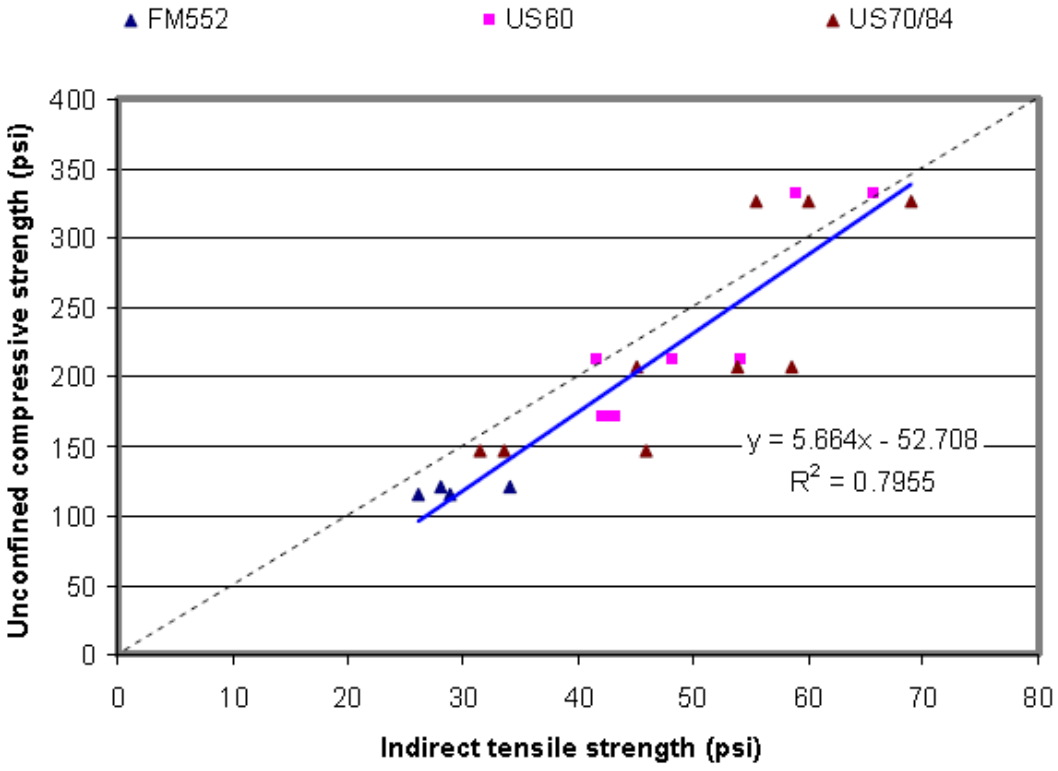

Figure 1.17 – Relationship between UCS and IDT (Scullion et al. 2012)

Description of Laboratory Testing Procedures for Fatigue Characterization of Cement Stabilized Materials

This section is aimed at summarizing the potential test protocols to characterize the strength, modulus and fatigue properties of cement-stabilized layers in the laboratory. Based on the comprehensive review of the literature, the following test protocols were selected and described for the laboratory assessment of stabilized materials:

- Unconfined compressive strength test
- Modulus of rupture and flexural beam fatigue tests
- Resilient modulus test
- Indirect tensile strength test
- Free-Free Resonant column test

Unconfined Compressive Strength (UCS) Test: UCS shall be conducted according to Tex-120-E, 2013. Essentially UCS is a strain-controlled compression test involving cylindrical specimens loaded along their vertical axes until failure.

Modulus of Rupture: This test will be incorporated in the experiment design and the procedure will be followed according to ASTM C 78. The flexural strength of stabilized material shall be determined using a simple beam with third-point loading employing bearing blocks to ensure that forces applied to the beam will be perpendicular to the face of the specimen and applied without eccentricity as shown in Figure 1.18. In general, the specimen beam size shall be of 6”x 6”x20”. Flexural fatigue tests will be carried out using similar setup, with capability of applying repeated loading under controlled load or displacement amplitude.

Figure 1.18 – Flexural Beam Test Setup for Modulus of Rupture Testing of Concrete

Indirect Tensile Test: The indirect tensile test set up in general is similar to traditionally used set up for asphalt mixtures as shown in Figure 1.19. However, appropriate loading rates, specimen geometry, deformation measurements need to be modified accordingly to measure the stress-strain response of the stabilized granular materials. Monotonic or static tensile test aims at measuring the tensile strength at constant displacement. Assuming the plane stress conditions, the split tensile strength can be calculated using relation as given in Equation 1.3. For repeated load indirect tensile test, percentages of the maximum load under the monotonic conditions shall be applied. The stress or strain ratio and the number of cycles can be used to determine the fatigue parameters for a particular type of mix.

$$\sigma = \frac{2p}{\pi dt} \tag{1.3}$$

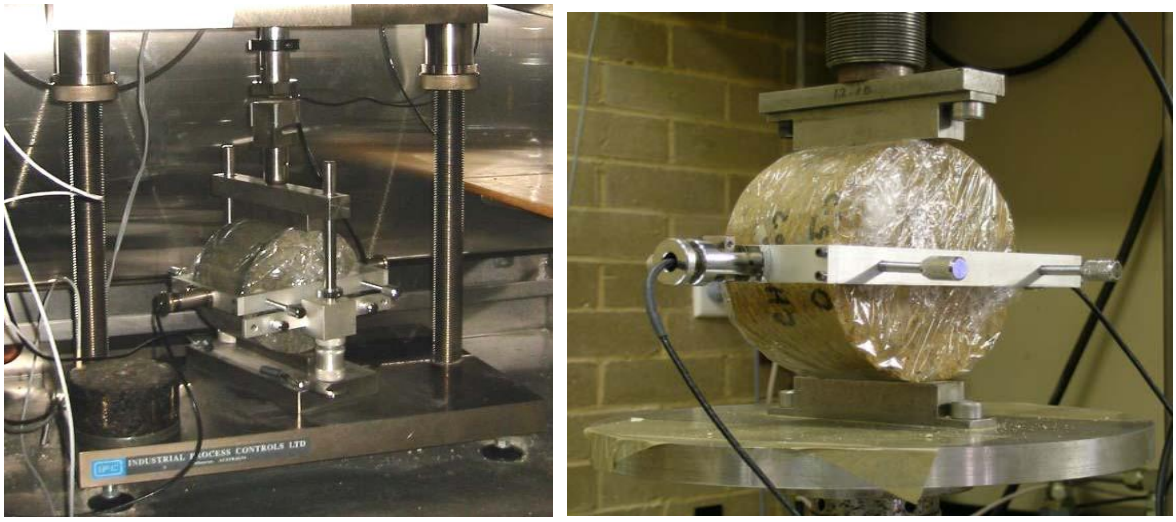

Figure 1.19 – Indirect Tensile Setup for Strength and Fatigue Testing (Midgley and Yeo 2008)

Resilient Modulus Test: The procedures for estimating the resilient modulus have been under continuous modification. AASHTO alone has adopted several test protocols in the last 20 years (e.g., T292-91, T294-92, TP46-94 and T307-03). The NCHRP 1-28A approach recommended as a part of the MEPDG is gaining popularity as well. These approaches differ in the specimen size, compaction method, loading time, stress sequence and the type and location of sensors (within or outside the confining chamber and mounted on specimen or platen-to-platen measurements). Despite the fact that loading protocols share similar concept, different stress path tests can potentially yield different stiffness parameters. Gupta et al. (2007) indicate that the resilient moduli obtained with internal displacement measurements can be up to three times greater than those when the displacement measurements are made outside the confining cell. The resilient modulus test shall be carried out using a repeated load triaxial test setup as shown in Figure 1.20. A haversine wave load pulse of 0.1 s loading and 0.9 s rest period will be applied to simulate traffic loading. The relationship used to estimate the resilient modulus is as given in Equation 1.4.

$$Mr = k_1 P_a \left(\frac{\theta}{P_a}\right)^{k_2} \left(\frac{\tau_{oct}}{P_a} + 1\right)^{k_3} \quad (1.4)$$

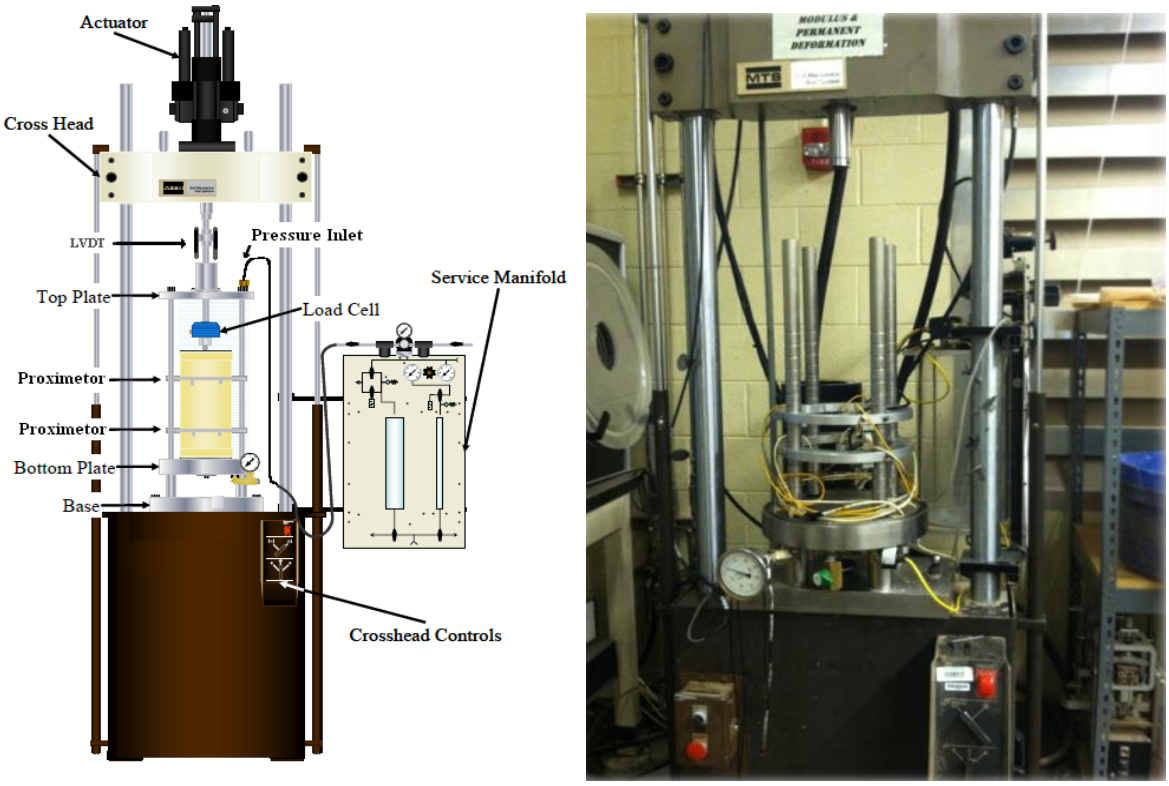

Figure 1.20 – Resilient Modulus (M_r) Test set up

Free-Free Resonant column: The free-free resonant column (FFRC) (Nazarian et al., 2003) tests can be conducted on the same specimens prepared for resilient modulus test. The FFRC method estimates the linear-elastic (low-strain) seismic modulus based on the determination of the fundamental resonant frequency of vibration of a specimen. The main components of the test setup are shown in Figure 1.21. An accelerometer is securely placed on top of the specimen, and the specimen is impacted with a hammer instrumented with a load cell. As an impulse load is applied to the specimen, seismic energy over a wide range of frequencies propagates within the specimen.

The resonant frequency, fL, and the length of the specimen, L, are used to determine the modulus, EFFRC, using the relation as given in Equation 1.5.

$$E_{FFRC} = \rho(2f_L L)^2 \quad (1.5)$$

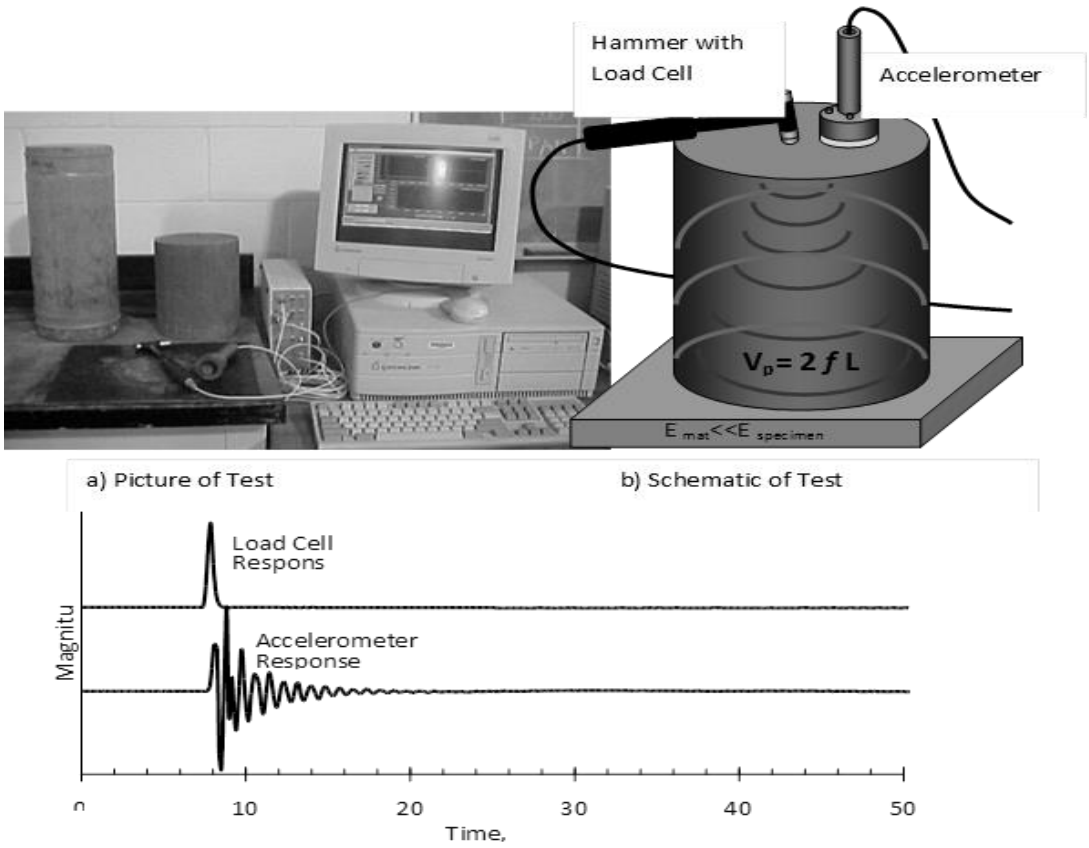

Figure 1.21 – Free-Free Resonant Column (FFRC) Test Setup

Summary of the Literature Search

An extensive literature search was carried out to identify the current state of the practice for the laboratory characterization of cement-stabilized aggregate layers. Table 1.5 summarizes various testing protocols found in the literature with their advantages and limitations. A significant number of researchers suggested that the use of flexural beam fatigue test has significant practical limitations to be incorporated in the testing protocol. The limitations include but not limited to the specimen preparation (uniform compaction of large beams), non-uniform distribution of the stresses in the four-point beam fatigue test, and practical issues associated with the specimen handling and transportation. This is more pronounced when small amount of stabilizer is considered to be added to the mixes and the specimen tends to disintegrate under self-weight. Based on the review of the literature it seems that a modified version of an indirect tensile test can be a potential alternative to the beam fatigue test. Table 1.5 presents a summary of the laboratory tests with their potential advantages, restrictions, and shortcomings.

Table 1.5 – Summary of test methods for characterization of stabilized materials

Test Types	Purpose	Specimen Size	Loading Pattern	Failure Criteria	Advantages	Limitations
UCS	Strength	6 X 8 in.	biaxial	until failure	ease of use	provides supplementary information
IDT	Strength	*4 X 6 in.	axial	until failure	provides supplementary information	relatively large measurement variation
Mrup	Strength	6 X 6 X 20 in.	three point	until failure	ease of use	provides supplementary information
Mr	Modulus	6 X 8 in.	axial	stress sequence	provides stiffness information of a mix under traffic loading condition	time consuming, measurement errors and availability in TxDOT district level
FFRC	Modulus	No restrictions	Hammer	NA	easy to use for cement-treated mixes and test results can be related to those from field modulus tests	available only in few district labs Summary
IDT Fatigue	Modulus and Fatigue properties	*4 X 6 in.	biaxial	50 - 60 % reduction in modulus	provides stiffness information of a mix under traffic loading condition	relatively large measurement variation
Flexural Beam Fatigue		*6 X 6 X 20 in.	three point		relatively large measurement variation	time consuming, failure of specimens due to self-weight and availability in TxDOT district level

*****Specimen dimensions vary with agency; UCS: Unconfined Compressive Strength; IDT: Indirect Tensile; M_{rup}: Modulus of Rupture; M_r: Resilient Modulus; FFRC: Free-Free Resonant Column

Chapter 2. Theoretical Background

Introduction

Proper characterization of cement-treated materials in the laboratory is of paramont importance for mechanistic characterization of stabilized base layeres. Logically, the material properties required for the design of the stabilized layers can be categorized into two distinct categories: material parameters that characterize the stiffness properties of the mix such as unconfined compressive strength, elastic material properties (resilient/elastic modulus and Poisson's ratio), and the modulus of rupture. The second category is associated with volumetric behavior such as shrinkage properties of the cement-treated mixes. Conventionally, thermal conductivity and heat capacity of the mixes are required to predict the volume change potential of the mixes. Currently, TxDOT is evaluating new approches and loratory test methods to characterize the fatigue resistance of the cement-treated base layers. The new approch is required to be inclusive of all environmental conditions and geologic litholigies to be considered for the new Texas Mechanistic-Emperical Design Guide (TxME). Traditionally, the large bending beam fatigue test, originally developed for concrete mixes, is used to determine the modulus of rupture of the cement-treated mixes. This chapter provides a theroetical review of this test and the practical issues associated with using such test to estimate the modulus of ruptire of cement treated materials.

Practical Issues in Four Point Test

Our previous experience with three-point beam fatigue test revealed that often times the large beam 6 x 6 x 20 in (152 x 152 x 508 mm) break under its own weight during transportation and handeling in the laboratory. This problem is more pronounced for lightly-cement stabilized materials with less than 3% stabilizer content. Therefore thisproject is aimed at developing an alternative laboratory testing method to characterize fatigue performance of cement-treated layers regardless of the stabilizer content.

Figure 2.1 shows the disintegration of the specimen during the de-moling process in our laboratory. This proved to be repeating pattern for materials stabilized with 2% cement content in the mix.Another major practical concern for the laboratory research team were the concerns associated with the uniformity of the compaction of large beams in the laboratory. Uniformity of the compaction cannot be assured due to the long and relatively shallow nature of the molds in the conventional four-point test. This should be noted that this test was originally developed for concrete and then extrapolated to stabilized materials; therefore, little thought was given to the compaction issues of stabilized materials when this procedure was adopted. Based on our experience with this test in the laboratory, we often observed pocket of air void trapped between the rigid mold and the specimen which is indication of the inconsistency of the compaction effort. This would ultimately manifest itself in reduced reliability of this test method.

Figure 2.1 – Sample Breakage during Demolding and curing at the CTIS Laboratory

Additionally, the heavy weight of the large beams requires two operators to safely handle the prismatic specimen to the test setup. Figures 2.2 and 2.3 shows the testing process for the 3% cement stabilized limestone materials sourced from El Paso after 7 days curing in the moisture room. Pockets of air voids are evident on the outside perimeter of the specimen.

Figure 2.2 – Large Beam Fatigue Test Setup before Loading at UTEP

Figure 2.3 – Large Beam Fatigue Test after Failure at UTEP

Figure 2.4 provides detailed process of specimen preparation, de-molding, handling, transportation to the test setup, and testing of stabilized materials in our laboratory.

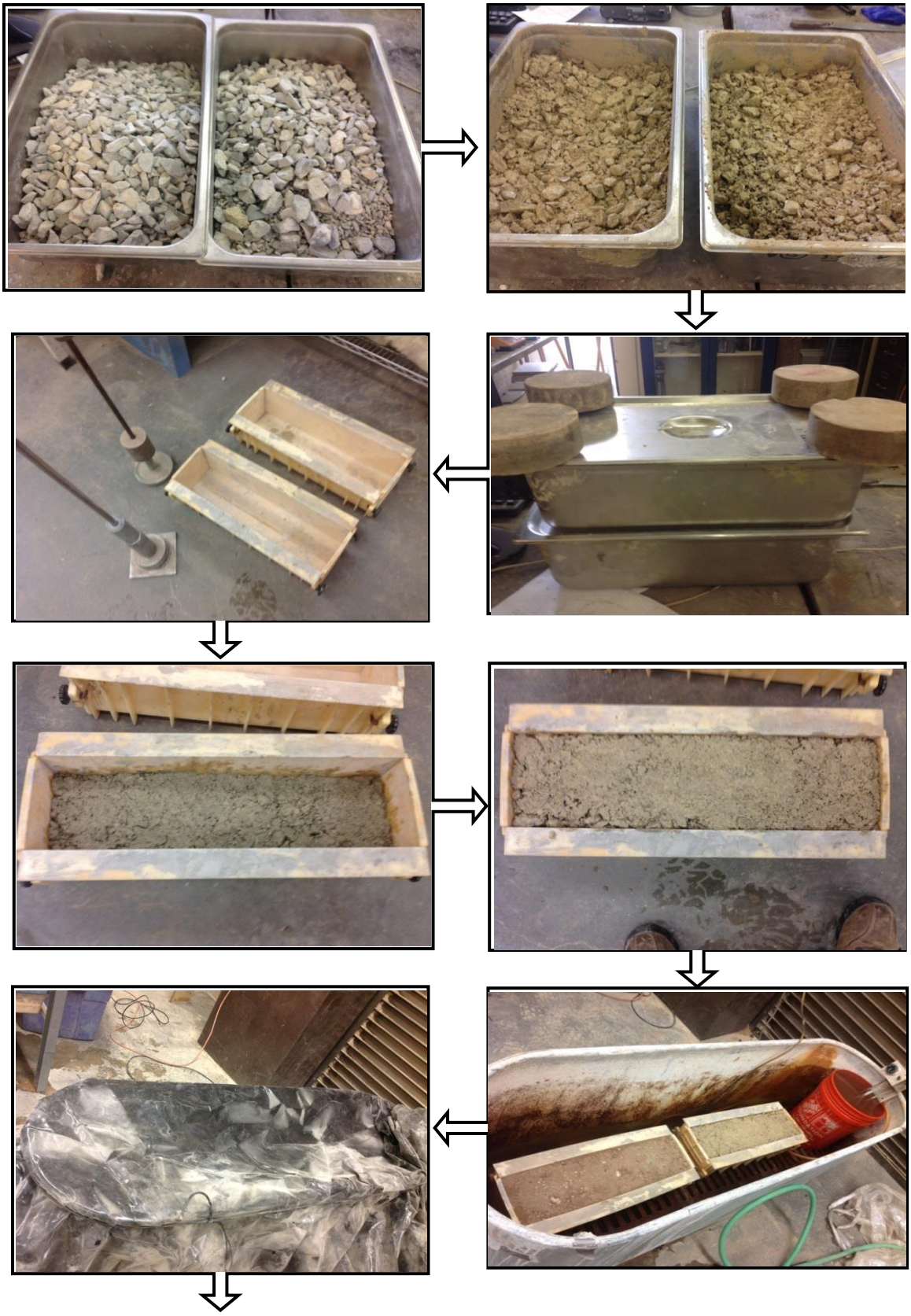

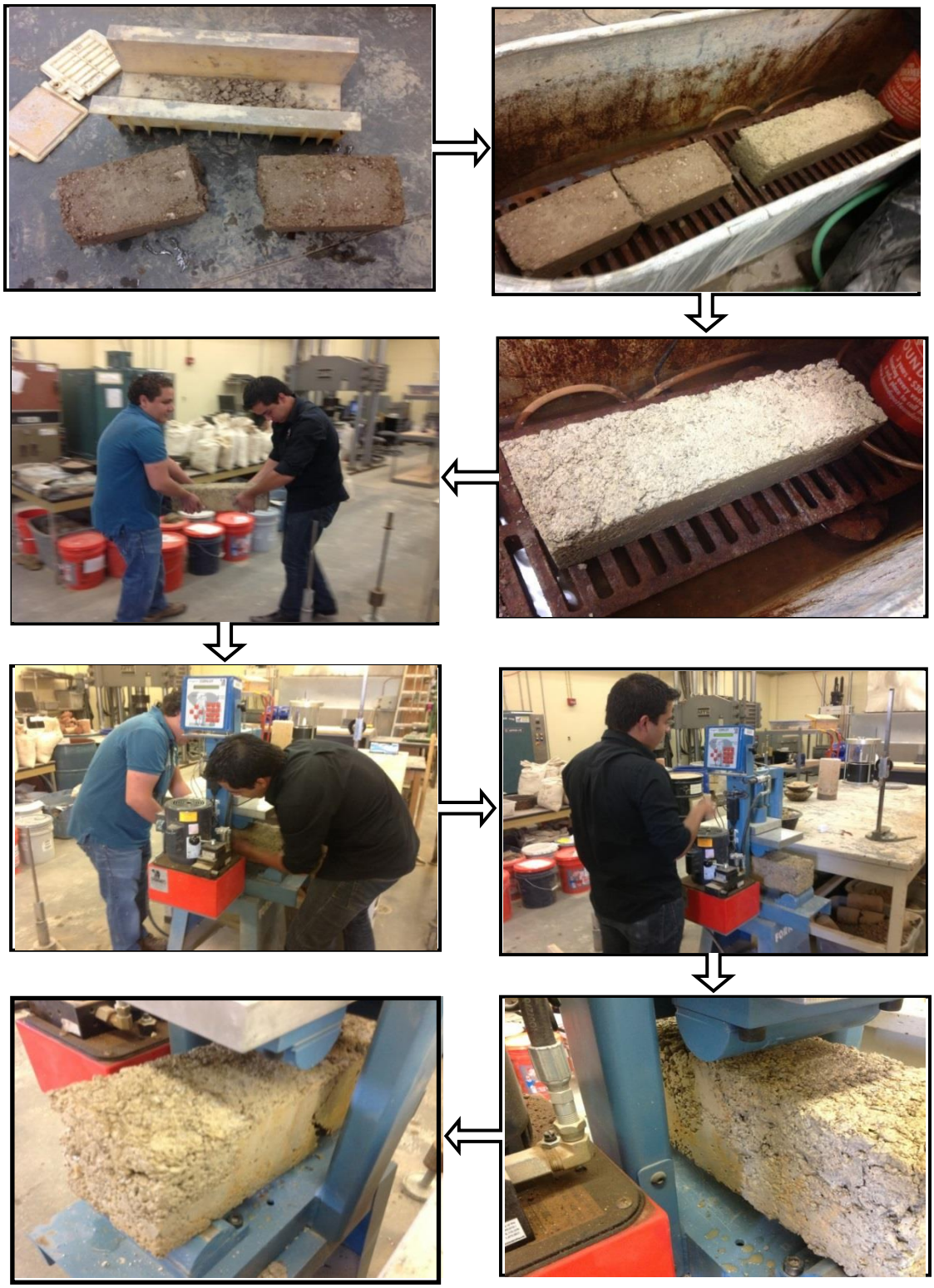

Figure 2.4 – Sample Preparation, Conditioning and Loading for Beam Fatigue Test at UTEP

Theoretical Discussion

Traditionally the tensile strength of the concrete materials is estimated using the ASTM C 496 splitting tension test and the ASTM C 78 third-point flexural loading test as show in Figure 2.5. The same type of tests is adopted for the characterization of the tensile strength of the stabilized systems in the laboratory.

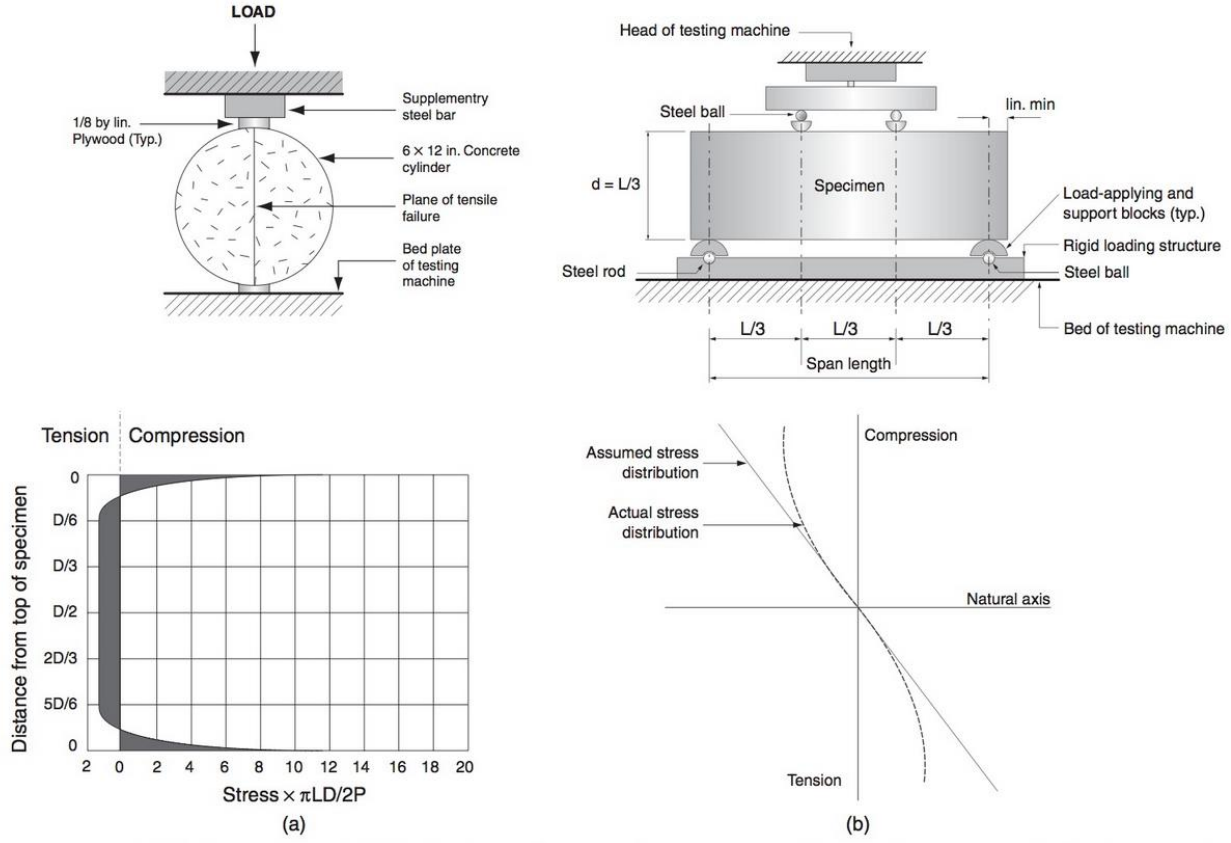

Figure 2.5 – Diagrammatic Arrangements of the Traditional Tensile Strength Tests Set up and Stress Distributions (a) Splitting Tension Test (ASTM C 496) (b) Flexural Four Point Test (ASTM C 78) (After Mehta, 2006)

In the splitting tension test a 6 x 12 in (152 x 305 mm) the cylindrical specimen is subjected to compressive loading condition along two axial lines. The load is applied monotonically at a constant rate to induce failure in the specimen. As evidenced in Figure 2.5 (a), the applied compressive stress results in a relatively uniform transverse tensile stress along the vertical diameter. The splitting tension strength is computed from Equation 2.1 as:

$$T = \frac{2P}{\pi ld} \tag{2.1}$$

Where:

T = tensile strength
P = failure load
l = length
d = diameter of the specimen

In the third-point flexural loading test, a 6 x 6 x 20 in (152 x 152 x 508 mm) concrete beam is subjected to constant rate of loading (stress-controlled condition) to induce fracture in the prismatic beam.

Flexural strength is commonly expressed in terms of the modulus of rupture, which is the maximum stress at rupture computed from Equation 2.2 as:

$$R = \frac{PL}{bd^2} \tag{2.2}$$

Where:

R = modulus of rupture
P = maximum indicated load
L = span length
b = width
d = depth of the specimen

Equation 2.2 is valid only if the fracture in the tension surface is within the middle third of the span length. If the fracture is outside by not more than 5 percent of the span length, the modified relationship presented in Equation 2.3 should be used.

$$R = \frac{3Pa}{bd^2} \tag{2.3}$$

Where a is equal to the average distance between the line of fracture and the nearest support measured on the tension surface of the beam. It should be noted that the results of the test should be rejected if the fracture is outside by more than 5 percent of the span length.

One of the other concerns associated with the characterization of the tensile behavior of cementitious materials is the fact the modulus of rupture test tend to overestimate the tensile strength by 50 to 100 percent as reported by Price in 1952 in Table 2.1. He noted that this systematic error is mainly because the flexure formula assumes a linear stress-strain relationship throughout the cross section of the beam. Conversely, in direct tension tests the entire volume of the specimen is under applied stress, whereas in the flexure test only a small volume of beam nears the bottom of the specimen is subjected to high stresses.

Table 2.1 – Relationship between Tensile Strength and the Modulus of Rupture (After Price, 1952)

Strength of concrete (MPa)			Ratio (%)		
Compressive	Modulus of rupture	Tensile	Modulus of rupture to compressive strength	Tensile strength to compressive strength	Tensile strength to modulus of rupture
7	2	1	23.0	11.0	48
14	3	1	18.8	10.0	53
21	3	2	16.2	9.2	57
28	4	2	14.5	8.5	59
34	5	3	13.5	8.0	59
41	5	3	12.8	7.7	60
48	6	4	12.2	7.4	61
55	6	4	11.6	7.2	62
62	7	4	11.2	7.0	63

The data in Table 2.1 show that for low strength concrete the modulus of rupture can be as high as twice the strength in direct tension; for moderate or high- strength concrete the values are about 70 percent and 50 to 60 percent higher, respectively.

This was the motivation for our research team at CTIS to perform a series of finite element analysis to evaluate this argument. Figures 2.6 and 2.7 provide the stress distribution in the body of the 6 x 6 x 20 in (152 x 152 x 508 mm) prismatic beam. As evidenced in this figure, due to the pure bending mechanism in the four-point test, the top portion of the beam is in compression, while the bottom fibers experience tension. The location of the neutral axis is a function of material properties of the cementitious materials as well as the parameters of the loading protocol such as magnitude and rate of loading in the test.

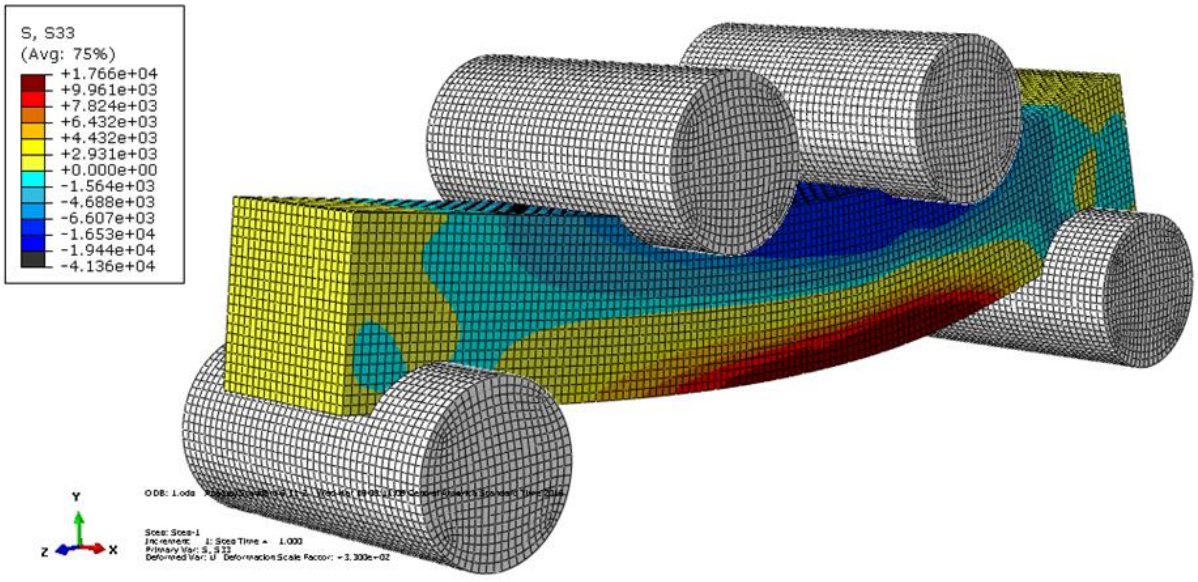

Figure 2.6 – Distribution of the Stresses in the Third Point Beam Test

The stress distributions in the mid-span of the cross-sectional area of the prismatic beam is provided in Figure 2.7. The warmer colors in this plot are an indication of the tension, and the cooler colors represent the compressive stresses.

A better visualization of the non-linear nature of the stress distributions is evident in the cross section of this plot. Based on the parameters selected for the finite element analysis, approximately 60% of the beam is still compression due to the pure bending loading in the third point test. This confirms the argument presented by Price on the systematic error of using simplified linear stress distribution to calculate the modulus of rupture of cementitious materials using the beam fatigue test. It is also worth noting that the degree of nonlinearity of the lightly cement stabilized materials is much larger compared to the traditional concrete. Detailed discussion on the reduction of the degree of nonlinearity of the mixes with higher percentages of cement is provided in chapter 5 of this report. This underscores the shortcoming of the third point beam test for lightly stabilized systems.

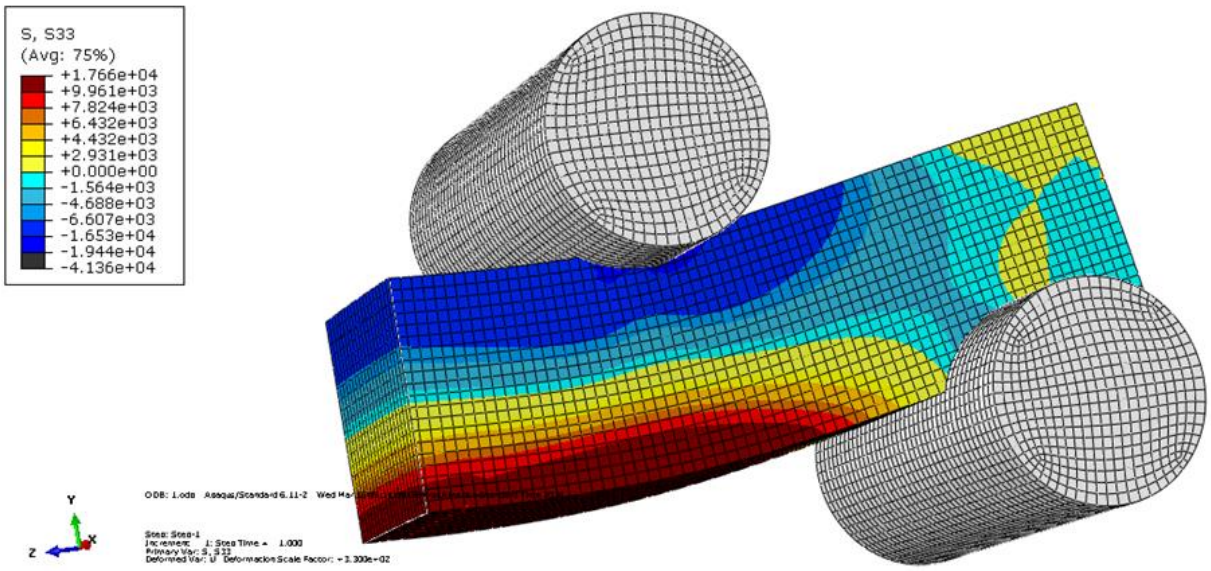

Figure 2.7 – Distribution of the Stresses in the Transverse Cross-Section in the Mid-Span of the Prismatic Beam

Figure 2.8 provides the stress distribution in the body of 6 x4.5 in (152 x 114 mm) cylindrical specimen subjected to a strain controlled split tension test. The compressive load applied on the rotated cylindrical specimen results in the failure of the sample in tension. The warmer colors in this plot (positive values of stresses) represent tension and cooler colors (negative values) represent compression in the sample.

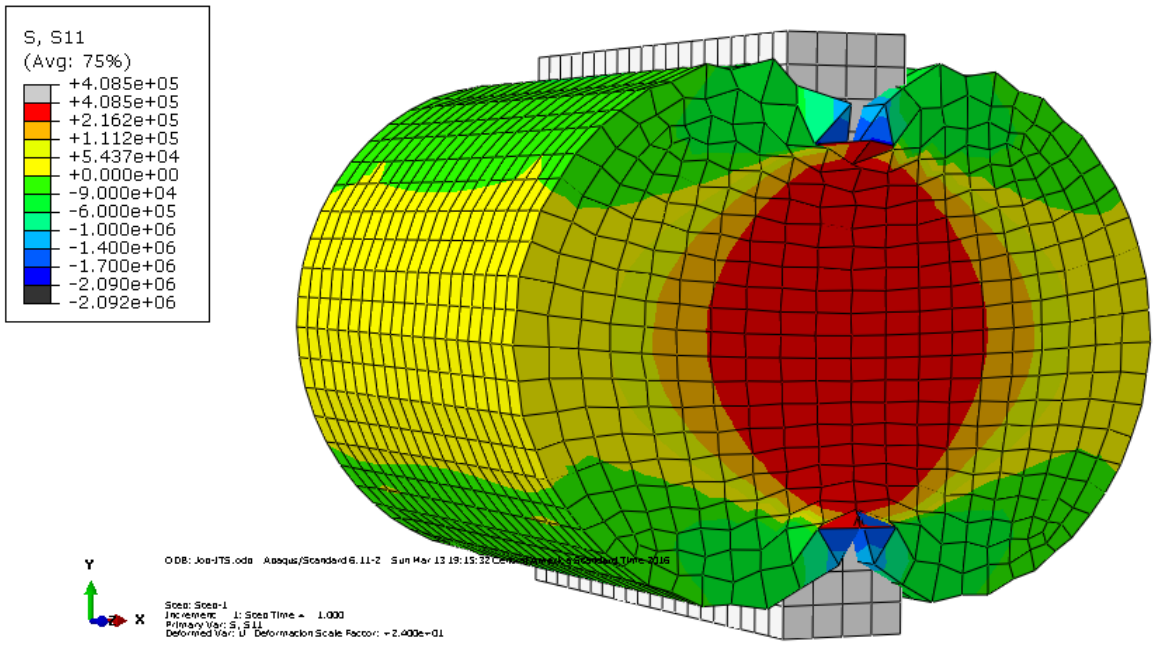

Figure 2.8 – Distribution of the Stresses in the Indirect Diametrical Tensile Test

Figures 2.9 and 2.10 provide the stress distributions along the longitudinal and transverse cross section of the specimen in the indirect diametrical tensile test.

These plots clearly show the capability of this test to induce relatively uniform tension along the axis of loading in the specimen. The exaggerated deformed meshes show the relatively small compression zones immediately beneath the loading platform and adjacent to the support at the bottom of the specimen, however the majority of the specimen stays in tension upon the application of the axial load.

The finite element results presented in this chapter provide to be in conformity with the schematic stress distributions presented in Figure 2.1 (a).

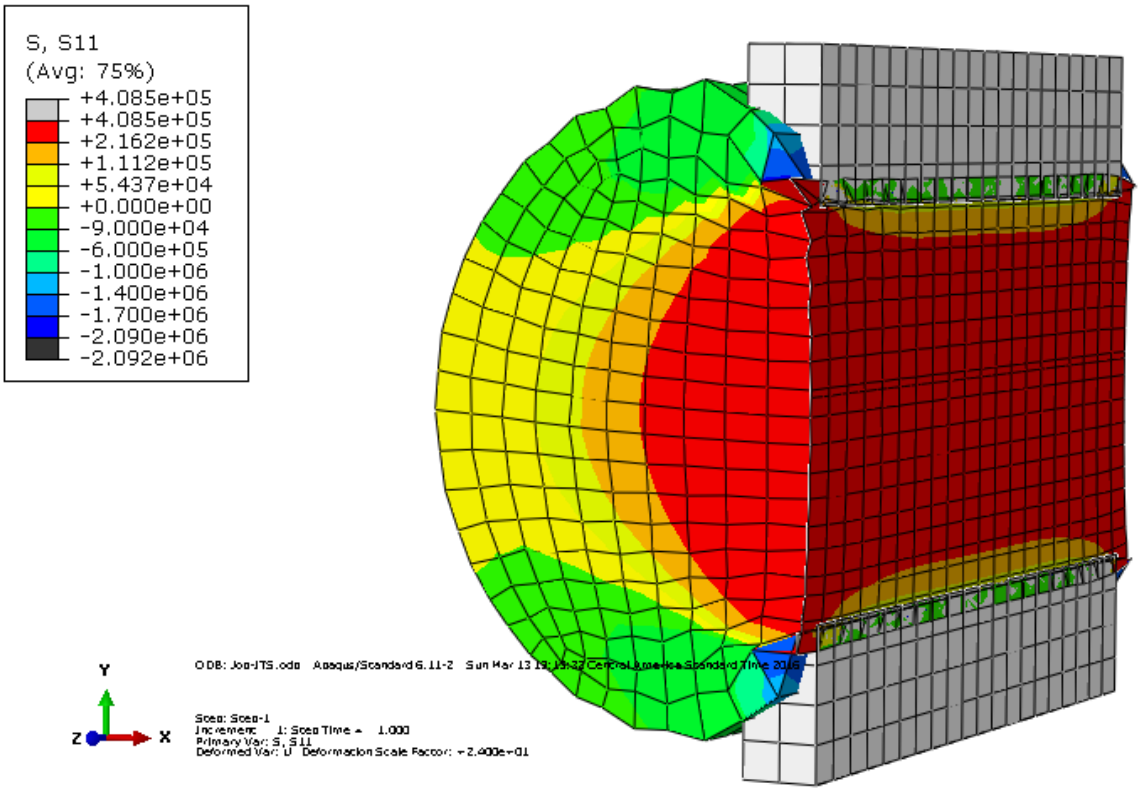

Figure 2.9 – Distribution of the Stresses in the longitudinal Cross-Section of the Specimen in the Indirect Diametrical Tensile Test

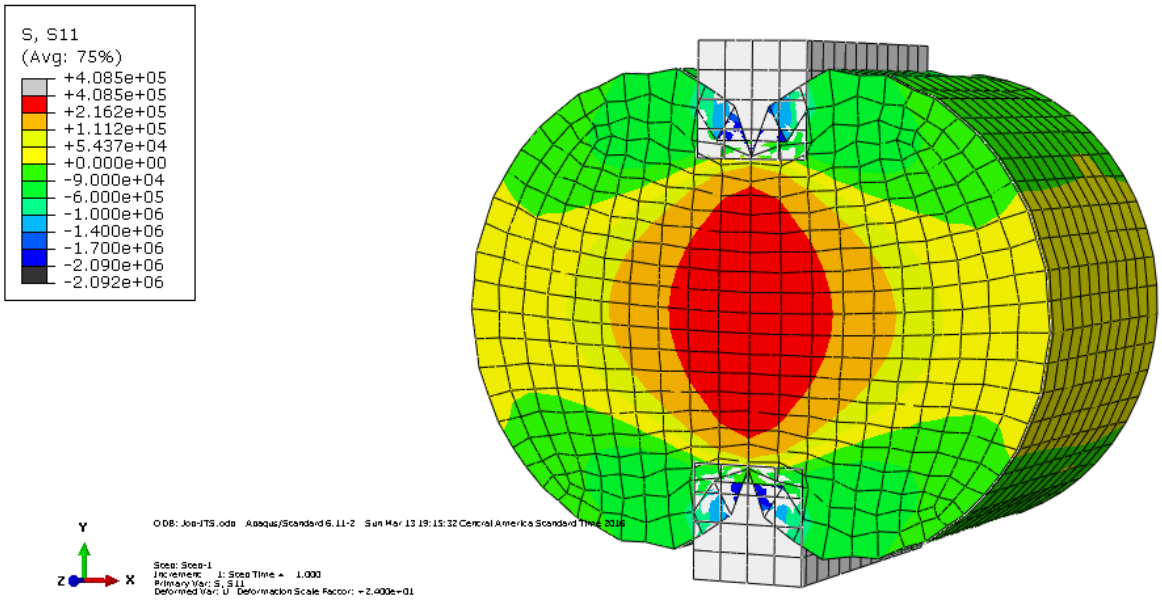

Figure 2.10 – Distribution of the Stresses in the Transverse Cross-Section of the Specimen in the Indirect Diametrical Tensile Test

Summary of the Major Points

This chapter provided details on the current state of practice to estimate the tensile behavior of the cementitious materials in the laboratory. Specifics of the third point beam test and indirect tensile test were discussed in this chapter. The disadvantages of the current state of the practice can be summarized as:

a. Practicality issues associated with specimen de-molding and handling of large beams in the laboratory for lightly stabilized materials.
b. Large sample size for four-point bending beam test 6 x6 x12 in (152 x 152 x 305 mm) and therefore the issues associated with the heavy weight of the beam for operators.
c. The bending beam test requires significantly larger amount of materials for testing in the laboratory.
d. Issues associated with the uniformity of compaction of the stabilized materials in the large beam specimen. Based on our experience the wall effect was evident in most of the stabilized samples.
e. The finite element analysis of bending beam test and IDT test revealed the systematic error associated with the linear stress distribution assumption for the calculation of the modulus of rupture in the bending beam test.

The theoretical issues and practical aspects of the third point beam test underscore the necessity of developing an alternative test method to effectively and efficiently provide an estimate of the tensile behavior of cementitious materials in the laboratory.

Chapter 3. Survey of Districts

Introduction

The use of soil stabilization for base layers with different percentage of cement is a common method among districts in Texas. The determination of a variety of materials for this research project was facilitated by the utilization of a short survey. There were 20 responses from 17 Districts with three Districts submitting multiple responses. In such cases, the responses were clarified and merged by contacting the Districts for further clarification. It is also worth mentioning that not all questions presented in the survey were answered completely by the Districts. The survey results are presented in this chapter.

Survey Results

Use of Portland cement as a stabilizer to improve the performance of the base layer

The seventeen Districts that responded to the survey answered how often the cement stabilization of base layers is used in their projects. The survey results presented in Figure 3.1 show that 11 districts responded "often" and 7 responded "sometimes." It is important to mention that the results clearly show that all districts are using cement stabilization for base layers. Figure 3.2 shows the number of projects that have been performed in the past five years or are scheduled for the future in each district. The chart in the figure shows that San Antonio has the highest amount of cement stabilized base layer incorporated projects, followed by Bryan, Paris, Fort Worth and Pharr.

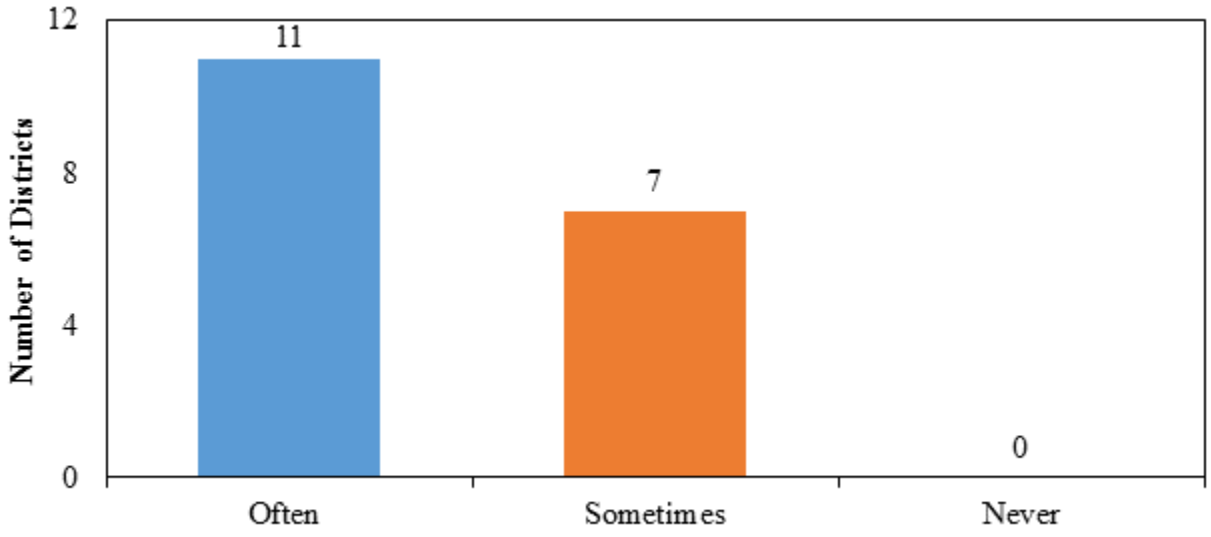

Figure 3.1 – Use of Portland cement to Stabilize Base Layers in the District

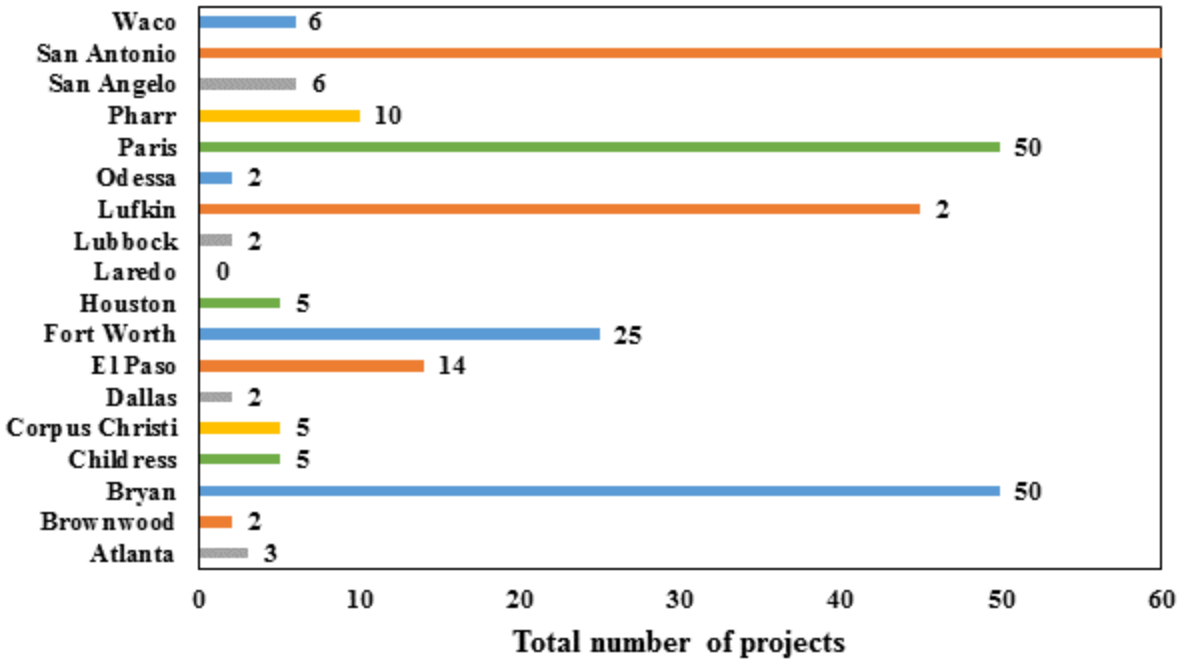

Figure 3.2 – Estimate of Projects that have been completed in the last 5 years or are scheduled in the near future

Determining the percentage of cement used in base stabilization

An important consideration in soil stabilization for base layers is the amount of cement typically used. Figure 3.3 demonstrates the range of percent of cement content for base layers to be from 2% to 5%. This range provides guidance to the amount of stabilization in the base layer that the researchers will consider in the experimental design for the laboratory portion of this project. The survey results show that 3% is the most common percentage of cement used. Figure 3.4 shows the range of stabilization used for each district.

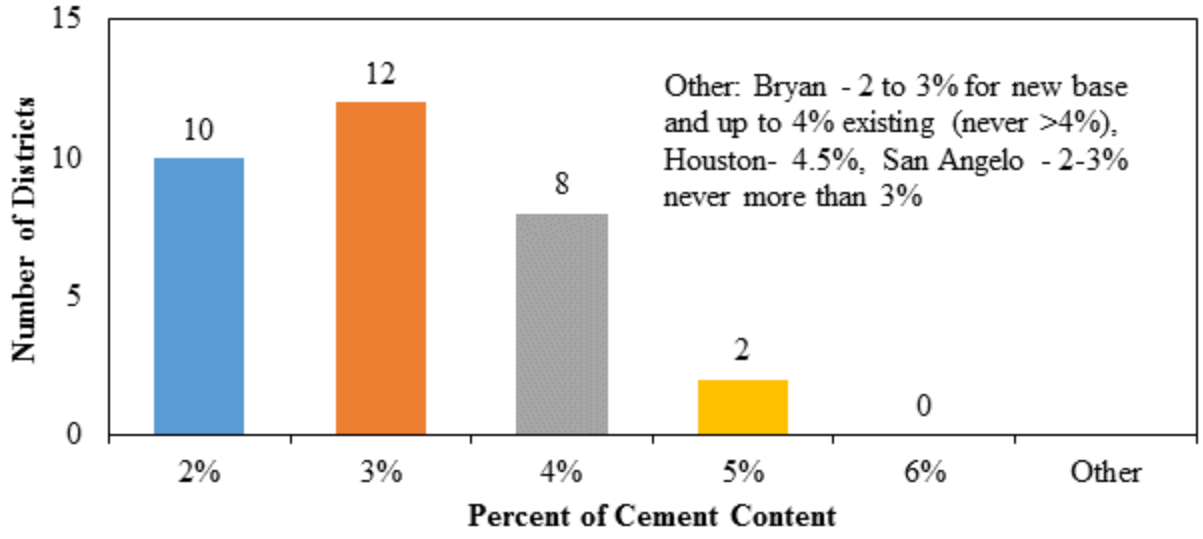

Figure 3.3 – Percentage of Cement Content Typically used for Stabilization of Base Layers

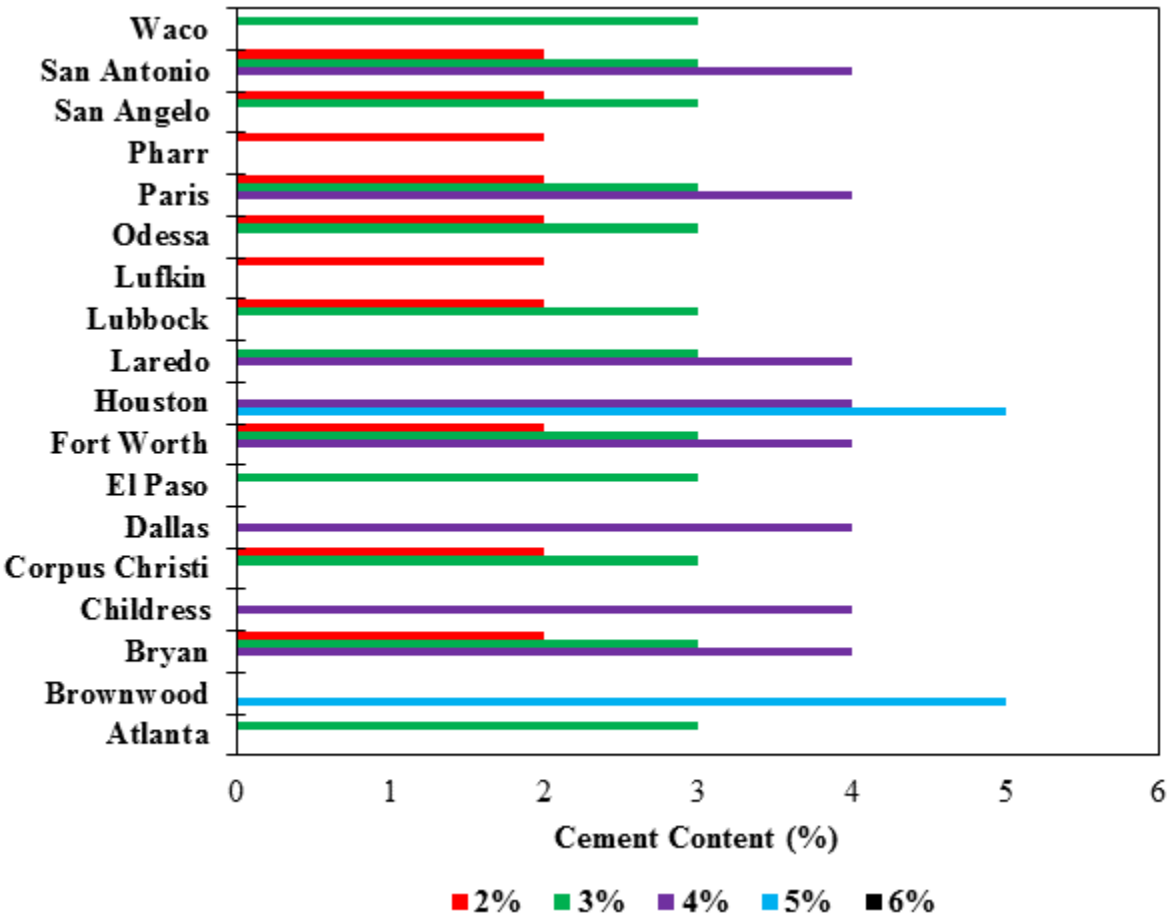

Figure 3.4 – Percentage of Cement Content Typically used for Stabilization by District

In terms of determination of the amount of cement added to the base layer, Figure 3.5 shows that the selection is based on laboratory testing followed by local experience from previous projects done. Ten of the seven districts responded that they follow a "strength based" requirement indicated in Figure 3.6. Several Districts such as El Paso, San Antonio, and Waco specify a strength requirement of 150 psi (1.03 MPa) for the Unconfined Compressive Strength (UCS) with 80% retained strength. Other Districts such as Atlanta, Fort Worth, Lubbock, Odessa, and Paris have a requirement of 300 psi (2.07 MPa) strength on UCS as criteria. Bryan has 210 psi (1.44 MPa) strength requirement at 85% retained strength. Additionally, Bryan District reported that they do not stabilize the base layer when the sulfate content is higher than 3000 ppm or the organic content is higher than 1%. This is important information that can be considered by those Districts dealing with high sulfate content in the soil. According to the collected responses from eighteen districts, most of the project use 2% to 4% cement to stabilize the base layers. Based on the feedback from the project technical team and the survey result, the amount of stabilizer used for this research were selected as 2%, 3%, 4%, and 5% to cover the range of conventional cement stabilization for base layers.

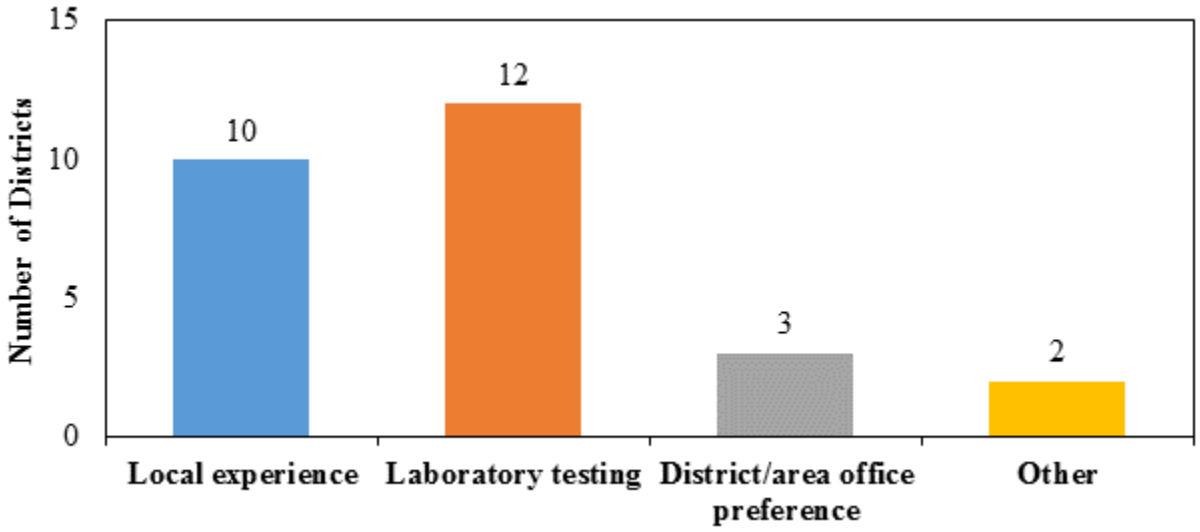

Figure 3.5 – Basis of Selection of the Percentage of Cement Content

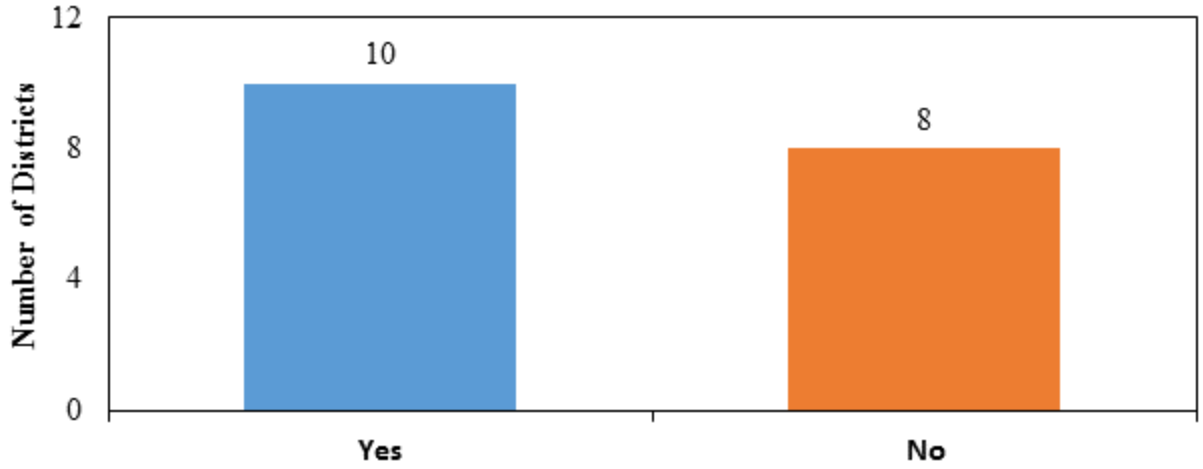

Figure 3.6 – Strength Requirements for Cement Stabilized Base Used by Districts

Aggregate type used in stabilized base layers

Another important factor particular to this research study was the type of aggregates and source materials used for cement stabilized base layers. As expected and shown in Figure 3.7, most districts use Limestone and gravel as the predominant aggregate type to construct base layers. Six of the surveyed districts reported that they utilize nonconventional aggregates such as Sandstone, Iron ore, recycled crushed concrete and Caliche. The quarries used by the District are listed in Table 3.1.

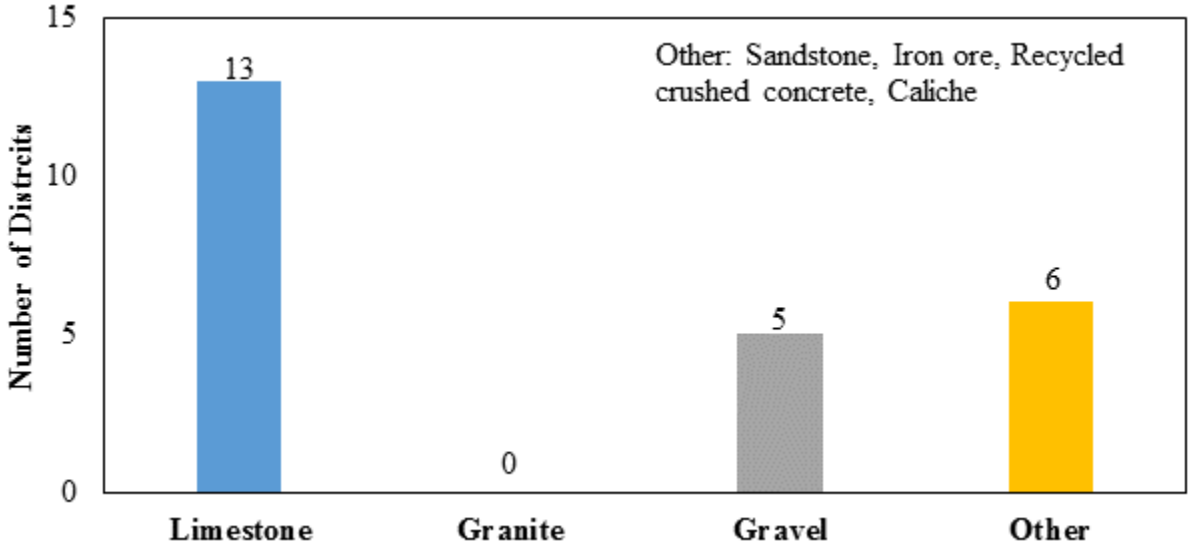

Figure 3.7 – Most Common Aggregate Types used for Cement Stabilized Base Layers

Table 3.1 – List of Districts and Quarries Used

District	Quarry
Atlanta	Sandstone & Iron Ore
Brownwood	Vulcan BWD & Eastland
Bryan	Usual Flexbase suppliers
Childress	Zack Burkett
Corpus Christi	Calica (Yucatan) Beckman
El Paso	Mckelligon Canyon or Ned Finney
Fort Worth	Bridgeport
Houston	Zack Burkett
Lubbock	Local quarries
Odessa	Local Pits
Lufkin	Hanson Perch Hill
Paris	Martin Marietta & Smith Buste Sandstone
Pharr	Fordyce Showers
San Angelo	Job Specific US83 Real Co.
San Antonio	Lonestar, Vulcan, Martin Marietta, S&J, Colorado Materials, South Texas Chapman's
Waco	A number of sources

Grade used in stabilizer base layers

Particle size distribution is another influencing factor for the performance of the stabilized aggregate layers. For this reason, the research team incorporated gradation requirements in the survey of the districts. Most of the responses were concentrated around Grade 4 and Grade 2 as the most commonly used gradation to construct the cement stabilized base layers as shown in Figure 3.8. Additionally Grade 5 was also reported to be used by a notable 4 districts.

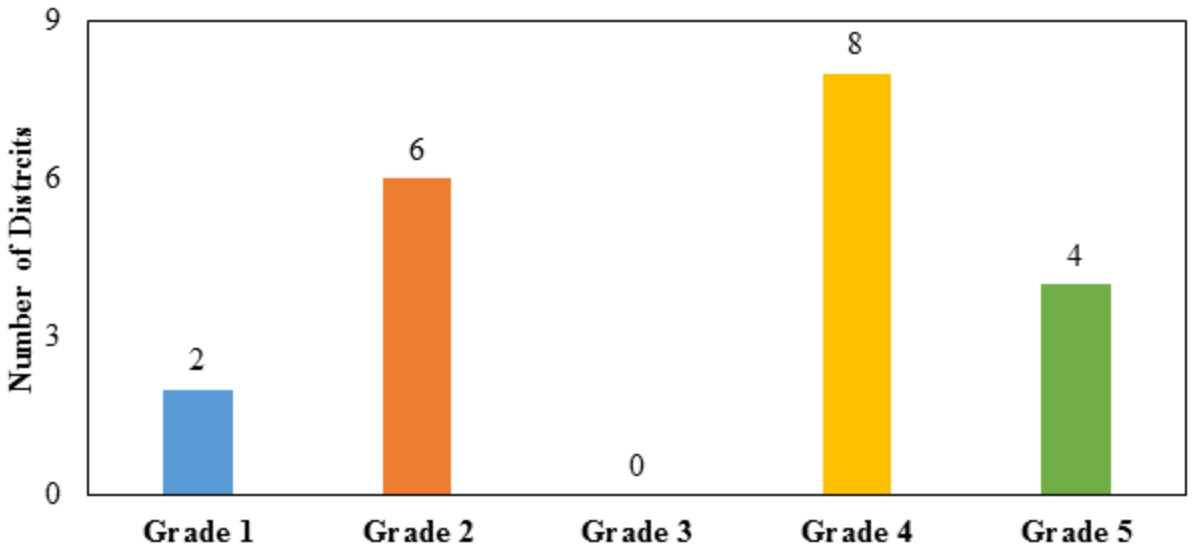

Figure 3.8 – Grade Selected as per Item 275 that is Most Frequently used for Cement Stabilized Base Layers

Materials selection

The following criteria were considered for the selection of the aggregate types/sources based on the analysis of the survey results:

- ***Number of projects*** reported to be completed in the coming five years by districts. San Antonio, being the district with the highest number of underway projects was thus incorporated in the test matrix.
- ***Type of aggregates***, such as limestone, gravel and sandstone, were considered by the research team in the test matrix to account for the influence of mineralogical properties of aggregate on the pozzolanic reactions during the cement stabilization process. Therefore, gravel and sandstone materials sourced from Pharr and Paris Districts respectively were included in the experiment design. Additionally, limestone materials sourced from El Paso and San Antonio were incorporated in the experiment matrix.
- ***Geographical distribution*** of the districts was also considered as a supplementary e=decision parameter. This criterion was considered to account for the diversity of the lithological properties and environmental conditions across the state of Texas. As indicated in Figure 3.9, materials from El Paso, Pharr, San Antonio, and Paris districts were incorporated in the experiment design. Notable, limestone materials sourced from El Paso and San Antonio were selected in this research. Based on our previous experience the physical and engineering properties of the El Paso and San Antonio materials are significantly different, therefore inclusion of the two limestone materials will improve the generalization aspect of the models in this project. The geographical distribution is shown in Figure 3.9 along with a geographical map.

Based on the analysis of the survey responses, direct contact with several districts, and feedback from the project technical team, the aggregate type and aggregate sources selected for this research are presented in Table 3.2.

Figure 3.9 – Geographical Distribution of Selected Aggregate Sources

Summary of the Major Points

The research team distributed a survey among the districts to better understand the current state of the practice for the characterization of the tensile strength of the materials in the laboratory. Based on the analyzed data and discussions with the project advisors, four different aggregate types, namely El Paso limestone, Pharr gravel, Paris Sandstone and San Antonio limestone were selected in the experiment matrix. Based on the collected responses one gradation, and five levels of cement contents were incorporated in the experiment design. Table 3.2 provides this information. The information collected on the policies for the selection of the stabilizer contents revealed the importance of developing a practical laboratory test, in conjunction with the unconfined compressive strength test, to characterize the mechanical behavior of stabilized materials for use in pavement foundations.

Table 3.2 – Determination of Materials and Cement Content

Material Selected	Range of Cement Selected	Grade Selected
El Paso (Limestone)	2%-5%	Grade 4
San Antonio (Limestone)	2%-5%	Grade 4
Pharr (Gravel)	2%-5%	Grade 4
Paris (Sandstone)	2%-5%	Grade 4

Chapter 4. Development of the Experiment Matrix

Introduction

This chapter pertains to the selection of the materials, gradation, cement contents, and the rationale for the inclusion of the laboratory tests in the experiment design. The selection of the aggregates was based on the diversification of the aggregate type, district activity (number of active projects), and geographical spread of the districts. The selection of particle size distribution and cement contents were based on the collected responses discussed in previous chapter. This section provides the laboratory procedures and condition/curing methods undertaken in our research approach.

Experiment Design

Table 4.1 represents the experiment matrix developed in this research effort. Four different aggregate materials, namely San Antonio limestone, Pharr gravel, El Paso limestone, and Paris sandstone were incorporated in this research study. One gradation and four levels of cement content were used in this effort. Based on the discussions with the technical advisory panel, two curing conditions were incorporated to study the influence of the moisture ingress on the mechanical performance of the stabilized materials.

Table 4.1 – **Laboratory Tests and Materials Selection**

	Aggregate Type															
	El Paso Limestone				Phar Gravel				Paris Sandstone				San Antonio Limestone			
	Cement Content (%)															
	2%	3%	4%	5%	2%	3%	4%	5%	2%	3%	4%	5%	2%	3%	4%	5%
Unconfined Compressive Strength (UCS)	√	√	√	√	√	√	√	√	√	√	√	√	√	√	√	√
Submaximal Test	√	√	√	√	√	√	√	√	√	√	√	√	√	√	√	√
Static Indirect Diametrical Tensile Test (S-IDT)	√	√	√	√	√	√	√	√	√	√	√	√	√	√	√	√
Dynamic Indirect Diametrical Tensile Test (D-IDT)	√	√	√	√	√	√	√	√	√	√	√	√	√	√	√	√
Dilective Value Test	√	√	√	√	√	√	√	√	√	√	√	√	√	√	√	√
Free-Free Resonant Coloumn (FFRC)	√	√	√	√	√	√	√	√	√	√	√	√	√	√	√	√

More details on the moisture susceptibility protocols will be provided in this chapter. Table 4.2 provides the details of the experiment design undertaken this study. A total of 570 specimens, considering the replicates, were prepared and subjected to various laboratory tests.

Table 4.2 – Experiment Design

			Aggregate Type															
			El Paso Limestone				***San Antonio*** Limestone				***Pharr*** Gravel				***Paris*** Sandstone			
			Cement Content (%)															
			2	3	4	5	2	3	4	5	2	3	4	5	2	3	4	5
7-Day Moist Cured	**UCS Test**		√	√	√	√	√	√	√	√	√	√	√	√	√	√	√	√
	Submaximal Modulus	@ 20% UCS	√	√	√	√	√	√	√	√	√	√	√	√	√	√	√	√
		@ 40% UCS	√	√	√	√	√	√	√	√	√	√	√	√	√	√	√	√
		@ 60% UCS	√	√	√	√	√	√	√	√	√	√	√	√	√	√	√	√
	IDT Test- Static		√	√	√	√	√	√	√	√	√	√	√	√	√	√	√	√
	IDT Test-Cyclic	@ 20% Strength	√	√	√	√	√	√	√	√	√	√	√	√	√	√	√	√
		@ 40% Strength	√	√	√	√	√	√	√	√	√	√	√	√	√	√	√	√
		@ 60% Strength	√	√	√	√	√	√	√	√	√	√	√	√	√	√	√	√
10-Day TST	**UCS Test**		√	√	√	√	√	√	√	√	√	√	√	√	√	√	√	√
	Submaximal Modulus	@ 20% UCS	√	√	√	√	√	√	√	√	√	√	√	√	√	√	√	√
		@ 40% UCS	√	√	√	√	√	√	√	√	√	√	√	√	√	√	√	√
		@ 60% UCS	√	√	√	√	√	√	√	√	√	√	√	√	√	√	√	√
	IDT Test- Static		√	√	√	√	√	√	√	√	√	√	√	√	√	√	√	√
	IDT Test-Cyclic	@ 20% Strength	√	√	√	√	√	√	√	√	√	√	√	√	√	√	√	√
		@ 40% Strength	√	√	√	√	√	√	√	√	√	√	√	√	√	√	√	√
		@ 60% Strength	√	√	√	√	√	√	√	√	√	√	√	√	√	√	√	√

Specimen Preparation

The research team performed dry sieve analysis to grade the aggregates based on the desired particle size distribution in the experiment design. Subsequently Atterberg Limits of the fine portion of the mixes were determined.

Initially, the unstabilized specimens were prepared in accordance with Tex-101-E part II for the moisture-density test. The M-D curves were established based on the Tex-113-E specification. The research team followed Tex-120-E specification to adjust for the molding moisture content with incremental increase of the cement in the mixes. The specimens were compacted using a 10-lb. hammer and 18-in. drop.

Two sets of sample sizes were incorporated in this study. The dimensions of the specimen for the UCS, Submaximal Modulus, and Static UCS was 6 x 12 in (152 x 305 mm) and the ones for the Static IDT and Cyclic IDT were dimensions of 6 x 4.5 in (152 x 114 mm).Specimens with dimensions of 6 x 4.5 in. were compacted in 3 layers with 50 blows per layer. Specimens with

dimension of 6 x 12 in. were compacted in 6 layers by Energy (750 ft-lb). Figure 4.1 shows the stepwise procedure of the sample preparation modification before compaction.

Figure 4.1 – Sample preparation modification

Specimen Conditioning

In the interest of adopting a common language to address the conditioning process of the specimen and moisture susceptibility of the stabilized materials, the following terminologies are uniformly used in this report:

- **7-Day Moist Cured**: this procedure pertains to the placement of the prepared specimen in the temperature-controlled chamber with at least 95% relative humidity for the duration of seven days. Dielectric and seismic modulus values were determined after specimen preparation (first day) and after the 7th day prior to subjecting to destructive laboratory tests, such as UCS or IDT tests.
- **10-Day Capillary Soak -Tube Suction Test (TST) Procedure:** According to the specification procedure Tex-144-E (draft) the prepared specimen were placed on porous stones in a tub of water at ambient temperature and subjected to capillary action for the duration of ten days prior to laboratory testing. Dielectric and seismic modulus values were determined every day ten consecutive days. The specimens were in turn subjected to destructive laboratory tests according to the experiment design. This procedure provides information on the affinity of the unbound moisture to travel and reach to the top of the sample. The dielectric value information when juxtaposed on daily progression (or degradation) of the seismic modulus values, provided an indication of the moisture susceptibility of the stabilized materials.

Material Testing

The following laboratory tests were incorporated in the experiment design to fully characterize the influence of aggregate type, stabilizer content and curing effect of the mechanical performance of the cement stabilized specimen.

Unconfined Compressive Strength (UCS) Test

The UCS test (Figure 4.2) was performed on all permutations of the experiment design to determine the compressive strength of the stabilized materials at different cement contents. UCS is a strain-controlled test at an imposed strain rate of 2% strain/min. Two sets of replicates of the 7-day moist-cured and 10-day capillary soak specimen were subjected to the UCS test. The results were used to identify the unconfined compressive strength, nature of stress-strain curves, variation of the degree of nonlinearity of stabilized materials with incremental increase of cement, and ultimately different measures of modulus such as tangent modulus and secant modulus at peak strength. This information was incorporated in the aggregate database for further post processing and trend analysis of the data. Figure 4.3 presents the flow chart that the research team followed for the execution of the UC strength test.

Figure 4.2 – Unconfined Compressive Strength Test Setup

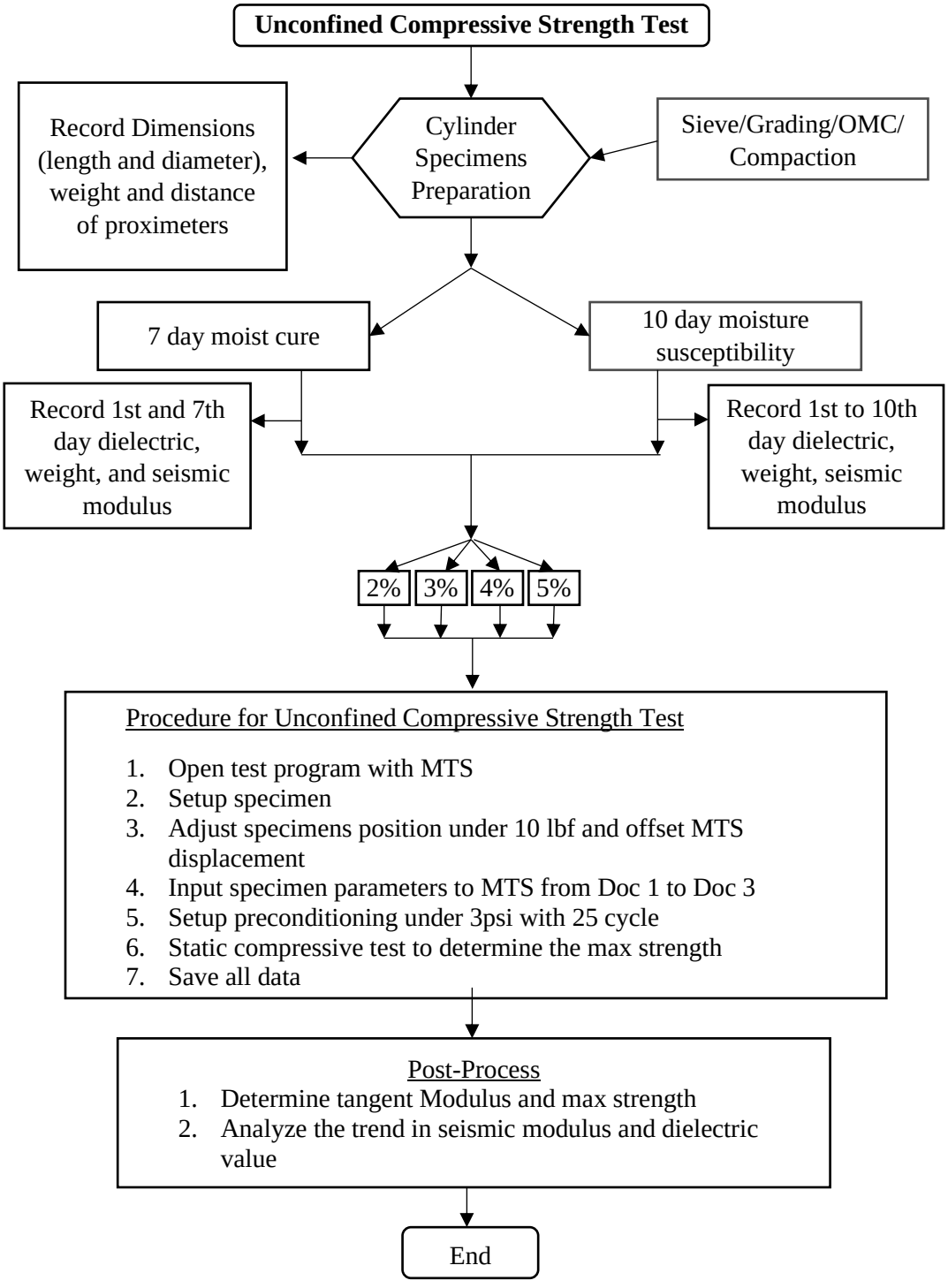

Figure 4.3 – Unconfined Compressive Strength Test Procedure

Submaximal Modulus Test

The submaximal modulus test was performed on all 6 x 12 in (152 x 305 mm) specimens in the laboratory experiment matrix. This test was performed on both seven-day moist-cured specimens as well as aggregate systems subjected to capillary soak for ten consecutive days. The results from the UCS test were the precursor to the repeated load submaximal modulus test. After the determinations of the unconfined compressive strength of two replicates of each variant, a fraction of the average of the UCS strength was applied for 5000 load cycles. Three levels of 20%, 40% and 60% of UCS strength were selected for this research effort to characterize both the resilient behavior and the permanent deformation under axial cyclic compressive loads. Vertical deformations were recorded using four proximeters attached to the specimens as illustrated in Figure 4.4. Figure 4.5 shows the schematic representation of the specimen set up for the execution of the submaximal modulus test. Figure 4.6 provides the flow chart for sample preparation, conditioning and execution of the submaximal modulus test.

Figure 4.4 – Submaximal Modulus Test Set Up

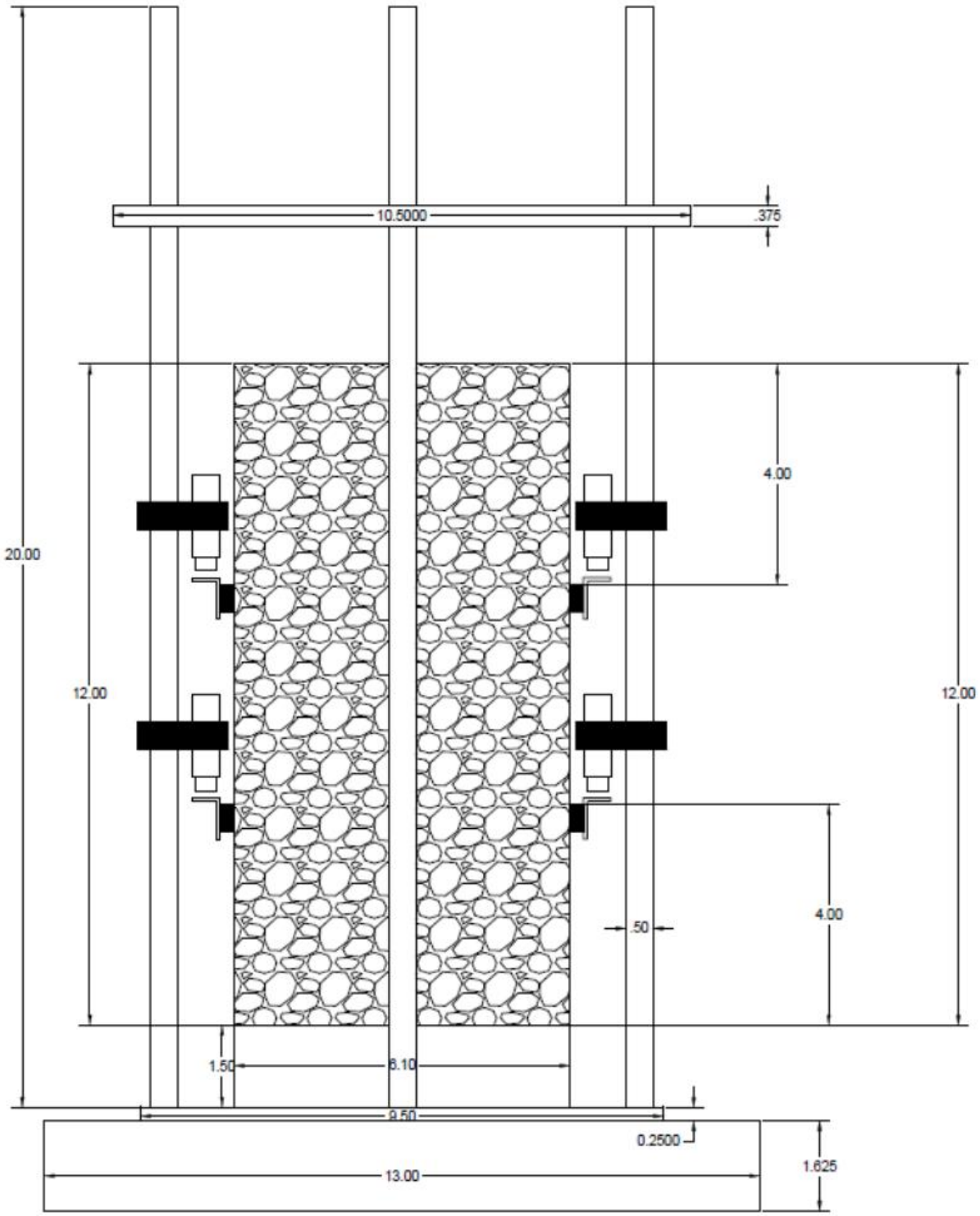

Figure 4.5 – Submaximal Dimensions

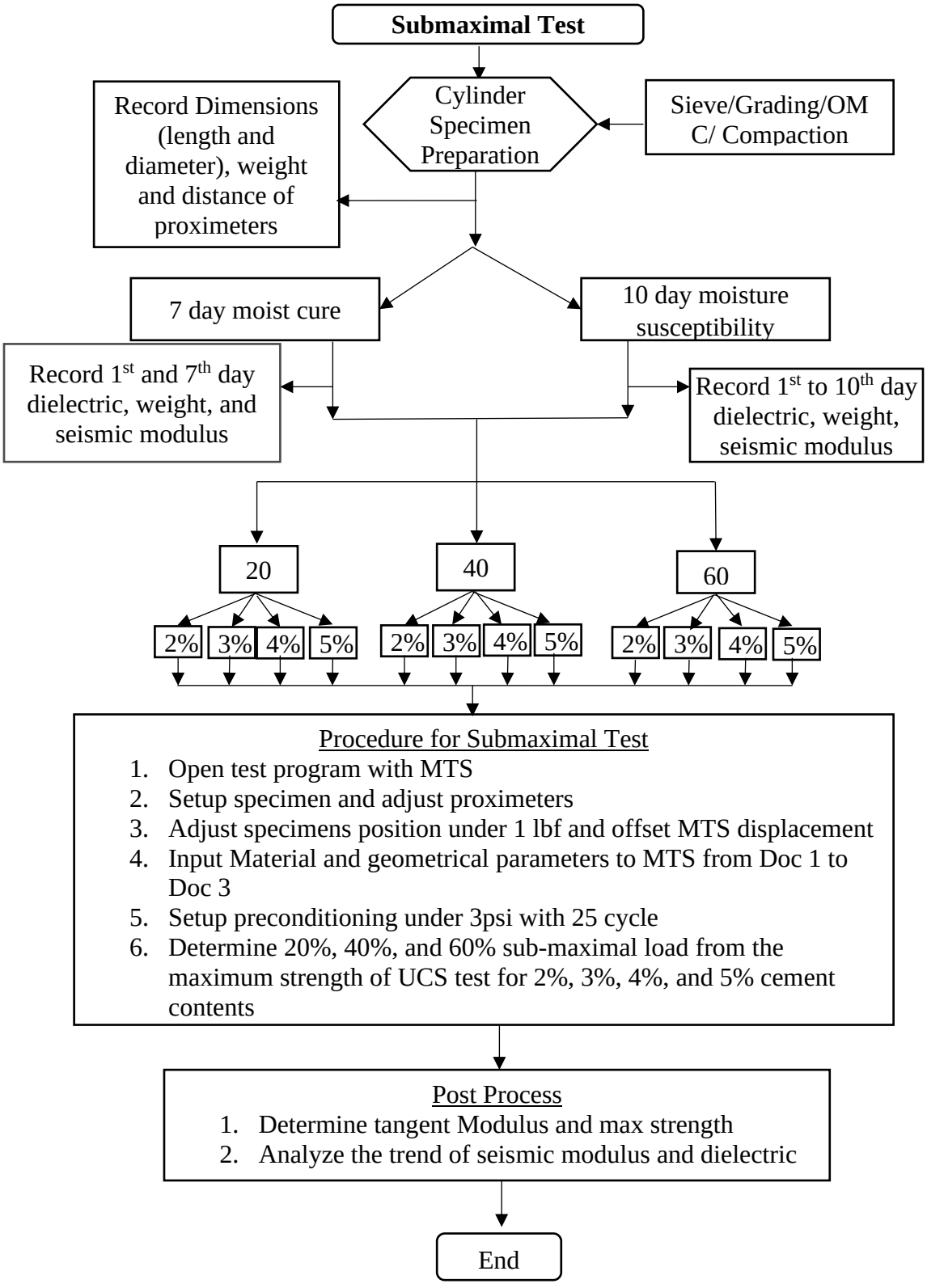

Figure 4.6 – Submaximal Modulus Test Procedure

Static Indirect Diametrical Tensile (IDT) test

The tensile behavior of stabilized materials was characterized using a strain-controlled Indirect Diametrical Tensile (IDT) test. A strain rate of 1 mm/min was imposed on the 4.5 x 6 in (114 x 152 mm) specimen to induce mid-span cracking or failure of the material. Similar to previous laboratory tests, two types of conditioning of specimen was considered to study the deleterious effect of moisture intrusion on the tensile strength of the stabilized materials. This provides valuable insights on the affinity of different aggregate types to hold moisture and perform differently in the field. Influence of moisture of the specimen IDT is a strain-controlled type test that will be performed at an imposed strain rate until the specimens fail. Figure 4.7 shows the specimen set up for the execution of the static IDT test. The research team followed the flowchart provided in Figure 4.8 for the static IDT test.

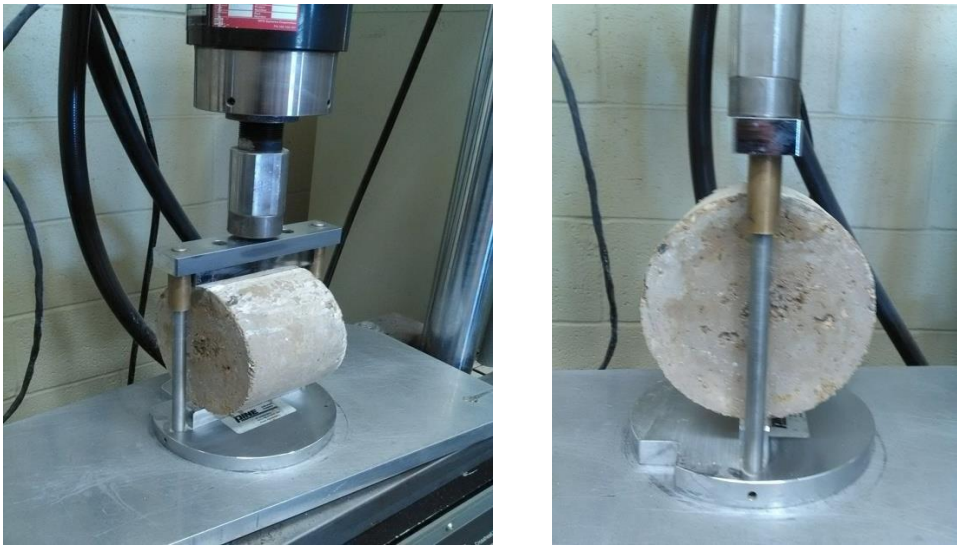

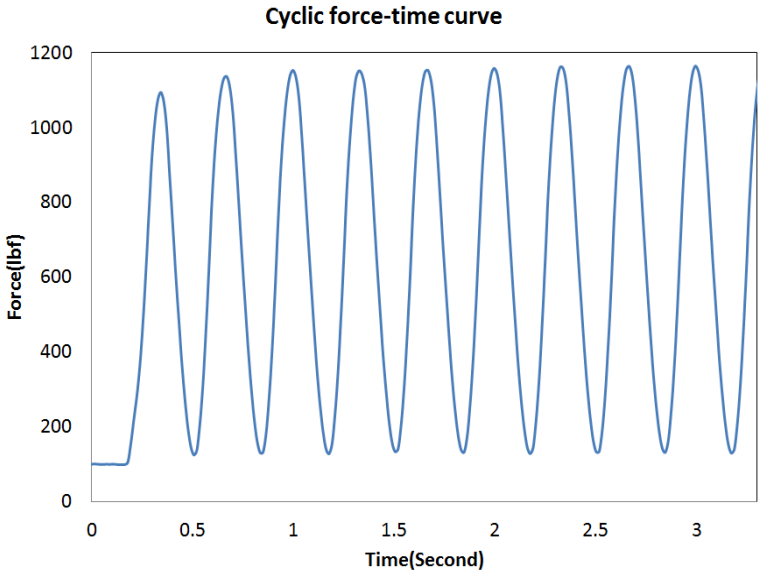

Figure 4.7 – Static IDT Test Set Up

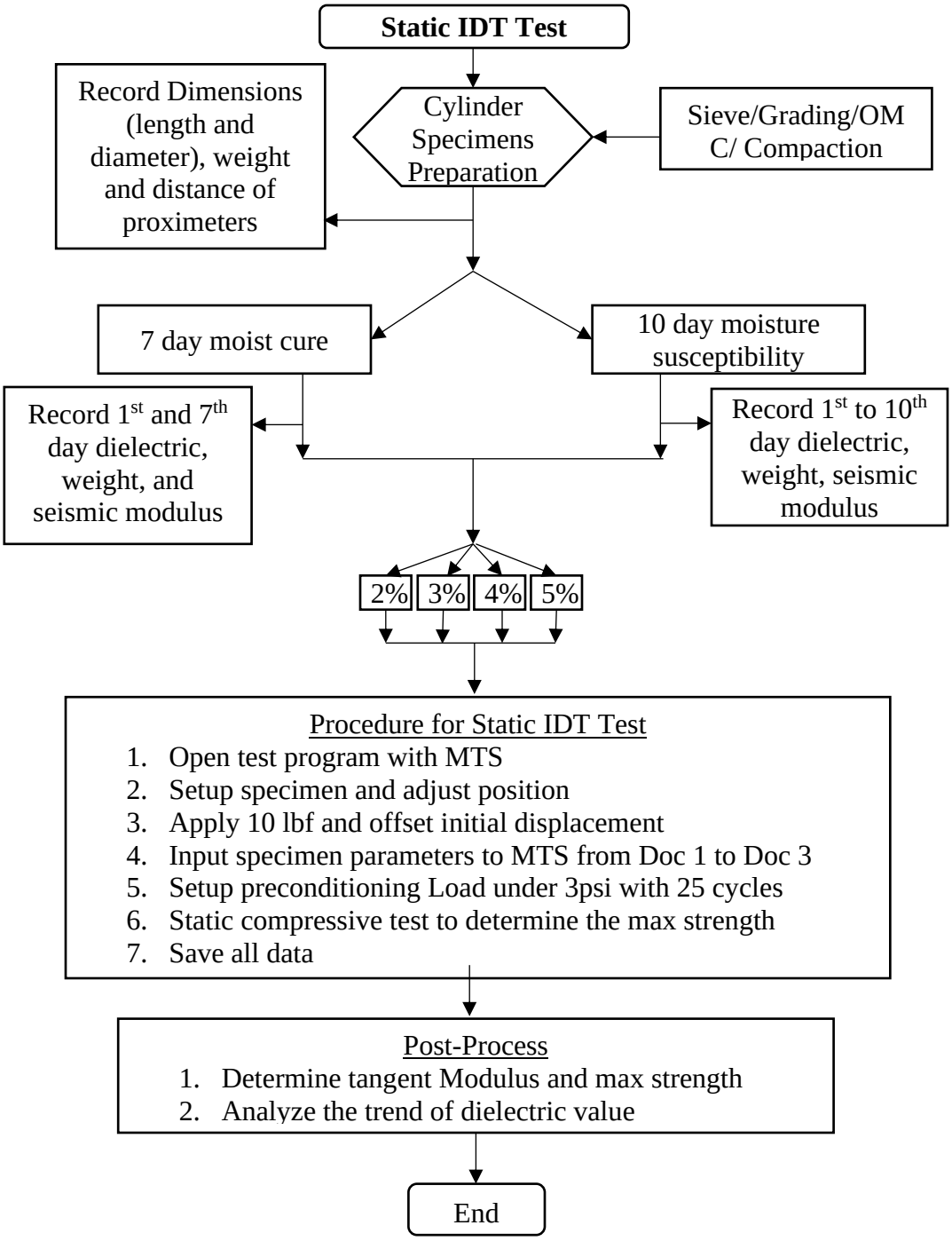

Figure 4.8 – Static Indirect Diametrical Test (IDT) Procedure

Cyclic Indirect Diametrical Tensile (IDT) Test

A new variation of the IDT was developed in this research to the study the performance of the cement stabilized materials subjected to repeated load in tension. Several prototypes and bonding agents were used to arrive at a reliable and repeatable test protocol. Similar to the concept

presented in the submaximal modulus test, the static IDT test results were used as a benchmark to determine the loading protocol in the dynamic IDT test. In other words, initially the IDT strength of each permutation of the experiment design was determined using the static IDT test. Subsequently a percentage of the static IDT strength was applied for 50,000 load cycles. The selected levels of the cyclic loads were 20%, 40% and 60% of the static IDT strength in this research effort. The tests were performed on two replicates for each moisture condition method. Figure 4.9 shows the specimen set up for the execution of the dynamic IDT test. The research team followed the flowchart presented in Figure 4.10 for the aforementioned test. Figure 4.11 represents the test set up, brackets arrangements, and the locations of the LVDTs for the accurate measurement of specimen deformations.

Figure 4.9 – Dynamic IDT Test Set Up

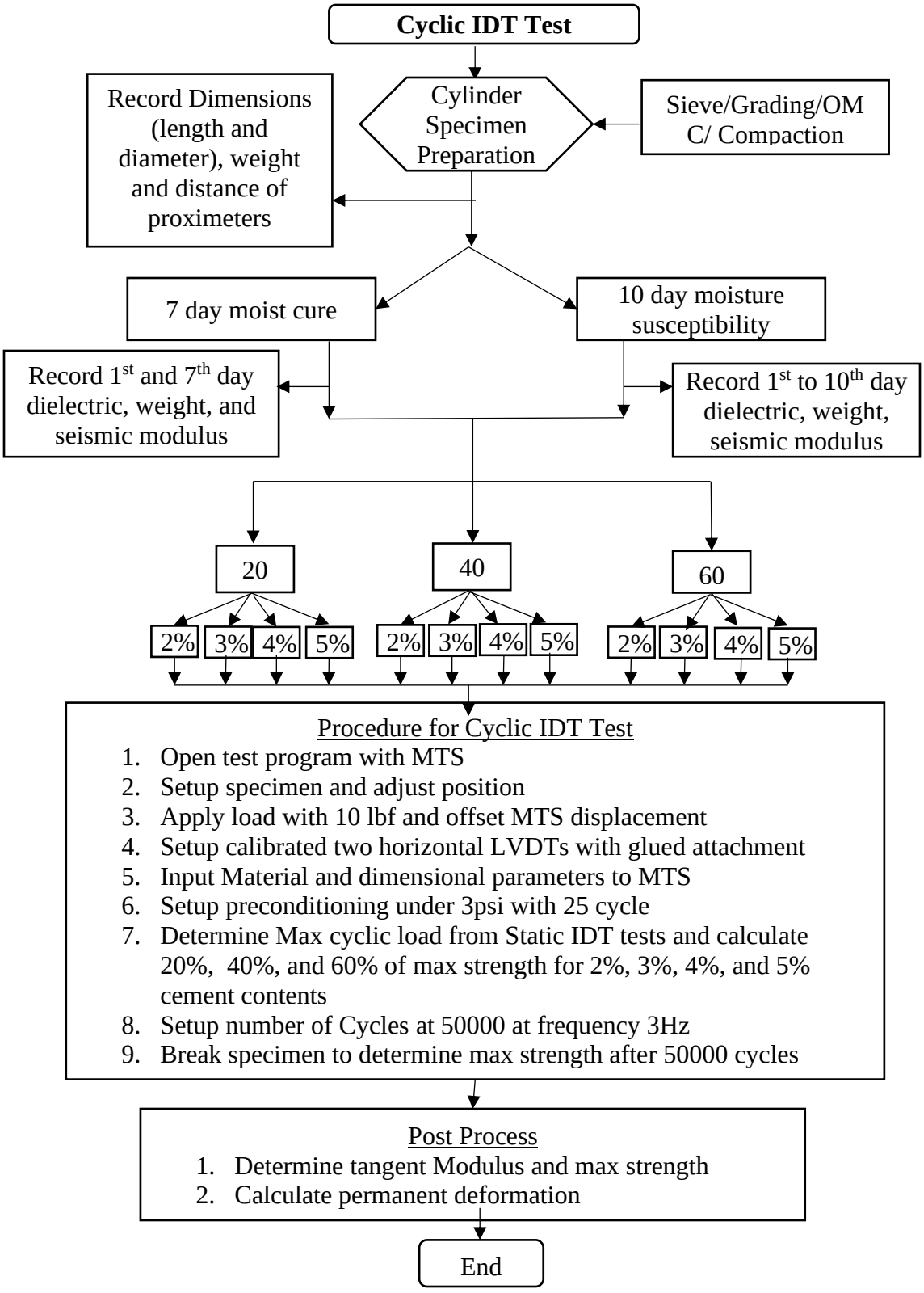

Figure 4.10 – **Dynamic Indirect Diametrical Test (IDT) Procedure**

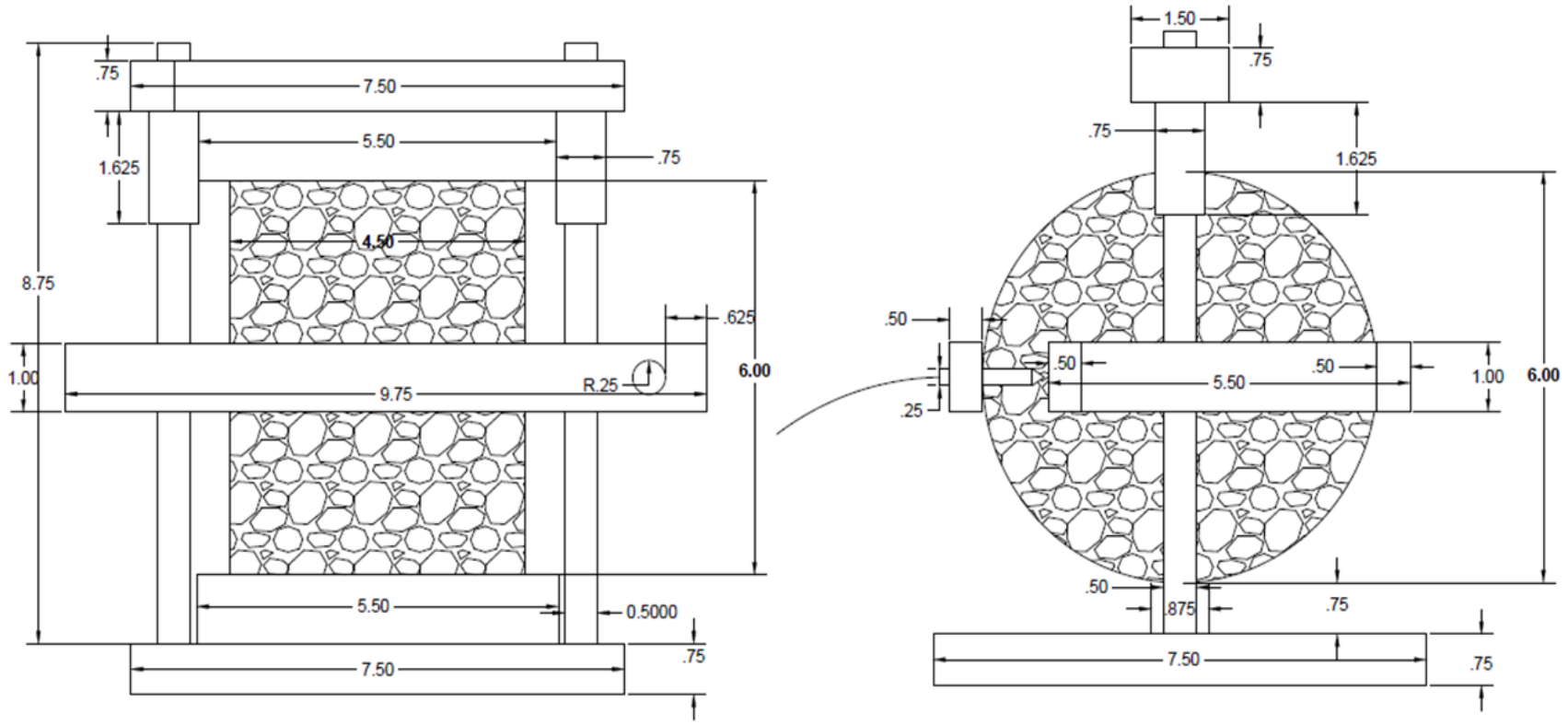

(a) (b)

Figure 4.11 – Indirect Diametrical Test Setup (a) Front View (b) Side View

Moisture Susceptibility Test

Moisture susceptibility of the stabilized materials was characterized by tracking the variations of the dielectric constants using a Rainbow dielectric constant meter in the laboratory. The change in the dielectric values of the stabilized specimen, when subjected to external moisture, such as environmental chamber or capillary soak, is an indication of the change in the available moisture in the pore structure. Therefore, monitoring the dielectric values at the top of the specimen can provide valuable information on the affinity of the specimen to transport moisture through the air void structure.

Figure 4.12 presents the dielectric test setup in the laboratory. The dielectric values of the TST specimen were measured every day for 10 consecutive days at five different points at the top of the specimen. The locations of measurements are presented in Figure 4.12-a. The dielectric meter was calibrated prior to each reading, as shown in Figure 4.12-b. The laboratory research team paid careful attention to perform the measurements at the same exact locations at each interval. The average values of the five measurements were then calculated and reported as the representative dielectric value for each variant of the experiment design. Additionally, the seismic modulus tests were performed every day during the course of ten days to mechanistically characterize the effect of moisture intrusion on stiffness properties of stabilized aggregate systems.

Figure 4.12 – Dielectric Value Test Setup

Seismic Modulus Test

The Free-Free Resonant Column (FFRC) test was adopted based on Tex-148-E (draft) procedure to provide measures of seismic modulus. Resonant frequencies were identified and small strain modulus values of the stabilized systems were determined using the principle of wave propagation. Figure 4.13 demonstrates the process of FFRC tests in this study.

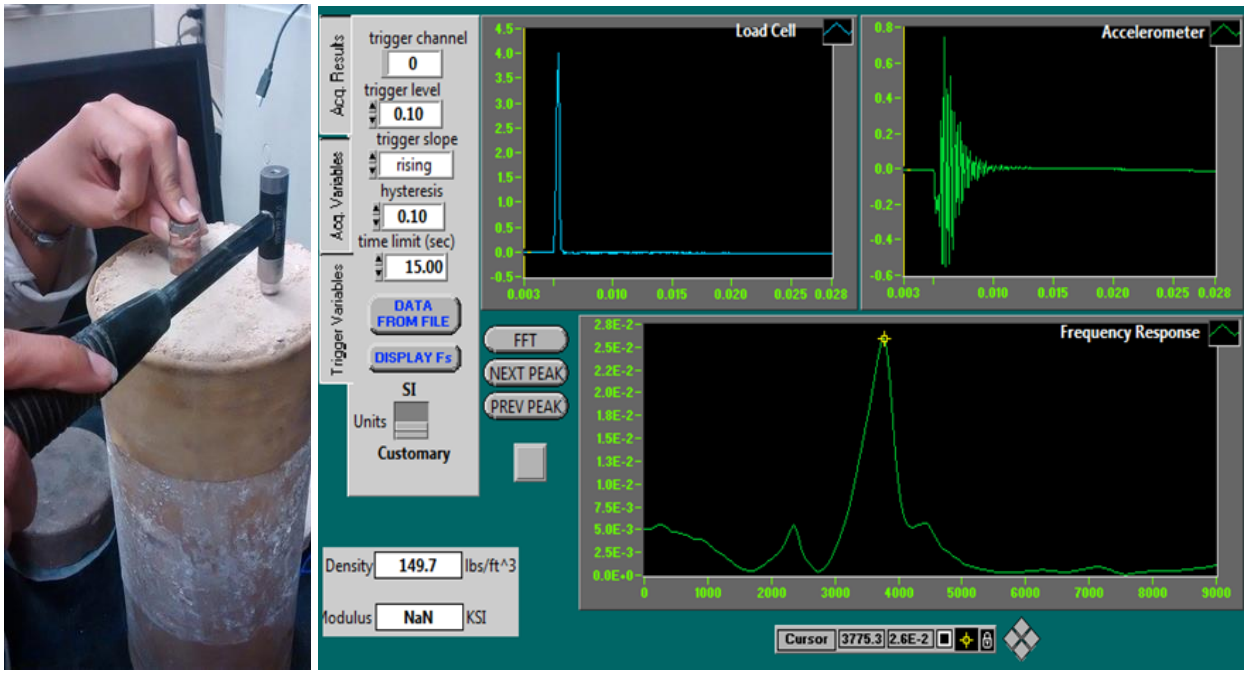

Figure 4.13 – FFRC Test Setup and Software Output

Chapter 5. Laboratory Test Results and Discussions

Introduction

This chapter provides information on the laboratory test results performed according to the experiment design outlined in chapter 3. The main focus of this chapter is to present laboratory performance test results of cement stabilized materials with different lithology and stabilizer content. Laboratory results pertaining to unconfined compressive strength, submaximal modulus, static indirect diametrical test, cyclic indirect diametrical test, seismic modulus, and dielectric test are presented in this chapter.

Gradations

Based on the survey of the districts, the particle size distributions adopted for this research effort were based on the Item 247 grade 4. Figure 5.1 represents the particle size for each material.

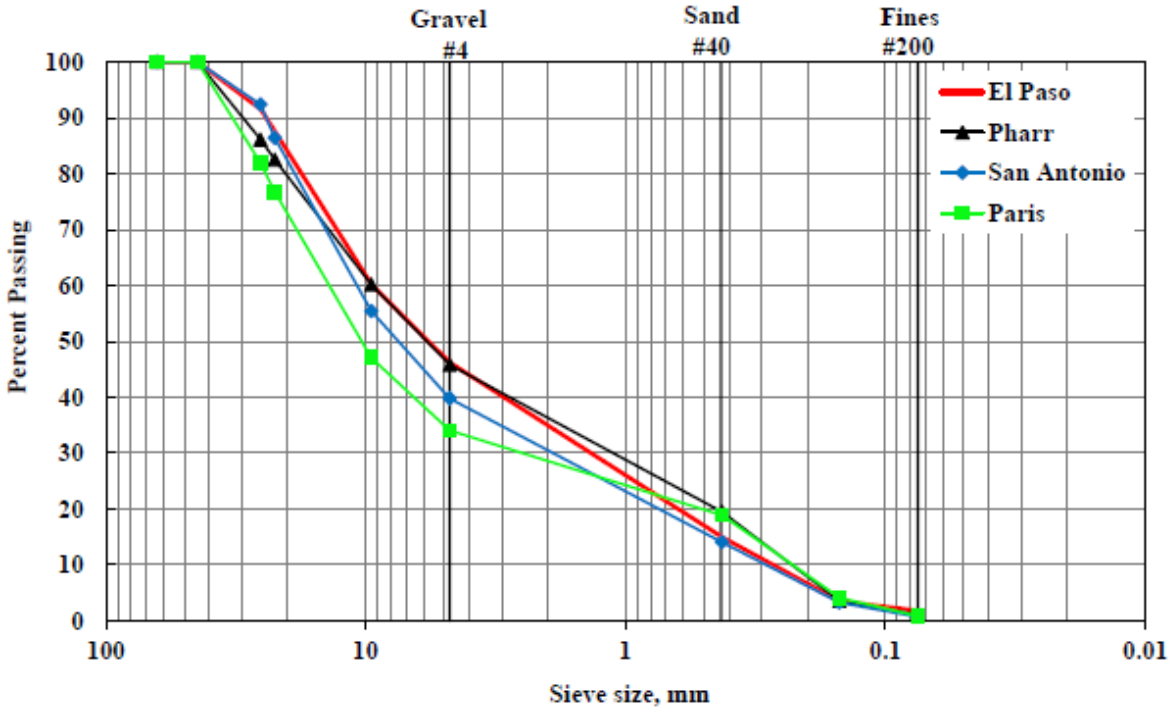

Figure 5.1 – Particle Size Distributions of Aggregate Materials

Moisture-Density Curves

Graded virgin aggregate materials were compacted using Tex-113-E procedure to prepare cylindrical specimen. Figure 5.2 shows the MD curves of moisture density test based on Tex-113-E for the graded aggregates without the stabilizer. Table 5.1 provides a summary of the results.

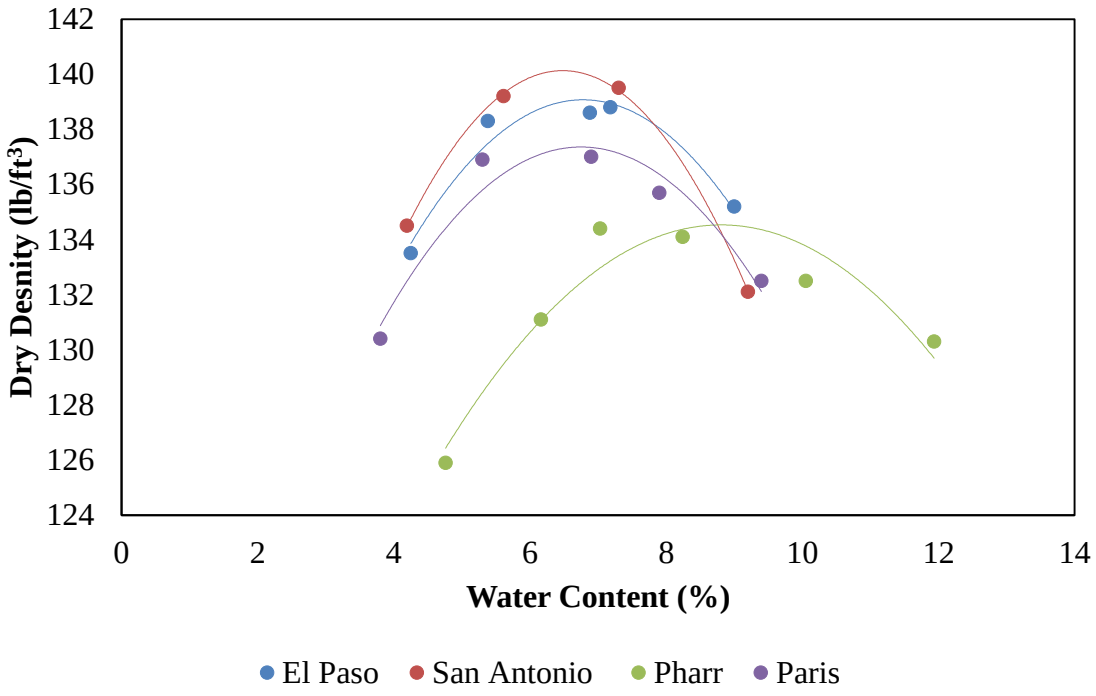

Figure 5.2 – MD Curves

Table 5.1 – Moisture-Density Test Results

Material	OMC (%)	Max Dry Density (lb/ft^3)
El Paso	6.8	139.1
San Antonio	6.5	140.1
Pharr	8.8	134.5
Paris	6.8	137.4

Unconfined Compressive Strength Test (UCS Test)

The UC strength test was performed on 6 x 12 in (152 x 305 mm) stabilized specimens until the specimen reached the pre-determined criteria for failure. For the execution of the UC strength test four cement contents, namely 2%, 3%, 4%, and 5% were added to the virgin materials and the water contents were adjusted based on the recommendation of Tex-120-E procedure to prepare 6 x 12 in (152 x 305 mm) stabilized cylindrical specimens. The specimens were subjected to two different curing conditions. One condition consisted of 7-day moist cured in a moisture room with at least 95% of relative humidity. Also, the specimens were subjected to 10-day capillary soak at ambient temperature to characterize the moisture susceptibility of the stabilized aggregate systems. The dialectic constant at the first and last days were measured as an indication of the affinity of the aggregate systems to hold moisture. The seismic modulus test was also performed on the stabilized specimen and results were exported to the aggregate feature database for further trend analysis and post processing of the laboratory test data.

Figure 5.3 show the stress-strain behavior of Paris materials subjected to strain-controlled UCS test. The results show the incremental increase in the cement content has significantly improved the strength properties of the stabilized mixes. In addition to the stress at failure or the strength of the material, several measures of modulus such as tangent modulus and secant modulus at failure can be extracted from the stress-strain curves from the UCS test. The tangent modulus can serve an indication of the small-strain behavior of the stabilized material. As depicted in Figure 5.3, the tangent modulus is also influenced by the increasing cement contents in the mix. Figure 5.4 presents the UCS results for the same Paris materials when subjected to 10-day capillary soak condition. Similar trends can be observed with increasing cement contents in the mixes.

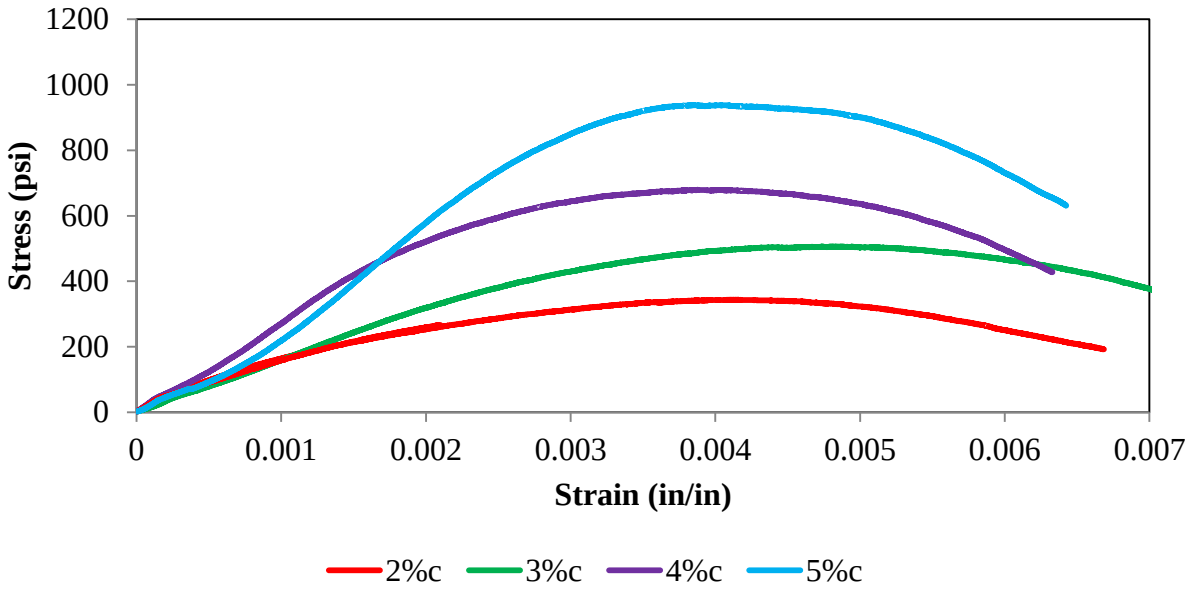

Figure 5.3 – UCS Results for Paris Materials for 7-day Moist Cured Samples

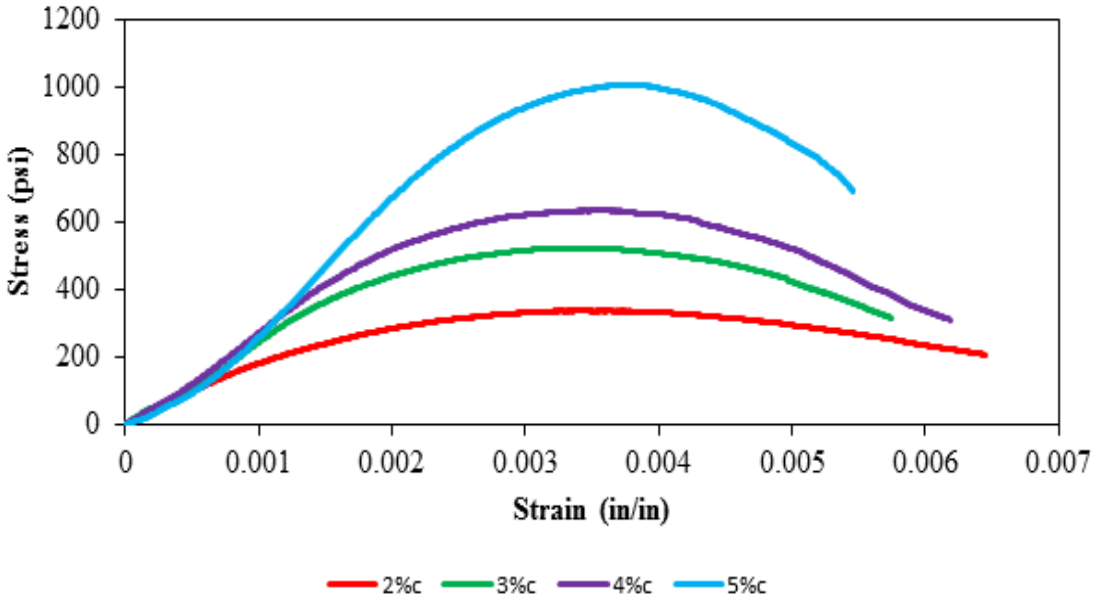

Figure 5.4 – **Paris Stress vs Strain Curve for 10-Day Capillary Soak Samples**

Figure 5.5 shows the laboratory results of the unconfined compressive strength test for 7-day moist cured specimens. The ascending nature of the trend lines is an indication of the favorable impact of increasing cement contents on the unconfined compressive strength of all the permutations of the experiment design. The slope of the trend lines, which represents the rate of improvements in the UC strength can provide valuable insight on the impact of the aggregate mineralogy and surface properties on the rate of the strength gain in presence of pozzolanic materials. As indicated in this plot, UC strength tests on the El Paso limestone materials resulted in sharper slopes which are an indication of the favorable influence of increasing cement contents to improve the strength of the stabilized materials. Comparatively, the UC strength results on siliceous gravel sourced from Pharr district exhibited flatter slope, which is an indication of lower influence of increasing cement content to improve the strength properties of the stabilized materials. This information can be utilized for selection of the optimum cement content for the stabilization of pavement foundations. The UCS test results clearly indicate that El Paso and Paris materials benefited more from the incremental increase of cement in terms of improvements in strength properties of the mixes. In contrast, Pharr materials significantly underperformed in terms of gaining strength compared to the other materials of the experiment design. In Figure 5.6, the similar behavior is observed for specimens subjected to 10-day capillary soak.

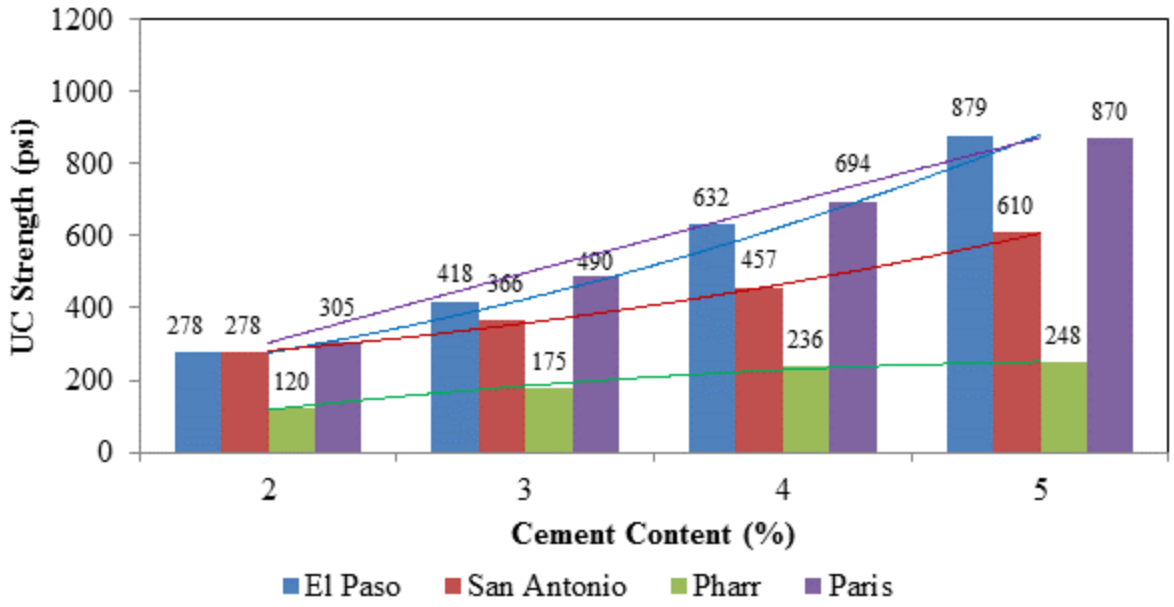

Figure 5.5 – Unconfined Compressive Strength Results for 7-day Moist Cured Samples

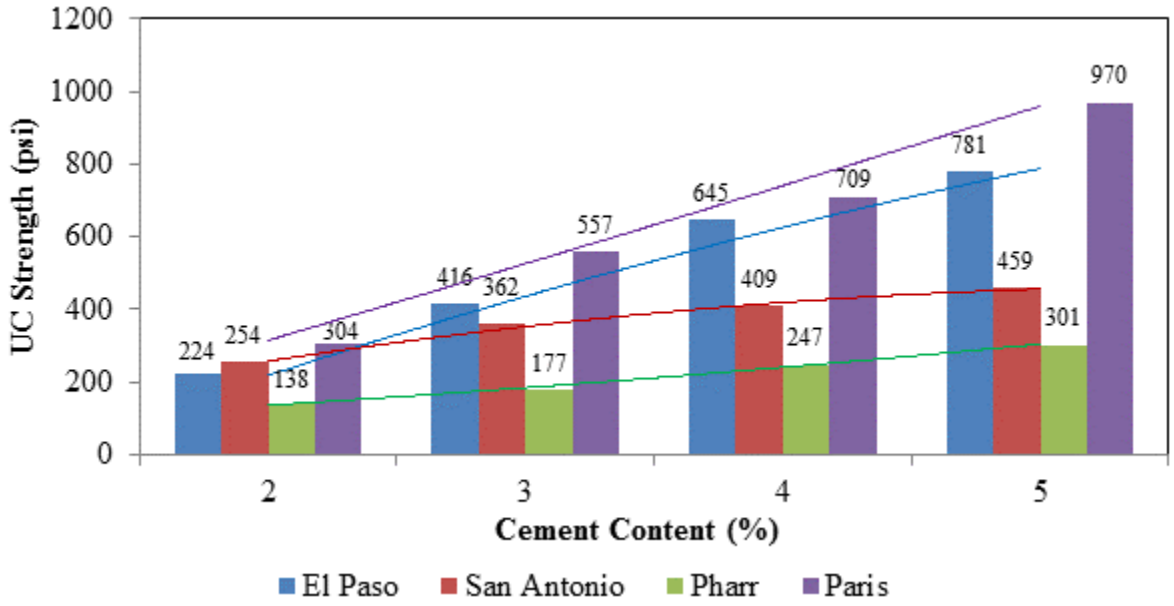

Figure 5.6 – Unconfined Compressive Strength Results for 10-Day Capillary Soak Samples

Figure 5.7 and 5.8 provide the improvements in UC strength with increasing cement content in the mix. The improvement plots were based on the comparisons with the lowest amount of stabilizer in the mix. In other words, 2% cement mixes for each aggregate type were used as the benchmark and the reference point to calculate the improvement plots. Subsequently, the percentage improvements were calculated based on incremental additions of cement. For example, 2-4% on the on the horizontal axes refers the improvement in the UC strength when the

cement content was increased from 2% to 4%. This provides valuable information for the efficient selection of the cement content needed for a specific aggregate type and gradation.

The increasing nature of the trend lines provided in Figures 5.7 and 5.8 is an indication of the favorable influence of stabilizer contents to improve the strength in the UCS test. Another noteworthy observation in Figures 5.7 and 5.8 is the role of aggregate mineralogy in the process of pozzolanic reactions. As illustrated in Figures 5.7 and 5.8, El Paso and Paris materials were benefitted more with incremental increase of cement in the mixes compared to the other counterparts.

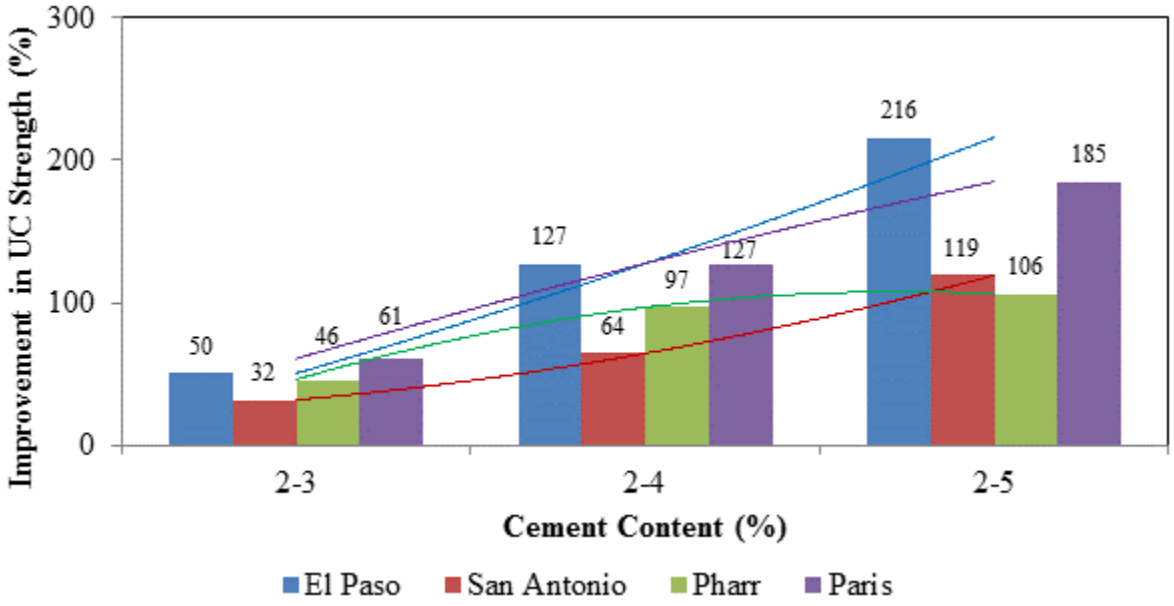

Figure 5.7 – Improvements in Unconfined Compressive Strength for 7-day Moist Cured Samples

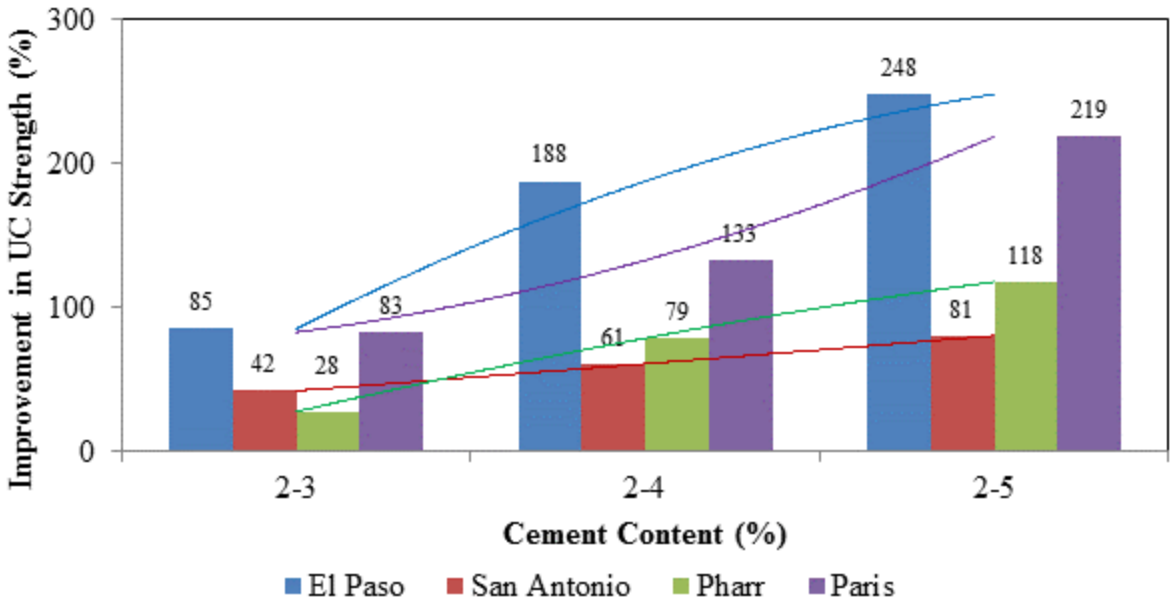

Figure 5.8 – Improvements in Unconfined Compressive Strength for 10-Day Capillary Soak Samples

Other important information than can be extracted from the UC strength test, especially from the stress-strain curves, is the tangent modulus of the specimens. This modulus is an indication of the undamaged small-strain modulus of the stabilized systems.

Figure 5.9 represents the tangent modulus values and trend lines for specimens prepared using 7-day moist cure condition. Similarly, Figure 5.10 represents the same information but for specimens subjected to 10-day capillary soak (TST condition). The monotonic increase of the tangent modulus values with incrementing cement content of the specimens is an indication of the positive effect in terms of higher modulus values with increasing the cement content in the mixes.

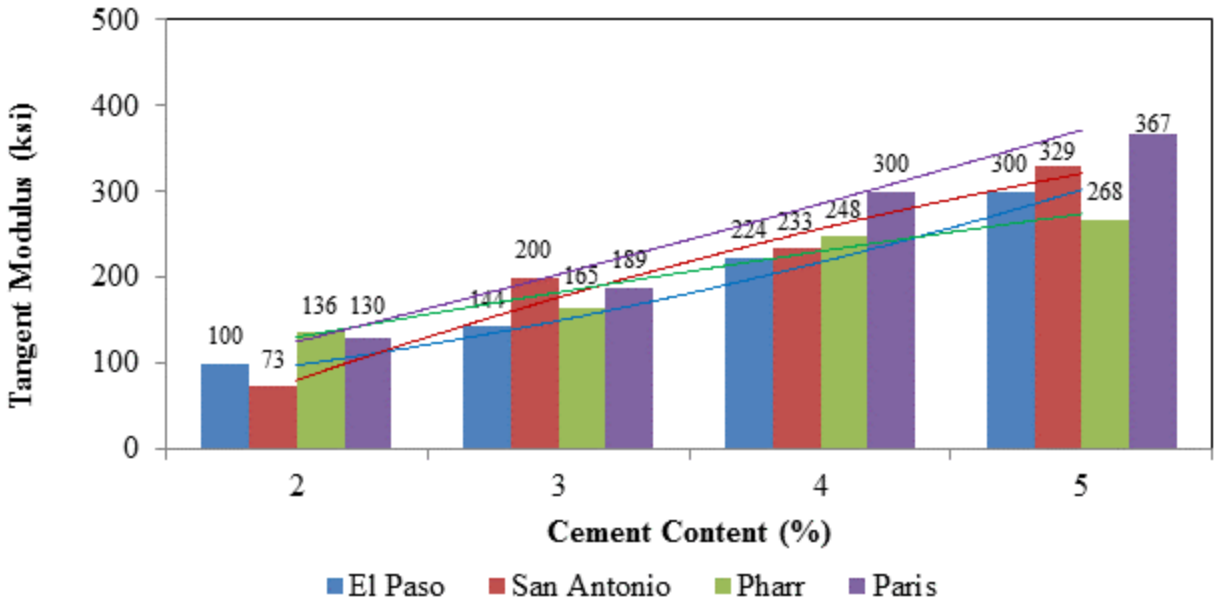

Figure 5.9 – Tangent Modulus for 7-day Moist Cured Samples

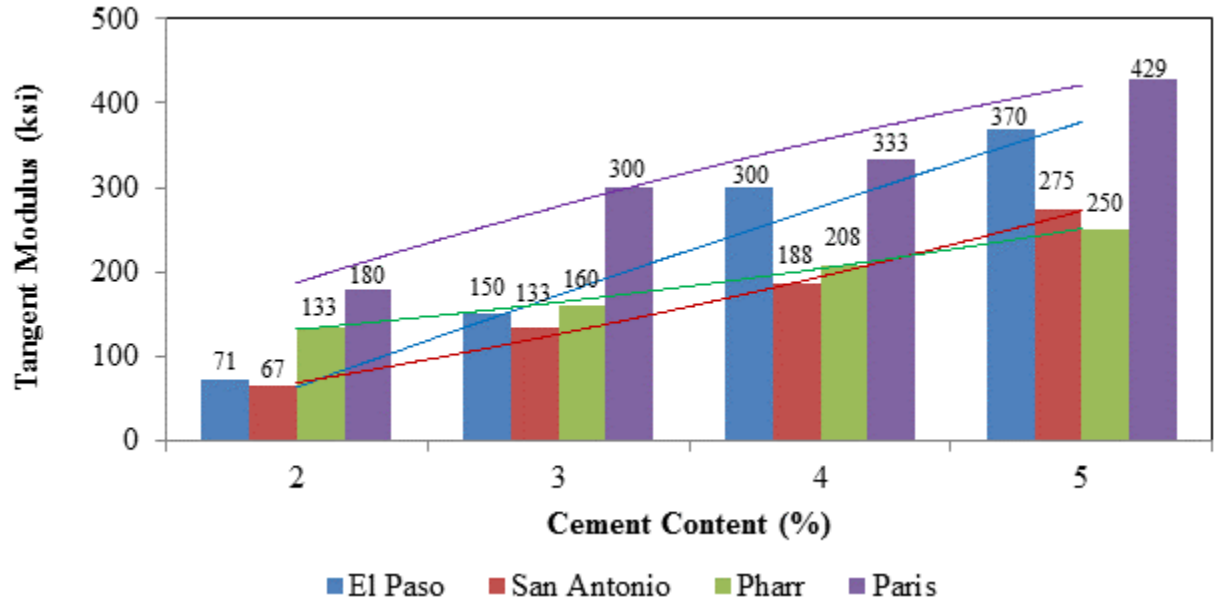

Figure 5.10 – Tangent Modulus for 10-Day Capillary Soak Samples

The degree of non-linearity is important feature that can be obtained from the USC test results. The method used to determine the degree of non-linearity was based on the deviatoric stress at failure over the maxim deviatoric stress of the linear part of stress-strain curves. Figures 5.11 and 5.12 illustrate the degree of non-linearity measured from the stress-strain curves using the UC strength test. The trends show a decreasing degree of non-linearity as cement content increases in the mixes. In other words, the specimens are more linear, and consequently show less ductile

behavior when cement content increases in the mix. This is another indication of the positive effect of increasing cement content in the mixes. The degree of non-linearity values is lower for specimens subjected to 10-day capillary soak (TST condition) than specimens subjected to 7-day moist cure condition.

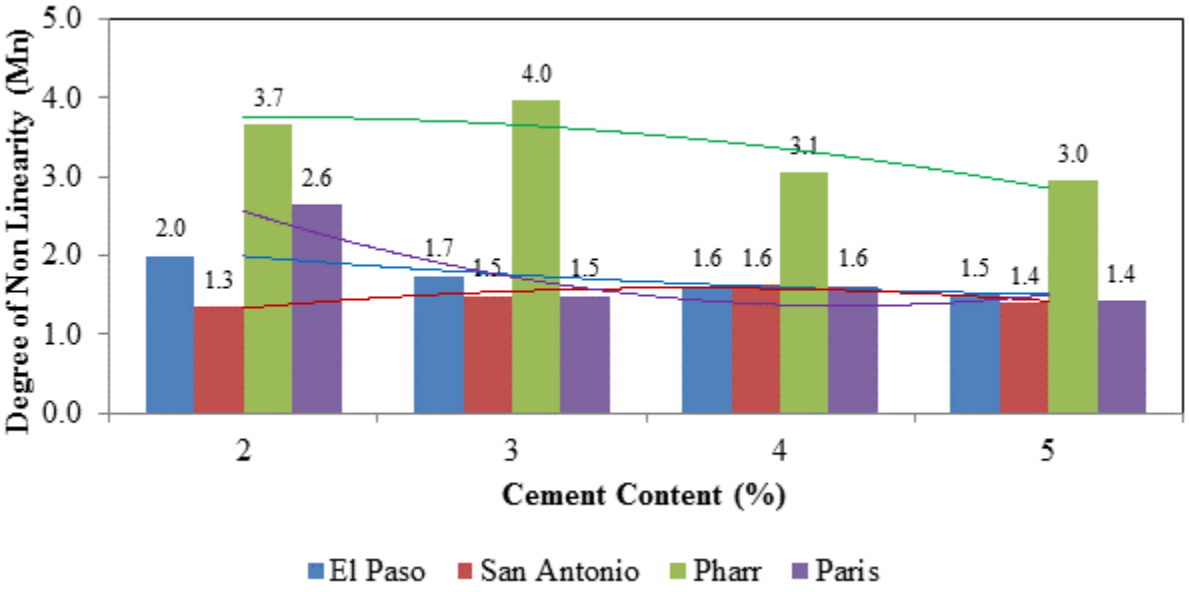

Figure 5.11 – **Degree of non-linearity for 7-day Moist Cured Samples**

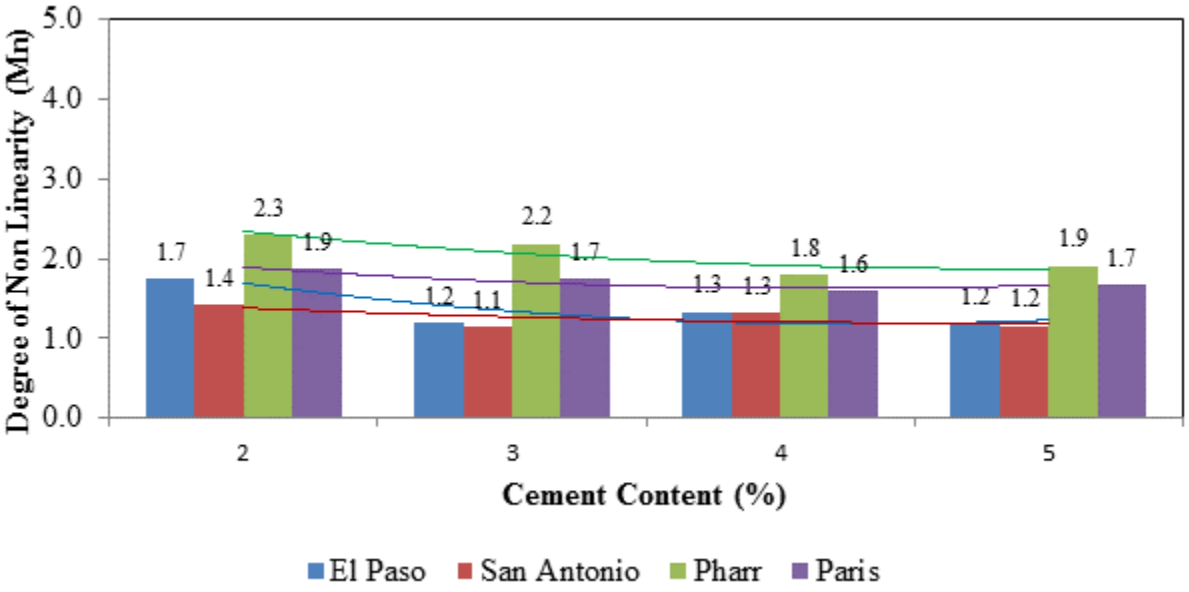

Figure 5.12 – Degree of non-linearity for 10-Day Capillary Soak Samples

Other important information obtained from the UC strength test is the strain at failure which is an indication of the stiffness and flexibility parameters of the stabilized systems. Figure 5.13 shows

the strain at failure for 7-day moist cure specimens. The nature of the trends represents a decreasing strain value at which the specimens fails, this means the specimens becomes more rigid and loses flexibility when cement content increases in the mix. As indicated by the nature of the trend lines in Figures 5.13 and 5.14, the strain at failure for El Paso and Paris materials stayed relatively constant with increasing the cement content in the mixes.

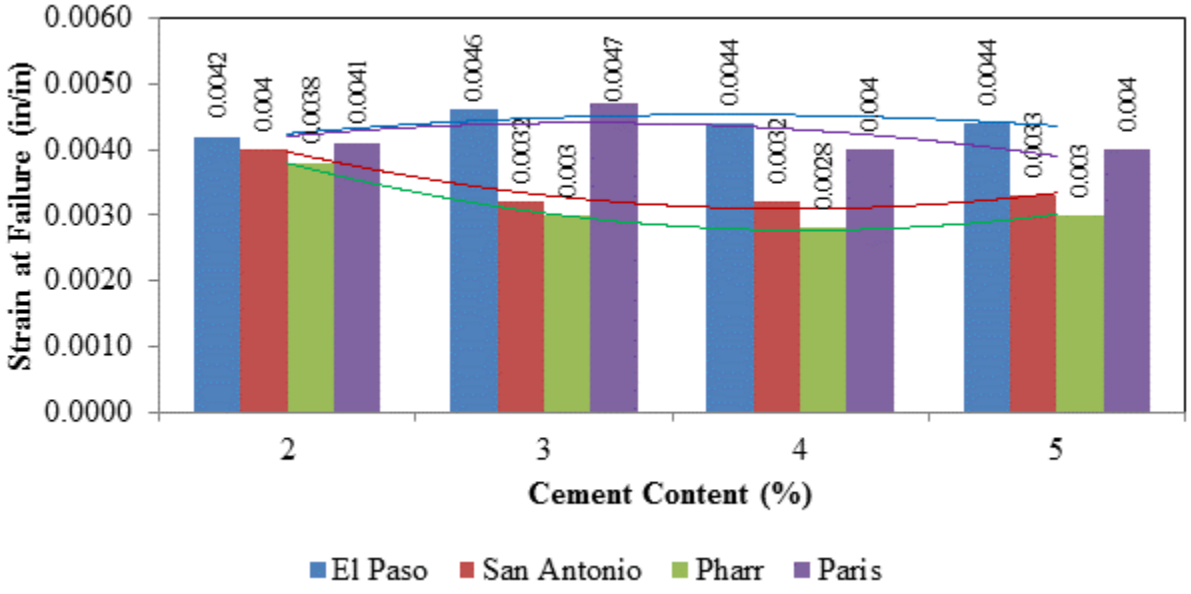

Figure 5.13 – Strain at Failure for 7-day Moist Cure Samples

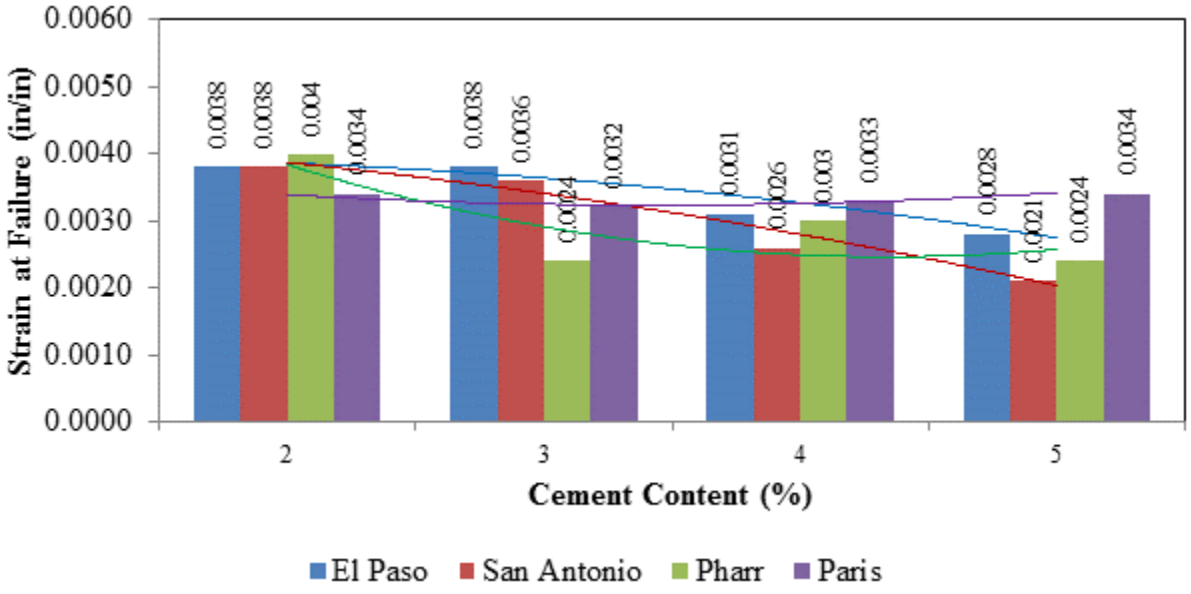

Figure 5.14 – Strain at Failure for 10-Day Capillary Soak Samples

Static Indirect Diametrical Test (S-IDT)

Strain controlled static Indirect Diametrical Tests (IDT) were performed on 6 x 4.5 in (152 x 114 mm) stabilized specimens. Similar to the previous case, two curing procedures were considered to better understand the influence of the moisture ingress on the tensile strength of the stabilized materials. The moisture content was adjusted based on the preliminary moisture density results and the recommendations of Tex-120-E procedure.

This section presents the laboratory results of the IDT test for 7-day moist cure and 10-day capillary soaked specimen. Similar to the UCS tests results, incremental addition of the stabilizer content improved the mechanical properties of the tested specimen. All permutations exhibited increase in the tensile strength with increasing stabilizer contents. However, as indicated in Figures 5.15 and 5.16, the rate and the magnitude of improvements were highly impacted by the lithology of aggregates.

The ascending nature of the IDT strength values with increasing cement content for all material types is an indication of the favorable effect of stabilizer content on the tensile strength of the stabilized systems. However, the rate of the increase in the IDT strengths was not similar as indicated by the trend lines in Figure 5.15. Similar to the UCS results presented in previous sections, El Paso limestone had benefited most from incremental increase in the cement contents. Conversely, the rate of the improvements in the tensile strength of siliceous gravel from Pharr district with increasing cement contents has been lower as indicated by trend lines in Figure 5.15. For instance, increasing the cement content from 2% to 4% for El Paso materials resulted in more than 135% increase in the IDT strength while the same incremental increase of stabilizer for the Pharr materials resulted in approximately 32% improvements in IDT strength. This underscores the influence of the lithology and surface properties of the geomaterials as potential candidates for stabilized layers. Additionally, this information can provide valuable insight on the benefit-cost ratio for the selection of stabilizer contents.

Figure 5.16 presents the laboratory results for the static IDT performed in 10-day capillary soaked specimens. The trend lines follow a similar pattern as in 7-day moist cure specimens. A comparison of the results presented in Figures 5.15 and 5.16 revealed the deleterious influence of moisture to degrade the tensile stiffness of the cement stabilized specimen.

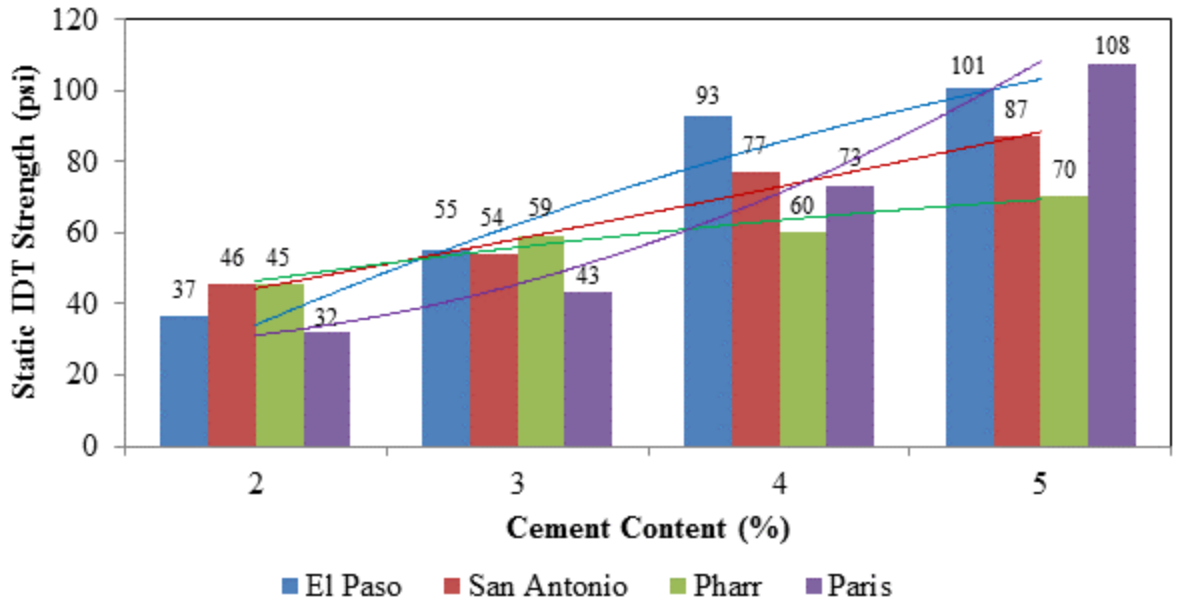

Figure 5.15 – Static IDT Test Results for 7-day Moist Cured Samples

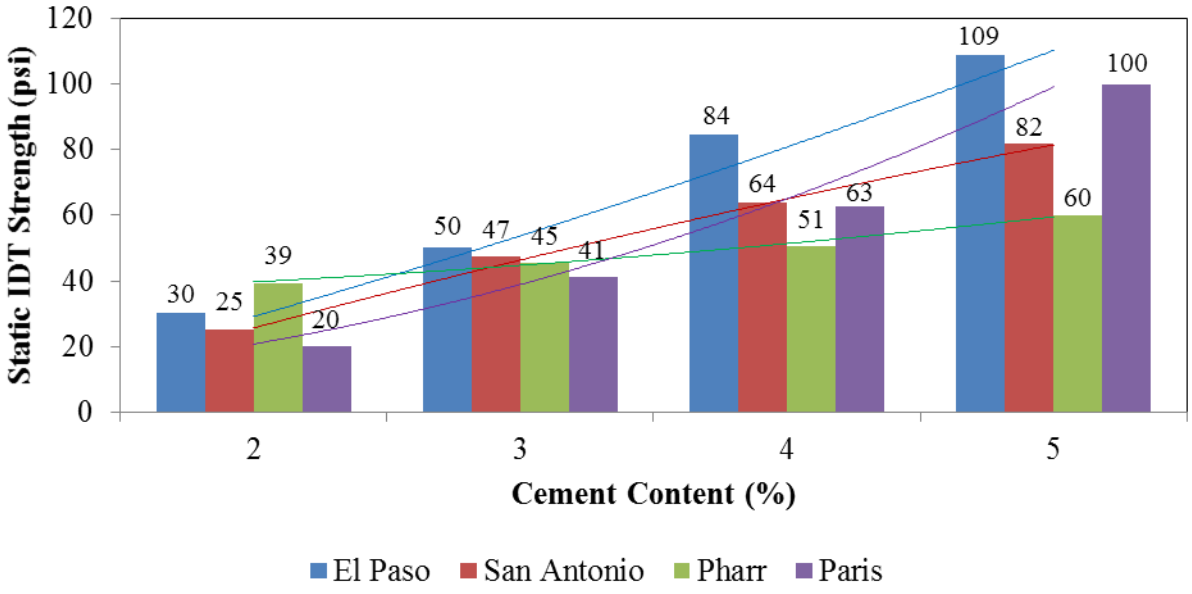

Figure 5.16 – Static IDT Test Results 10-Day Capillary Soak Samples

Figures 5.17 and 5.18 represent the improvement in tensile strength of the specimen for 7-day moist cure and 10-day capillary soaked (TST) specimen, respectively. A notable observation in these plots is the significant underperformance of Pharr materials at high stabilizer contents, 4% and 5%, compared to other materials in the experiment design. The underperformance of Pharr materials is more pronounced in the TST results presented in Figure 5.18. For instance, the tensile strength of Paris samples improved by 397%, by increasing the cement content from 2%

to 5%, while it showed a relatively modest improvement of 52% for Pharr samples. Again, Paris material is the most benefited in terms of tensile strength improvement by incrementing cement in the mix.

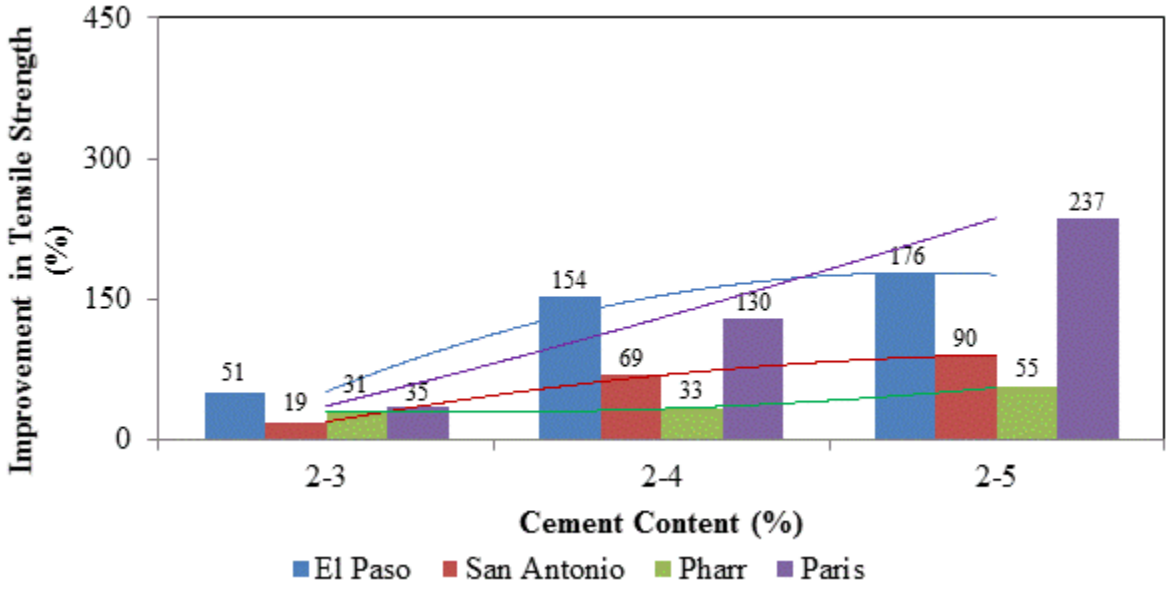

Figure 5.17 – Tensile Strength Improvement for 7-day Moist Cure Samples

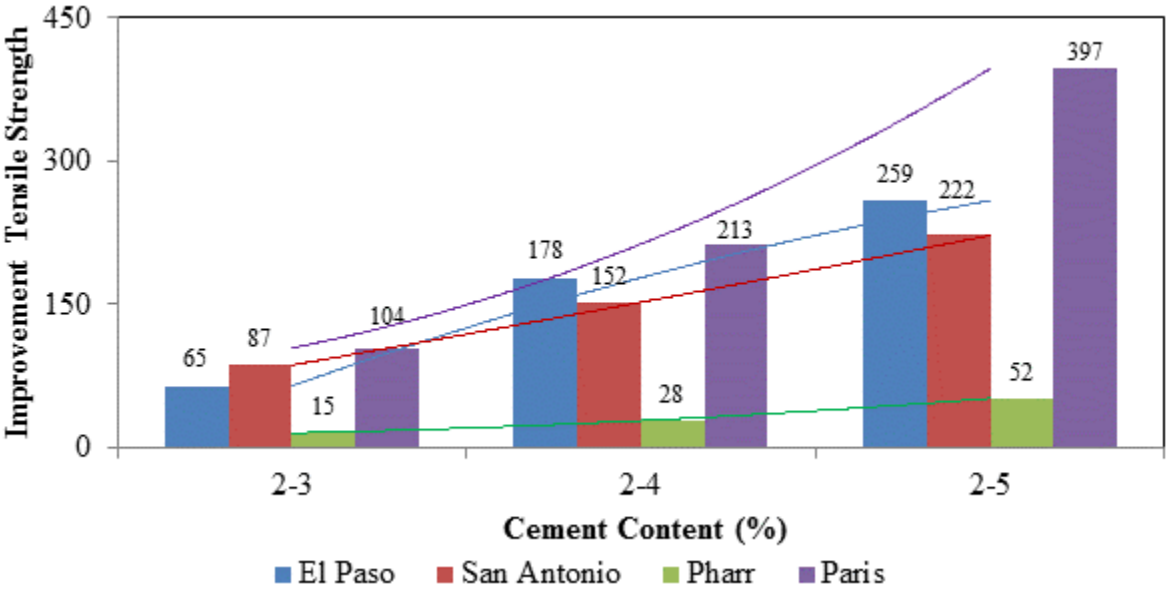

Figure 5.18 – Tensile Strength Improvement for 10-Day Capillary Soak Samples

Figures 5.19 and 5.20 show the tangent modulus values calculated based on the stress-strain curves in the static IDT using 7-day moist cure and 10-day capillary soak samples, respectively. As expected, the nature of the trend lines is increasing when cement content increases.

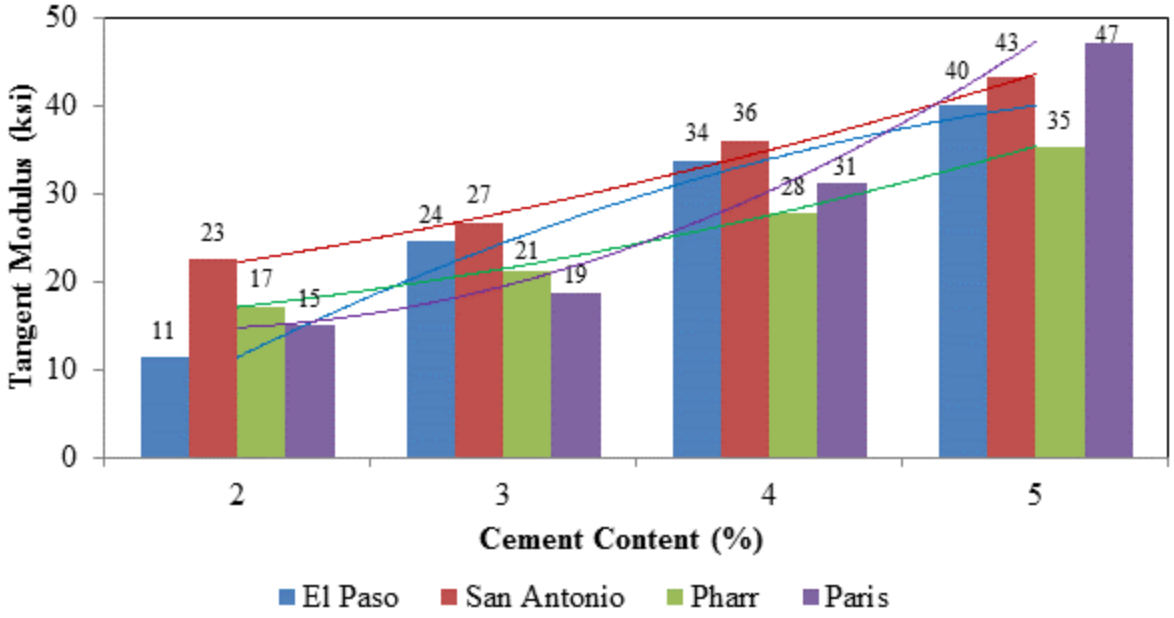

Figure 5.19 – Tangent Modulus for 7-day Moist Cured Samples

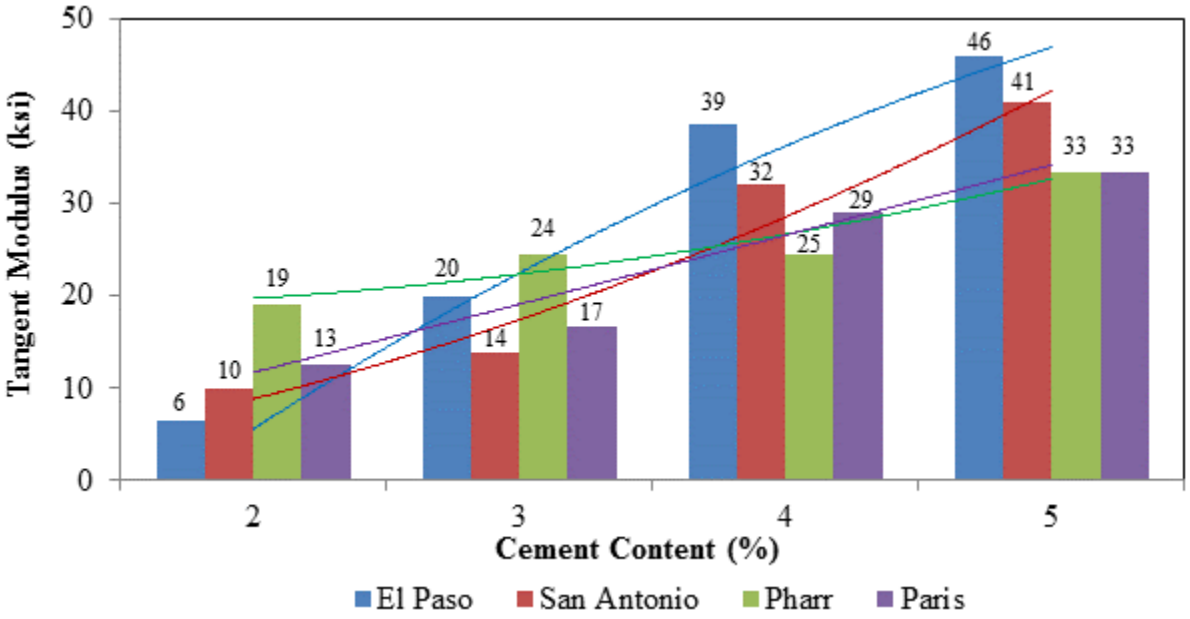

Figure 5.20 – Tangent Modulus for 10-Day Capillary Soak Samples

Figure 5.21 shows the compressive behavior when the specimen is subjected to strain-controlled test for Pharr materials. Figure 5.22 represents the tensile behavior for Pharr materials. Both behaviors are very different even for the same material.

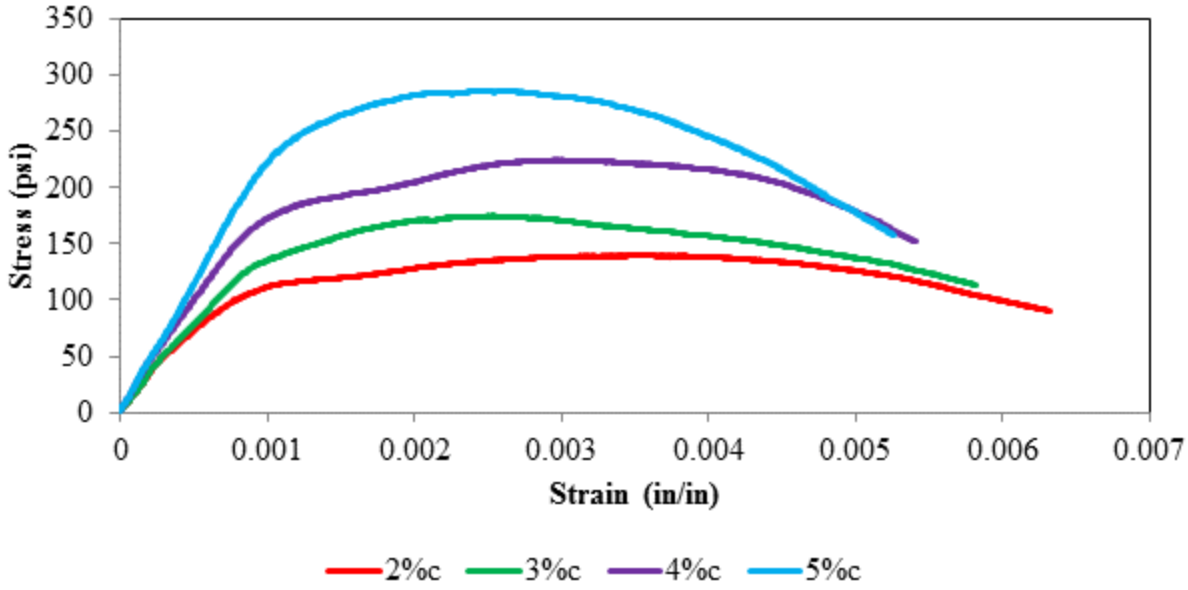

Figure 5.21 – Stress vs Strain Curves under UCS Test for Pharr Materials (Compressive Behavior)

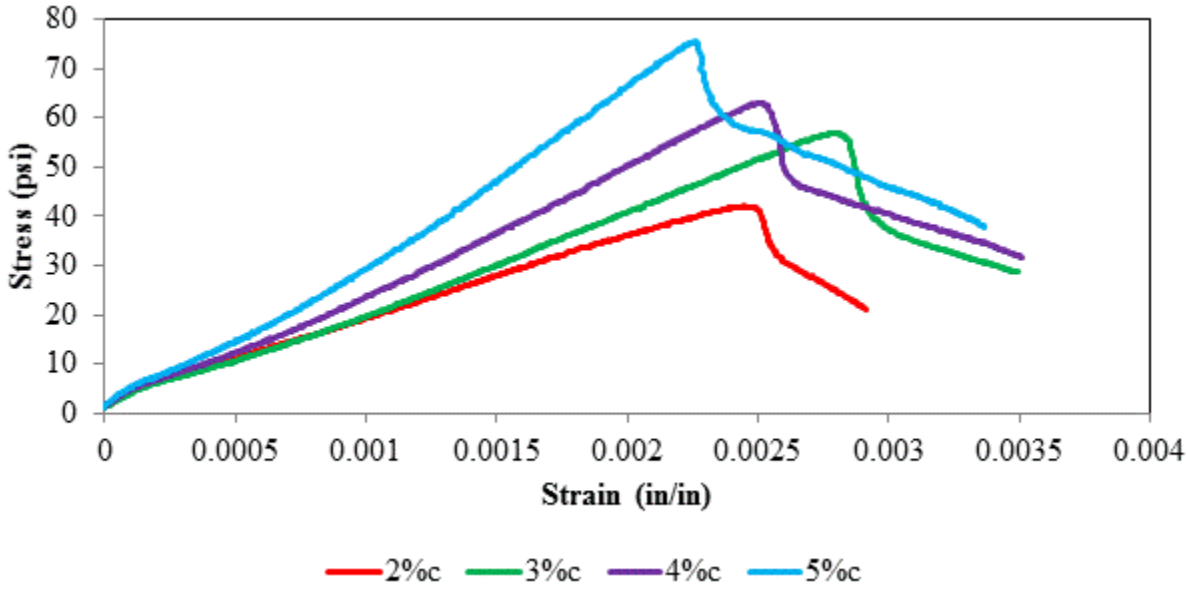

Figure 5.22 – Stress vs. Strain Curves under Static IDT Tests for Pharr Materials (Tensile Behavior)

Another noteworthy analysis derived from the static IDT was the calculations of the degree of the nonlinearity of the stabilized specimen. The results presented in Figures 5.23 and 5.24 clearly indicate that the "flexibility" of the materials is significantly reduced by increasing the stabilizer contents in the mixes.

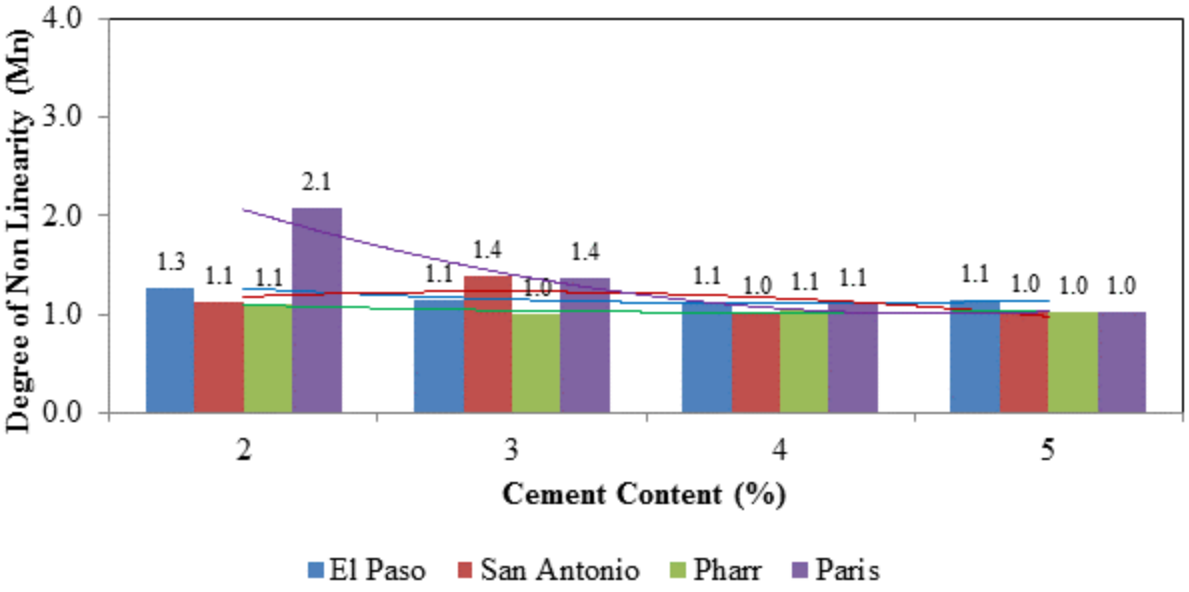

Figure 5.23 – Degree of Non-linearity for 7-day Moist Cure Samples

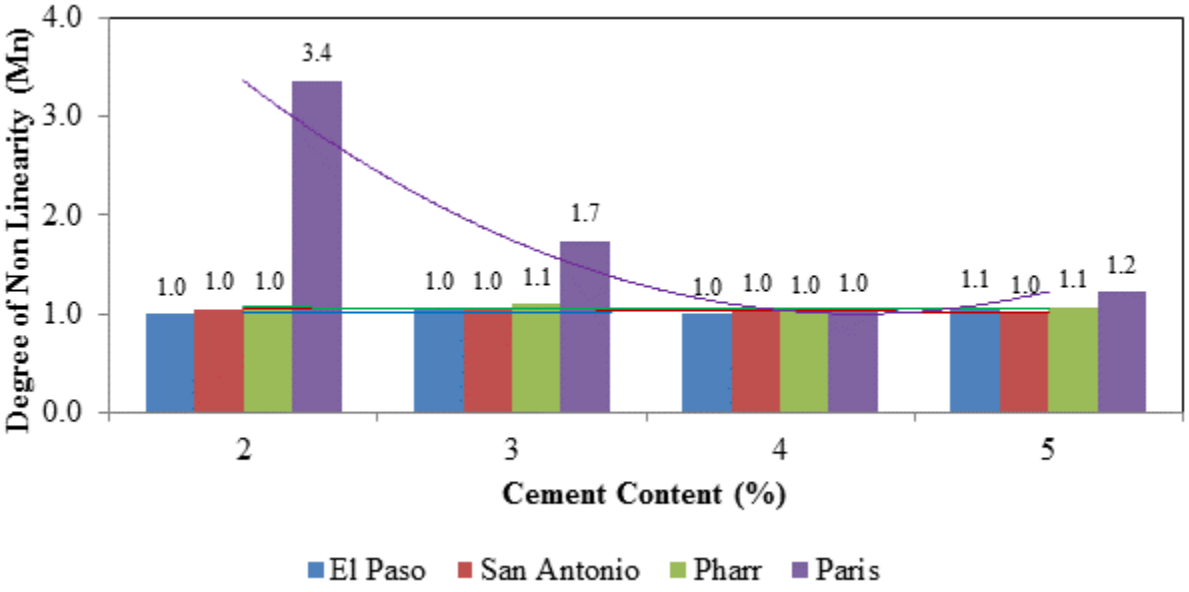

Figure 5.24 – Degree of Non-linearity for 10-Day Capillary Soak Samples

Pair-Wise Analysis of Compressive and Tensile Behavior of Stabilized Systems

Compressive behavior and tensile behavior of the stabilized specimen were independently presented and discussed in previous sections of this document. The simultaneous improvements in tensile and compressive behavior of stabilized systems can be visualized in Figure 5.25. As evidenced in this plot, the orthogonal improvements of strength are anisotropic for all variants.

This is more pronounced for Pharr materials that showed nearly twice the rate of improvement of strengths in compression compared to strength gain in tension.

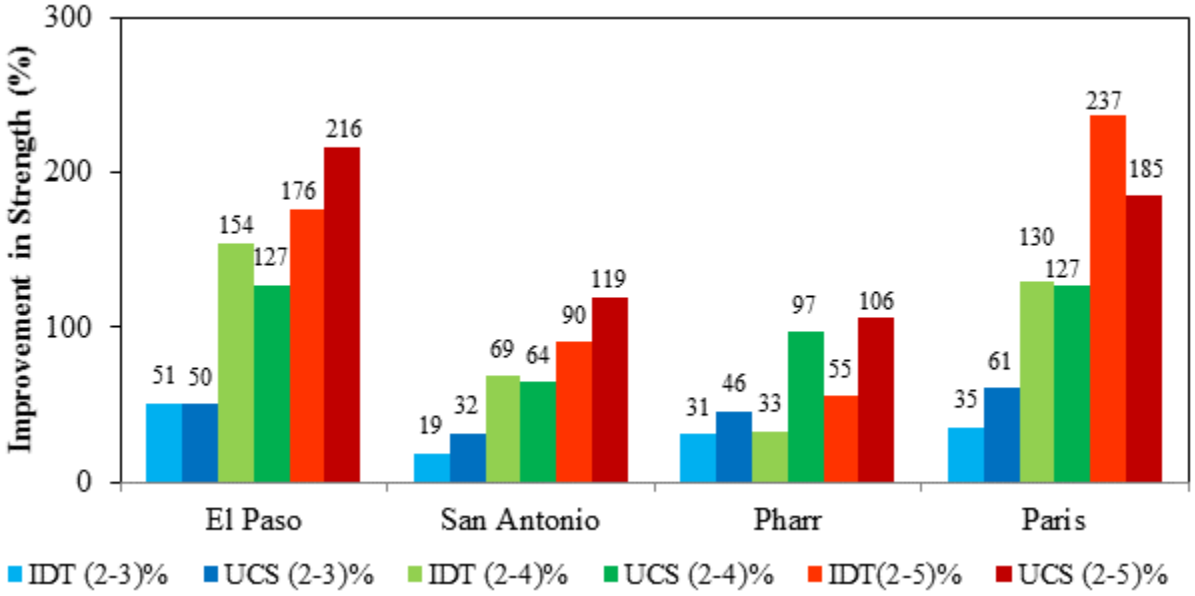

Figure 5.25 – Improvements in Tensile and Compressive Strength Dynamic Indirect Diametrical Test (IDT)

Submaximal Modulus Test

Stress-controlled Submaximal Modules Tests were performed on the 6 x 12 in (152 x 305 mm) cylindrical aggregate specimen stabilized with varying cement contents. The strength values obtained from the UCS test were basis for the selection of the stress amplitudes applied to the permutations of the experiment design. Pre-determined fractions of the UCS-value, namely 20%, 40% and 60% were cycled for 5,000 repetitions for each variant. The motivation for incorporation of this test in the experiment design was to identify the permanent deformation behavior of stabilized systems subjected to vertical load repetitions. Similar to the procedure outlined for the UCS tests, two sets of samples for each [Material Type-Stabilizer Content] were subjected to seven-day moist cured and 10-day capillary soak at ambient temperature (TST procedure) to study the softening role of moisture in repeated load permanent deformation tests. Figure 5.26 shows the specimen setup and sample failure in the Submaximal Modulus Test.

Figure 5.26 – Submaximal Modulus Test (a) Specimen Setup (b) Fractured Specimen

Figure 5.27 illustrates the normalized permanent deformation after 5,000 load applications for 7-day moist cured specimens at 20% UC strength. Since the percentage of strength is constant, it is imperative to normalize the measured deformations by strength values (or stress amplitudes) for proper comparison of deformations. This is simply due to the fact that 20% UC strength of a stabilized material X with w% cement content is significantly different compared to a material Y with w% cement content; therefore, the selected stress amplitude in two test are different.

For instance, 20% of the UC strength for Paris specimens is significantly higher than 20% strength for Pharr specimens.

The results show reduction in the final permanent deformation for all materials tested. Figure 5.27 clearly shows the underperformance of the Pharr materials in terms of higher permanent deformation after 5,000 cycles for 7-day moist cured specimens. As illustrated in Figure 5.27, the magnitude of the terminal permanent deformations observed for El Paso, San Antonio and Paris materials were close each other.

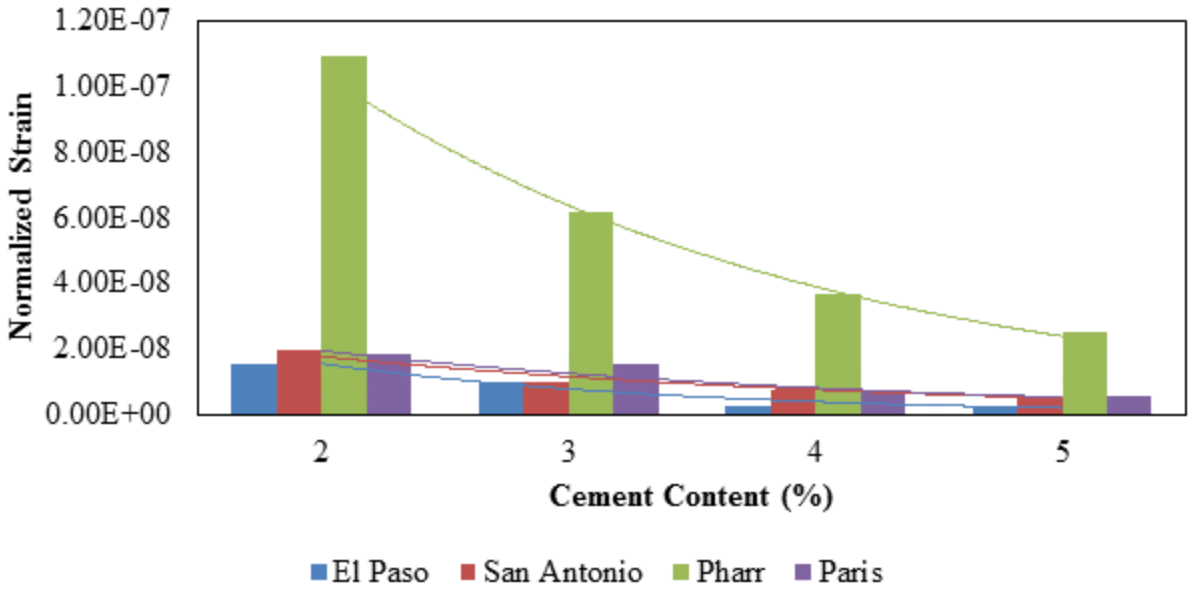

Figure 5.27 – Plastic Deformations for 7-day Moist Cured Samples

Figure 5.28 represents the normalized plastic strains for 10-day capillary soaked specimen. One interesting observation when comparing Figures 5.27 and 5.28 results was the significant reduction of deformations of Pharr materials in the 10-day soaked specimen. This could be due to the time-dependent nature of the pozzolanic reactions and its sensitivity to the rate and velocity of silica solubility in the mixes. The trends show that Pharr and San Antonio Materials deforms more than Paris and El Paso materials.

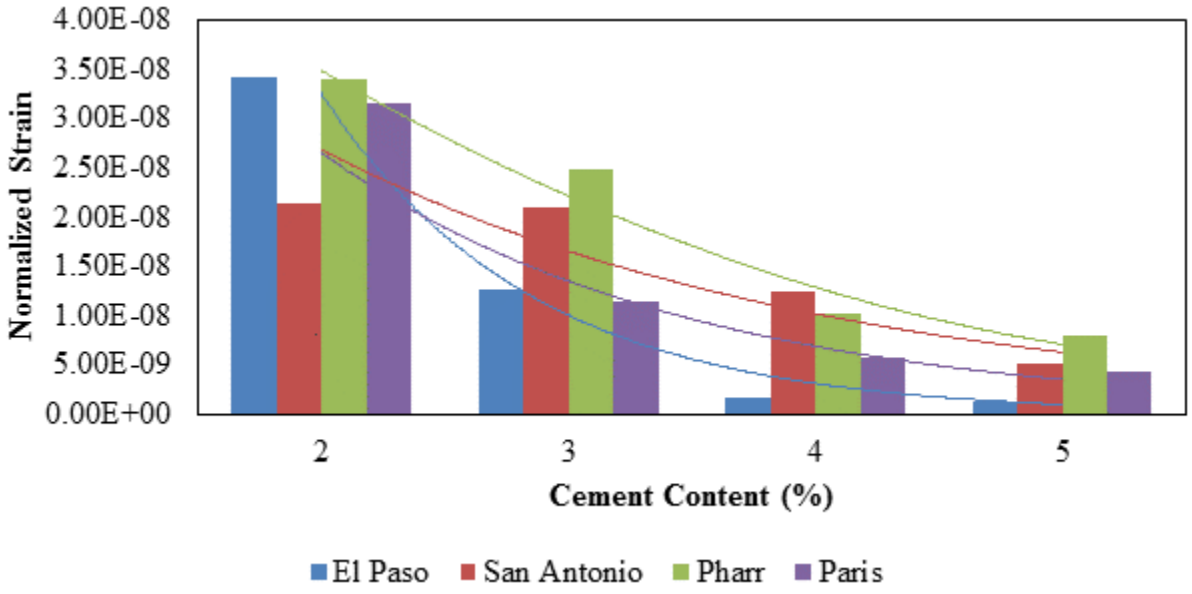

Figure 5.28 – Plastic Deformations for 10-day Capillary Soak Samples

Figure 5.29 illustrates the reduction in the cumulative plastic deformations due the increase of cement content in the mixes for 7-day moist cured specimens. Similarly to the argument presented for analysis of the previous testing procedures, the deformations for the 2% cement content were selected as the benchmark for to establish comparative improvement plots. The results clearly demonstrate the reduction in the permanent deformation by increasing the cement content in all permutations of the experiment design. This positive influence is more pronounced for El Paso materials as compared to Pharr materials.

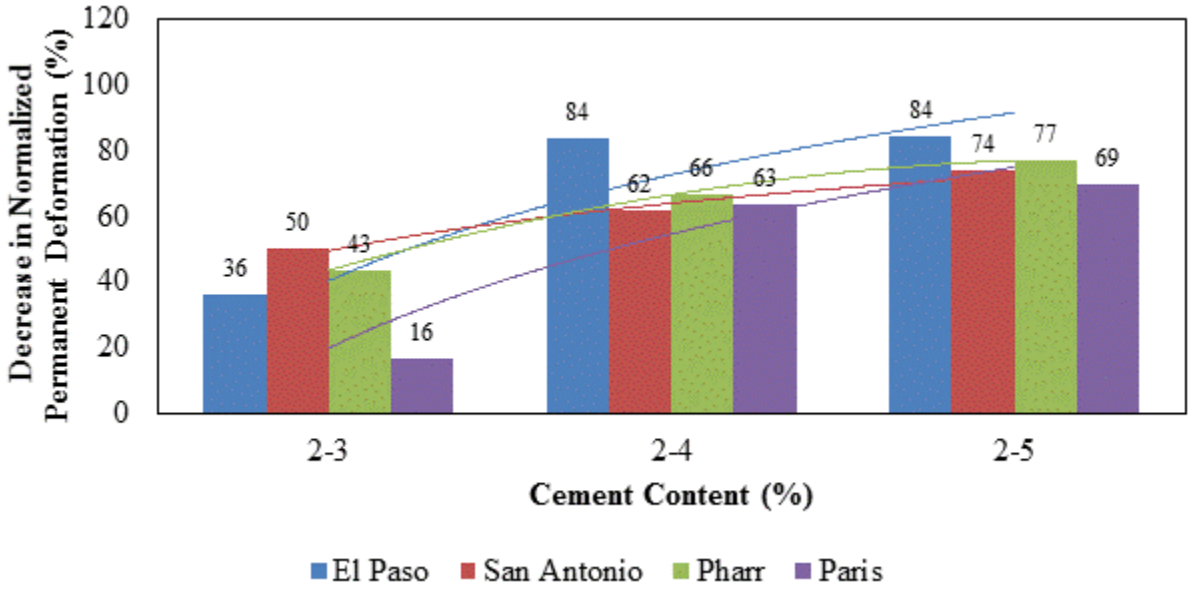

Figure 5.29 – Reduction of Plastic Deformations after 5,000 cycles for 7-day Moist Cured Samples

A similar argument is valid for the 10-day capillary soaked specimen as illustrated in Figure 5.30. The trend of the data shows the reduction plastic deformations by incremental increase of cement contents in the mixes. One noteworthy observation was the significant reduction of the normalized plastic deformations in 10-day capillary soak specimen. This could be due to the time-dependent nature of the pozzolanic reactions as well as the role of provided moisture through capillary action in the 10-day soaked specimen.

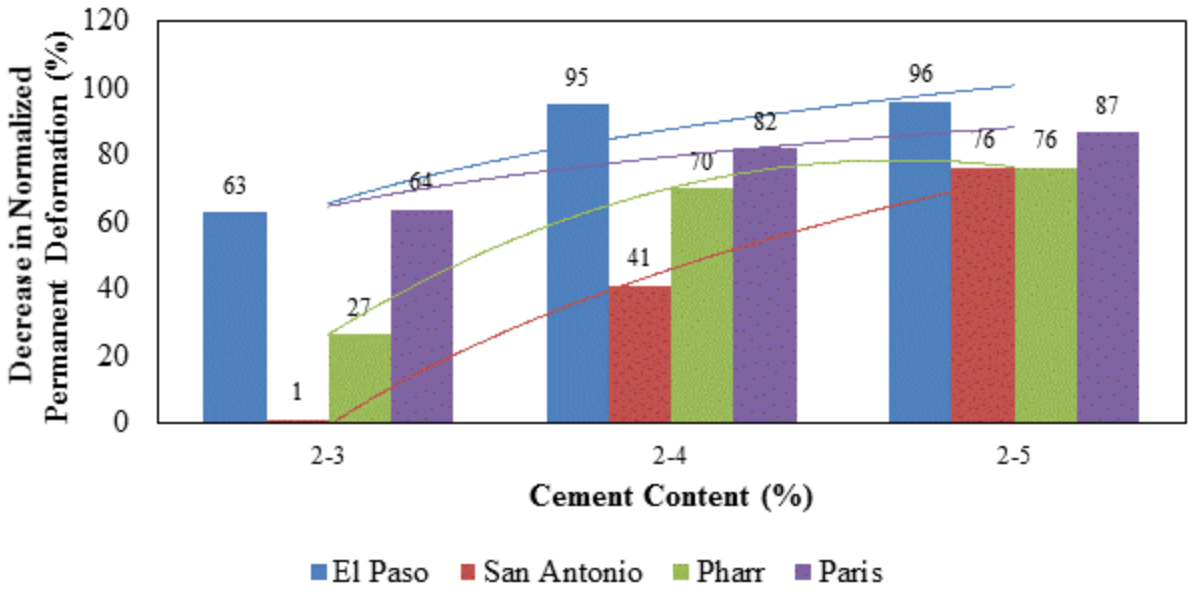

Figure 5.30 – Reduction of Plastic Deformations after 5,000 cycles for 10-day Capillary Soak Samples

Dynamic Indirect Diametrical Test (IDT)

Stress-controlled dynamic IDTs were performed on the 6 x 4.5 in (152 x 114 mm) cylindrical aggregate specimen stabilized with varying cement contents. The test setup and the sample geometry are similar to the static IDT. The dynamic load pulse amplitude was selected as fractions of the static IDT strength. Three incremental strength levels of 20%, 40% and 60% of IDT strength were cycled for 50,000 repetitions to characterize the fracture behavior of stabilized materials subjected to high number of load cycles. Figure 5.31 shows the specimen setup and sample failure in the dynamic IDT test.

Figure 5.31 – Dynamic Indirect Diametrical Test (IDT) (a) Specimen Setup (b) Fractured Specimen

Figure 5.32 illustrates the normalized cumulative plastic deformations of 7-day moist cured specimens after 50,000 cycles applied 20% static IDT strength. The nature of trend of the data clearly shows a favorable influence of the increasing stabilizer content to control the rutting of stabilized systems. Similarly Figure 5.33 shows the normalized cumulative plastic deformations for TST samples.

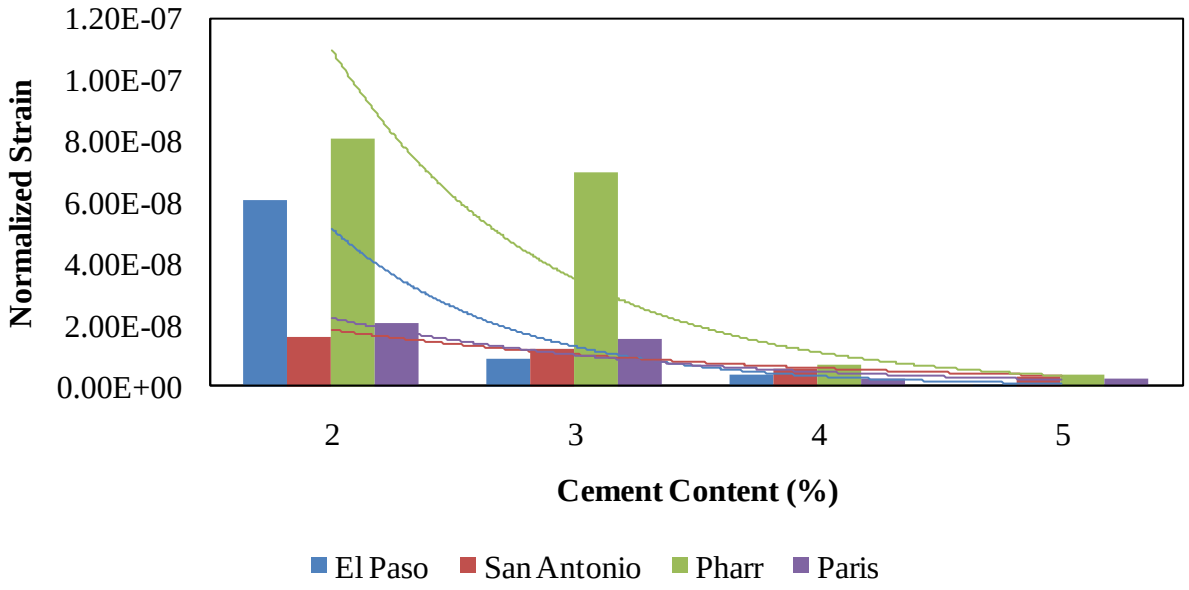

Figure 5.32 – Cumulative Plastic Deformation after 50,000 Load Cycles for 20% Dynamic IDT for 7-day Moist Cured Samples

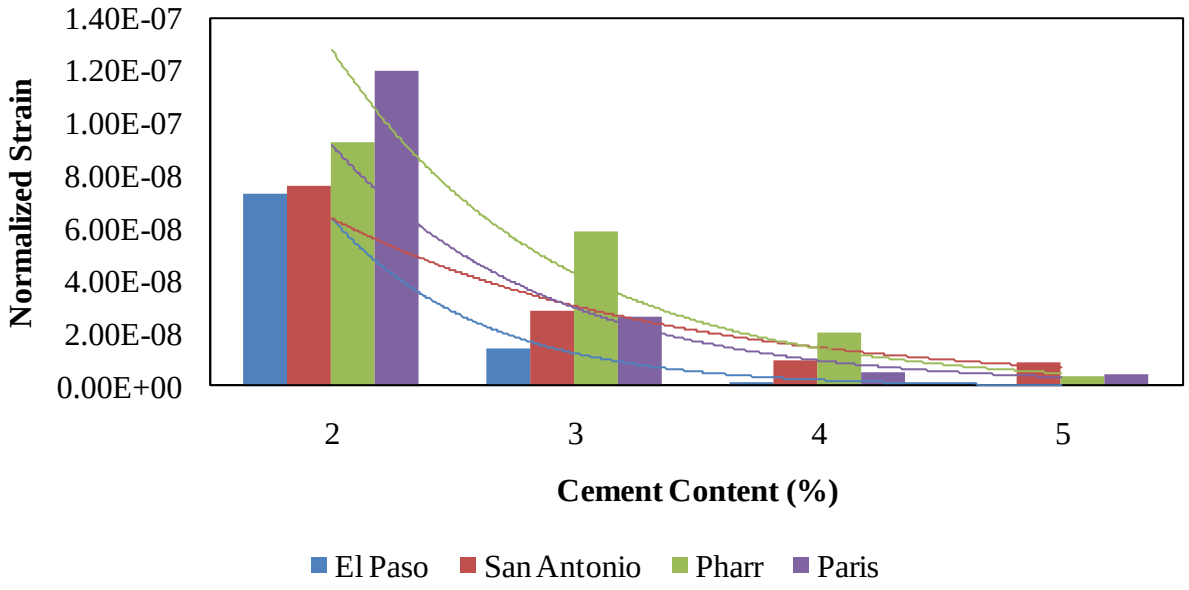

Figure 5.33 – Cumulative Plastic Deformation after 50,000 Load Cycles for 20% Dynamic IDT for 10-day Capillary Soak Samples

Figures 5.34 and 5.35 shows the percent reductions in the plastic deformation as cement content increases for 7-day moist cured samples and 10-day capillary soak samples respectively. This figure clearly shows the favorable effect of increasing cement contents to 4% and 5% for Pharr materials.

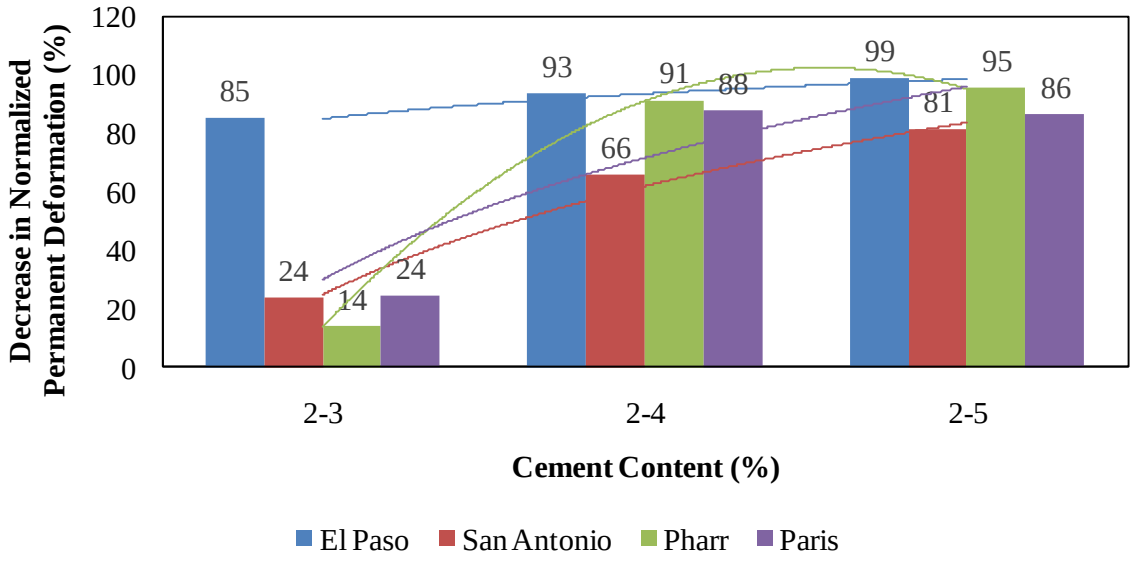

Figure 5.34 – Percent Decrease in Plastic Deformation after 50,000 Load Cycles in Dynamic IDT Test for 7-day Moist Cured Samples

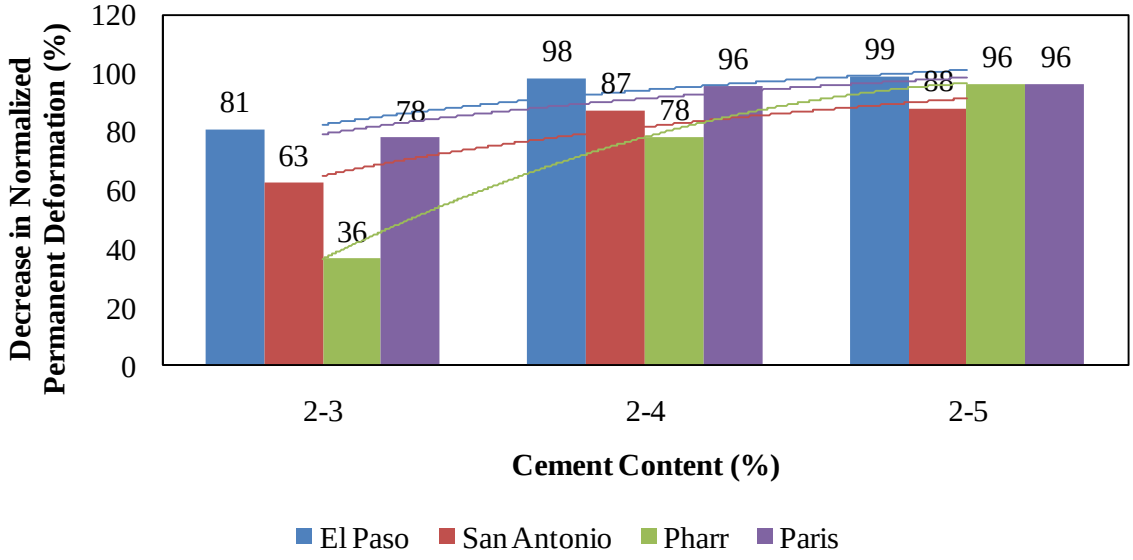

Figure 5.35 – Percent Decrease in Plastic Deformation after 50,000 Load Cycles in Dynamic IDT Test for 10-day Capillary Soak Samples

An interesting observation depicted in this graph is the fact that increasing the cement content from 4% to 5% did not have a significant influence to mitigate plastic deformations after 50,000 load cycles. A plausible explanation could be the fact that the (ε_p-N) curve has already reached an asymptotic behavior; therefore, further increase in the cement content has negligible influence on the rutting of the mixes.

Dielectric Test

Moisture susceptibility of the stabilized materials was characterized by tracking the variations of the dielectric constants using a Rainbow dielectric constant meter in the laboratory. The change in the dielectric values of the stabilized specimen, when subjected to external moisture, such as environmental chamber or capillary soak, is an indication of the change in the available moisture in the pore structure. Therefore, monitoring the dielectric values at the top of the specimen can provide valuable information on the affinity of the specimen to transport moisture through the air void structure.

Figures 5.36 and 5.37 illustrate the variations of the dielectric values for two replicates of the San Antonio limestone and Paris sandstone subjected to 10-day capillary soak at ambient temperatures (TST procedure). The dielectric values of the TST specimen were measured every day for 10 consecutive days at five points at the top of the specimen. Our laboratory research team paid careful attention to perform the measurements at the same exact locations at each interval. The average values of the five measurements were then calculated and reported as the representative dielectric value for each variant of the experiment design. The plot presents the results for a 6 x 12 in (152 x 305 mm) inch specimen for all the permutations of the experiment design.

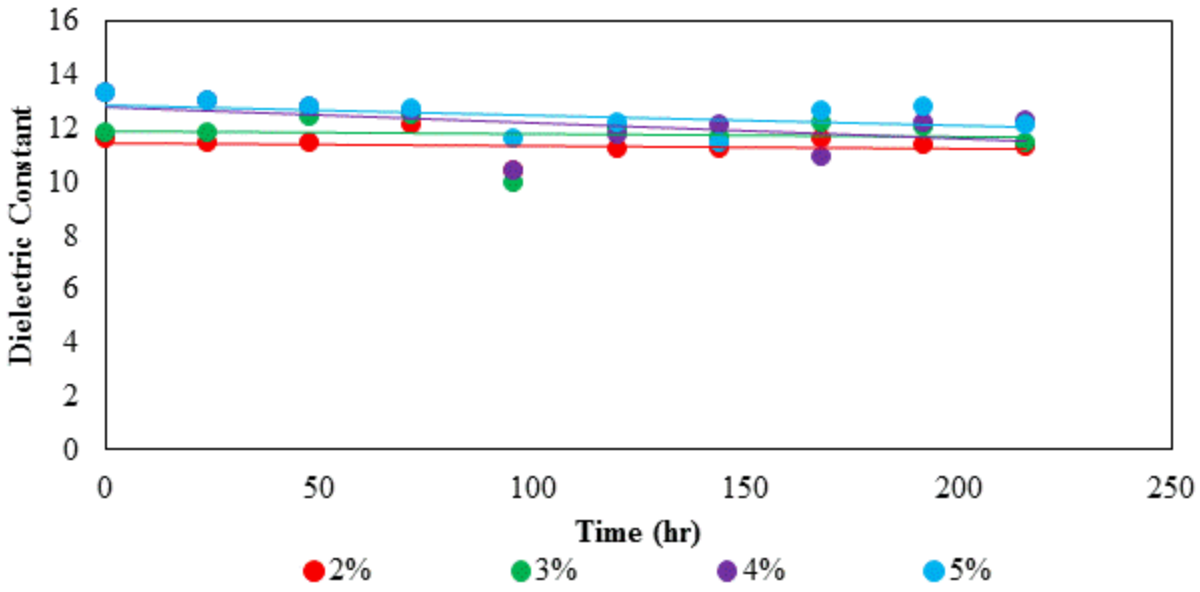

Figure 5.36 – Variations of Dielectric Values for San Antonio Limestone for 10-day Capillary Soak Samples

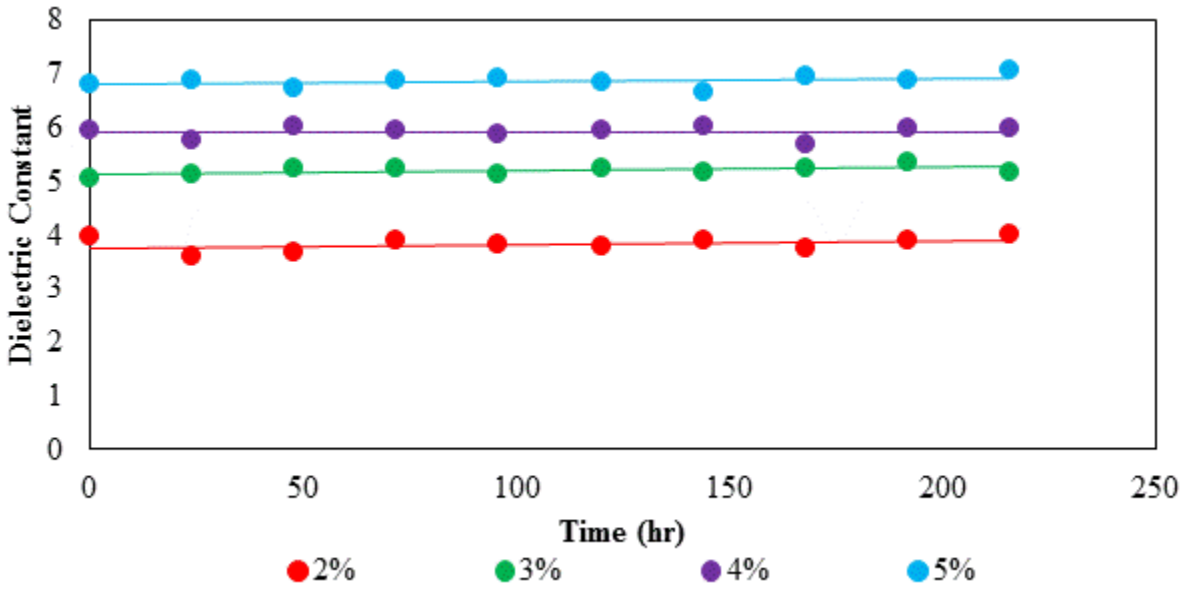

Figure 5.37 – Variations of Dielectric Values for Paris Sandstone for 10-day Capillary Soak Samples

The small variability of the dielectric values during 10 days of testing for all stabilizer contents indicates that the unbound moisture was not able to travel and reach to the top of specimen. This is an indication of insignificant sensitivity of the selected aggregates to hold and transport moisture in the pore structure.

Figure 5.38 presents the cumulative results of the dielectric value measurements for 10-day capillary soak (TST) procedure. In order to construct this plot, initially the averages of the five point-measurements for each specimen were determined. Subsequently, the averages of the dielectric values for 10 consecutive days were calculated. Lastly, the averages of the two replicated were determined and reported as the representative dielectric value for each variant. In other words, every single bar in Figure 5.36 is the average of 100 data points [5 (measurements at the top of specimen) x 10 (days) x 2 (Replicates) = 100]. Same procedure was repeated for each combination of [aggregate type-stabilizer content] and reported in the aggregate feature database. Therefore, Figure 5.38 summarizes 1600 dielectric value measurements into one plot. This will provide valuable information for comparative analysis of the moisture susceptibility of the stabilized materials. One interesting observation that can be clearly visualized from this figure is the superior performance of Paris materials in terms of lower dielectric constants compared to other materials in the experiment design. This could be attributed to either low moisture retention capacity of aggregates sources from Paris district, or the consumption of the available moisture in strength gain reactions to improve the mechanical properties of the mixes.

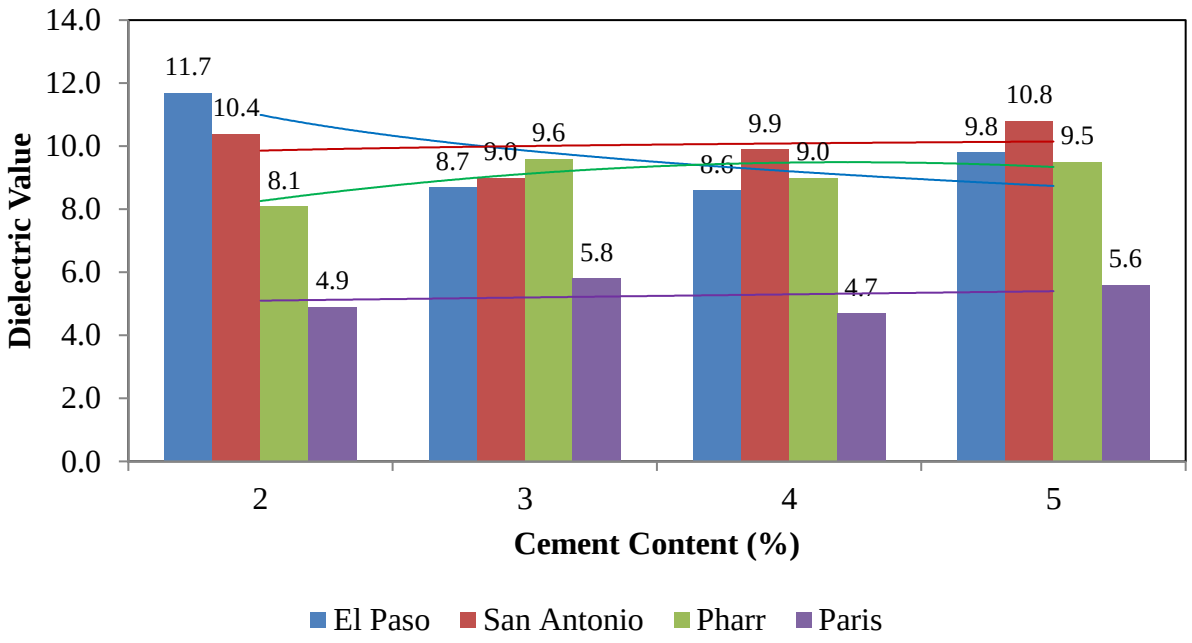

Figure 5.38 – Average Dielectric Values for 10-day Capillary Soak Samples

Seismic Modulus Test

Free-Free Resonant Column (FFRC) test was used to estimate the small strain seismic modulus of the stabilized specimen in the laboratory. FFRC test is primarily based on the estimation of the seismic modulus by means of wave propagation techniques in the continuum. The test is based on Tex-148-E (draft) procedure.

Figure 5.39 through Figure 5.42 present the variations of seismic modulus test results for El Paso, San Antonio, Pharr, and Paris material for 10 consecutive days. The analysis provided in these plots pertains to 6x12 inch specimen for the 10-day capillary soak (TST) procedure. As evidenced in Figure 5.39 through Figure 5.42, increasing the stabilizer contents resulted in higher small strain modulus values. This is in line with expectations and observations in other laboratory tests provided earlier in this chapter.

The ascending nature of the plots is an indication of the favorable influence of the provided moisture to contribute to the strength gain reactions. This information, when combined with the observations outlined for Figure 5.36 and 5.37, explains the insensitivity of dielectric values in 10-day period.

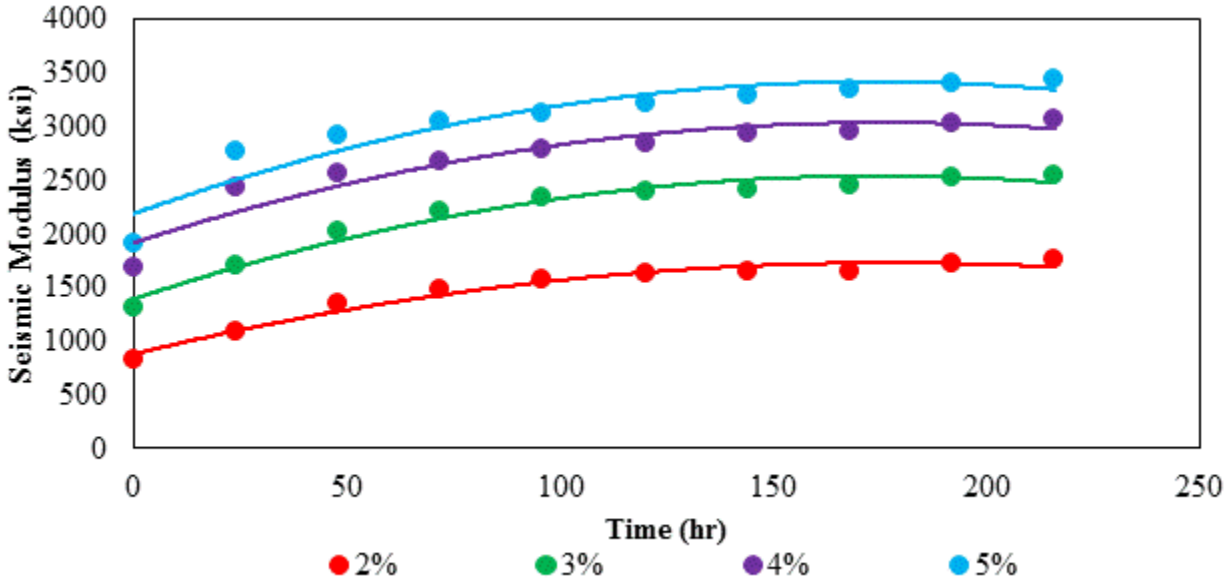

Figure 5.39 – Variations of Seismic Modulus for Paris Sandstone for 10-day Capillary Soak Samples

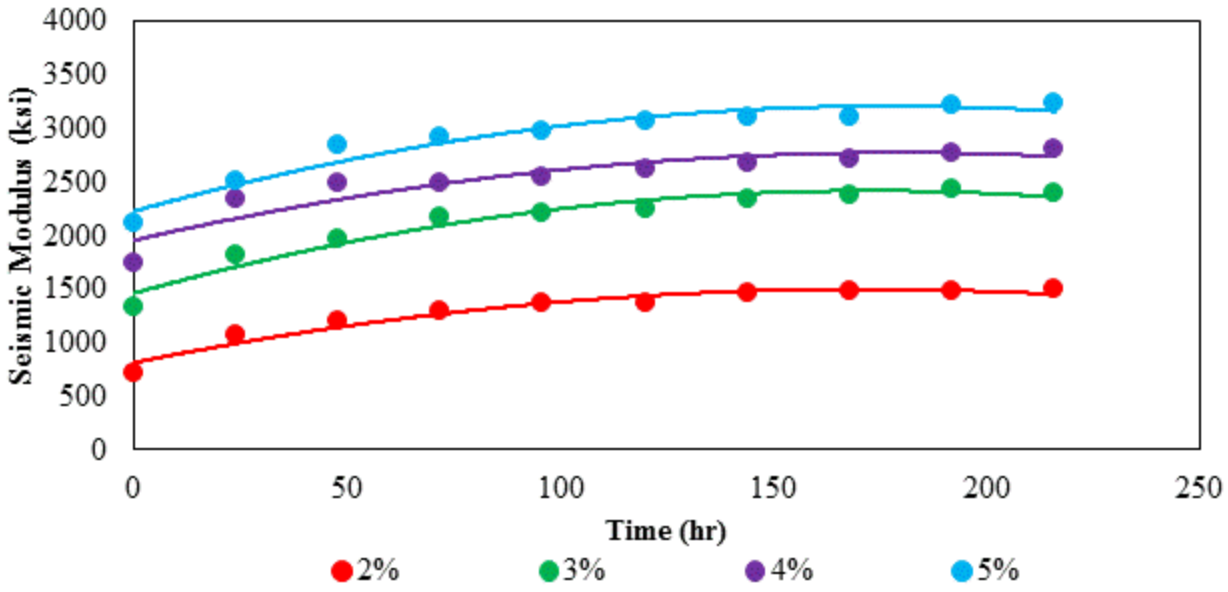

Figure 5.40 – Variations of Seismic Modulus for El Paso Limestone for 10-day Capillary Soak Samples

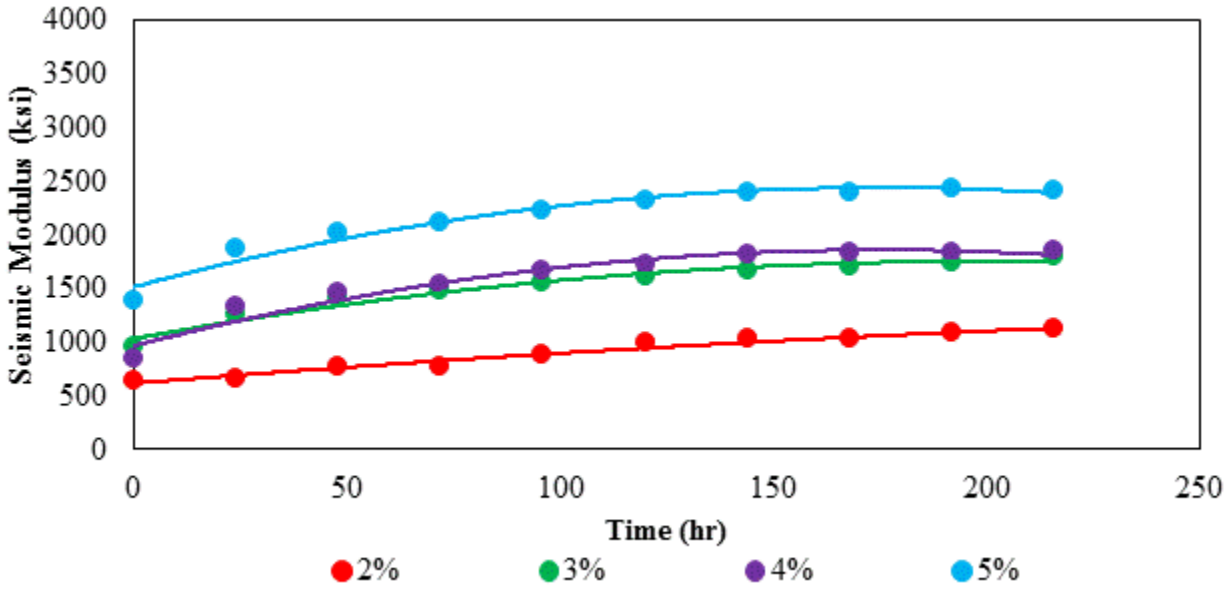

Figure 5.41 – Variations of Seismic Modulus for San Antonio Limestone for 10-day Capillary Soak Samples

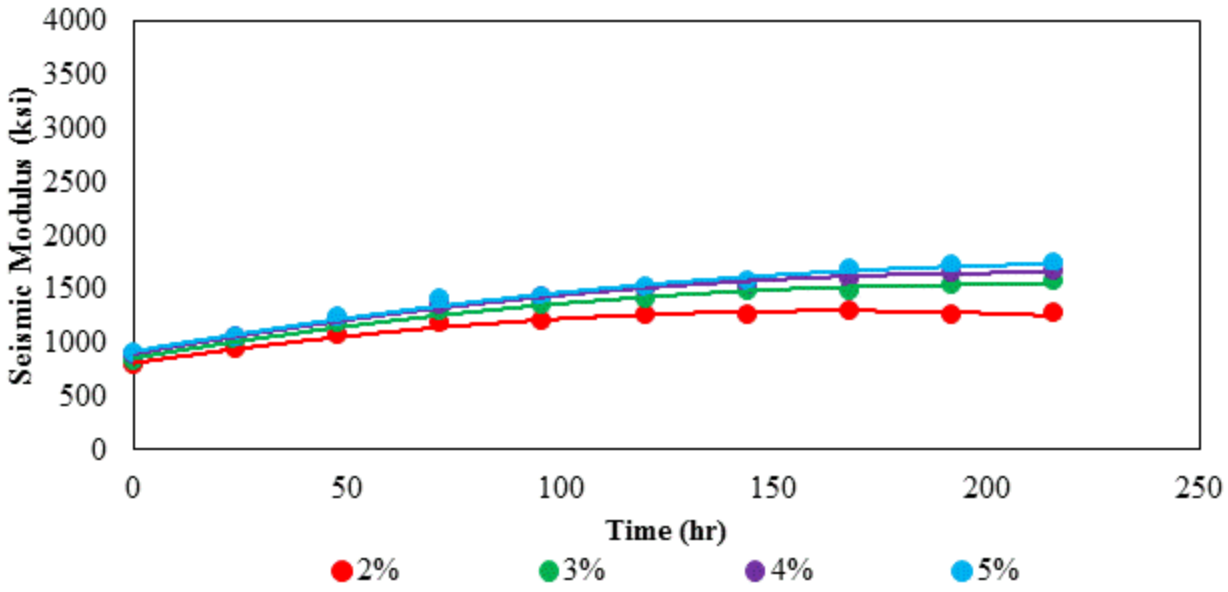

Figure 5.42 – Variations of Seismic Modulus for Pharr Gravel for 10-day Capillary Soak Samples

Figure 5.43 provides the comparative visualization of the seismic modulus values for all [aggregate type-stabilizer content] combinations. Similar to the argument presented for the dielectric constants charts, the calculated seismic modulus values were averaged over the 10 consecutive days to generate Figure 5.43. Therefore, each bar represents the average of 10 measurements, and the plot is generated based on 192 data points for each material or 768 total data points.

Figure 5.44 provides the improvements in the seismic modulus with increasing the stabilizer contents in the mix. The seismic modulus improvements were calculated considering the lowest stabilizer content, two percent cement, as the reference level for each material. The rate of improvements, characterize by the slope of the trend lines, is additional information provided in this plot. As evidenced in Figure 5.44, El Paso and Paris materials were considerably benefitted from the increase in the cement contents in the mix compared to San Antonio and Pharr materials.

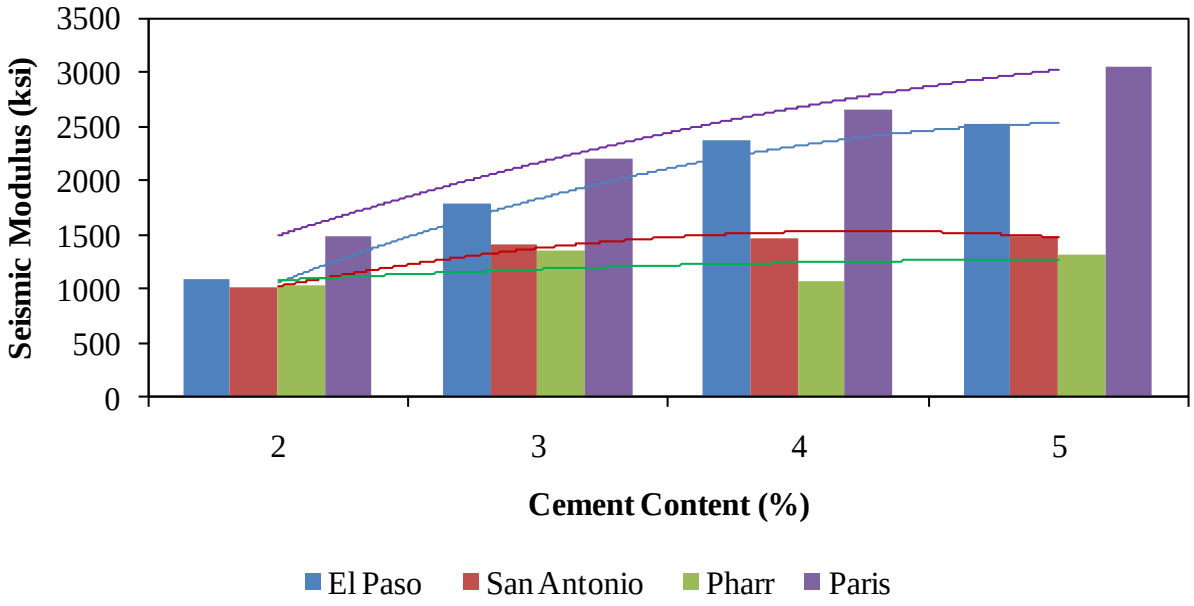

Figure 5.43 – Average Seismic modulus Values for 10-day Capillary Soak Samples

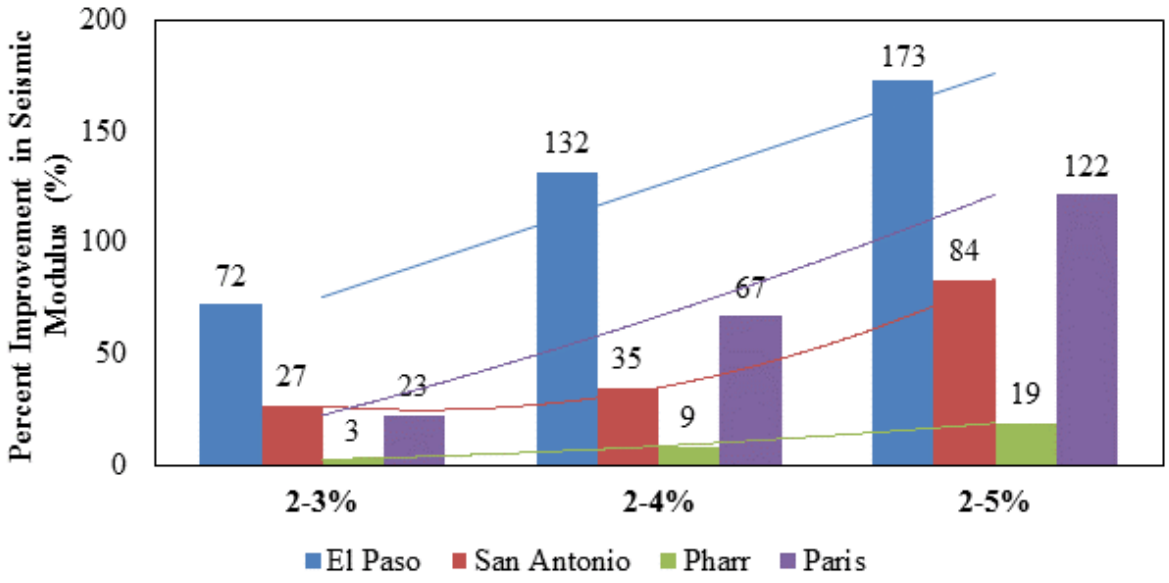

Figure 5.44 – Improvements in Seismic Modulus for 10-day Capillary Soak Samples

Chapter 6. Conclusion and Recommendations

Introduction

The major goal of this project was to develop a reliable and repeatable laboratory testing protocol to assess the fatigue performance of cement stabilized materials. Current Mechanistic Empirical Pavement Design Guide (MEPDG) performance models consider the strength ratio and the modulus of rupture of the stabilized materials as the determining factors that influence the fatigue life of the stabilized layers. There are several systematic errors and practical issues associated with the use of conventional laboratory test methods for the estimation of the modulus of rupture of stabilized materials. These anomalies are more pronounced when low levels of stabilizers are considered by the design engineer. The major sources of inaccuracies, outlined in Chapter 2, are itemized in the following:

a. Practicality issues associated with specimen de-molding and handling of large beams in the laboratory for lightly stabilized materials. Based on our experience and the arguments presented in Chapter 2, the beams tend to disintegrate during the sample extrusion, transportation or even during the conditioning/curing period in the environmental chamber. This potentially compromises the generalization of the developed models as most of the lightly stabilized systems are not testable.

b. Large sample size for third point bending beam test 6 x 6 x 20 in (152 x 152 x 508 in) and therefore the issues associated with the heavy weight of the beam for handling by operators. Based on our laboratory experience, it requires at least two operators to handle and safely transport beams with approximate weight of 60 lbs. to the environmental chamber and later to the test setup.

c. Issues associated with the uniformity of compaction of the stabilized materials in the large beam specimen. Uniformity of the compaction cannot be assured due to the long and relatively shallow nature of the molds in the conventional bending beam test. It should be noted that this test was originally developed for concrete and then extrapolated to the stabilized materials; therefore, little thought was given to the compaction issues of stabilized materials when this procedure was adopted. Based on our experience with this test in the laboratory, we often observed pockets of air void trapped between the rigid mold and the specimen which is indication of the inconsistency of the compaction effort.

d. Systematic error associated with the linear stress distribution assumption in the third point beam test. The commonly used equations for the calculation of the modulus of rupture of materials are based on the linear distribution of the stresses in the cross section of the beam.

A finite element analysis was performed on an arbitrary beam in this research to make the case for the realistic nature of the nonlinear stress dissipation in the traditional tests. This erroneous assumption can be eliminated by proper selection of an alternative laboratory test method.

To achieve the objective of the project, the research team performed a thorough study of the available test methods in the US and abroad for proper characterization of the stabilized materials in the laboratory (Figure 6.1). Additionally, a survey was designed and distributed between the districts to collect relevant data of the ongoing stabilization projects in the state of Texas. The main questions were related to the policies and the rationale behind the selection of the type and the stabilizer contents in the districts across the state. This information was in turn used to develop laboratory experiment design in this project.

Based on the feedback from the project advisory panel, a comprehensive experiment matrix was developed to fully characterize the mechanical behavior of the stabilized materials in the laboratory. This is information was essential for the cross validation of the trend analysis of the newly developed laboratory test. The following tests were incorporated in the experiment matrix:

- ***Unconfined Compressive Strength (UCS) Test:*** This test was performed to provide an indication of the compressive strength of stabilized systems subjected to vertical axial compressive load. This test was the precursor to the submaximal modulus test which helped to determine the dynamic stress levels in the submaximal test. In addition to the compressive strength, features such as degree of nonlinearity, tangent modulus and two measures of secant modulus were extracted from the stress-strain curves in the UCS test.

- ***Submaximal Modulus Test:*** resilient and permanent deformation properties of the stabilized mixes at different stress levels were characterized by the submaximal modulus test. This test was essentially a stress-controlled test utilizing fractions of the UC strength as the imposed dynamic stress level for 5,000 load cycles. This provided valuable information on the influence of the incremental increase in cement contents on the cumulative plastic deformation of the stabilized mixes. Additionally, the deleterious (or beneficial) influence of provided moisture through capillary action on the cumulative plastic deformations was studied using the submaximal modulus test.

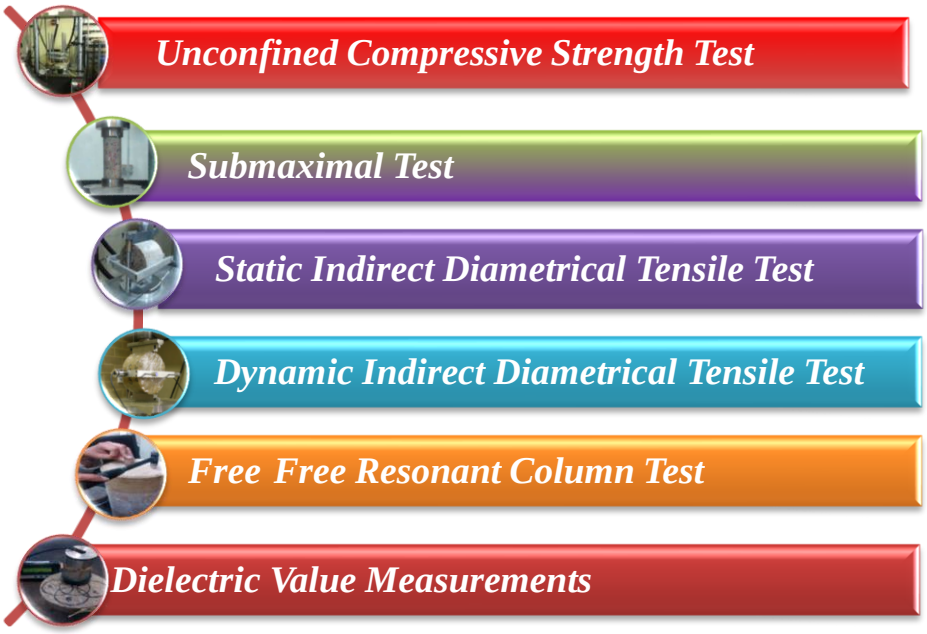

Figue 6.1 – Laboratory Tests Envisioned in the Experiment Design

- ***Static Indirect Diametrical Tensile (S-IDT) Test:*** the static IDT tests were performed at an imposed strain rate of 0.04 in/min to characterize the tensile strength of the stabilized materials. Based on our laboratory observations, this test proved to be a reliable and repeatable test for the determination of the tensile strength of the stabilized materials. Additionally, the relatively uniform tensile stress distribution in the general form of split tension tests, as previously discussed in the FE analysis in chapter 2, would make this a viable option to replace existing third point bending beam test. This test was the precursor to the dynamic IDT test.

- ***Dynamic Indirect Diametrical Tensile (D-IDT) Test:*** the permanent deformation behavior of the stabilized specimen subjected to induced tension was characterized with the D-IDT test. The traditional IDT test setup was modified in this project to study the rate and the magnitude of the progression of plastic deformations due to the induced tension in the samples. Similar to the argument presented for the submaximal modulus tests, a fraction of the tensile strength of the material, namely 20%, 40% and 60% of the S-IDT strength were cycled for 50,000 load repetitions to study the deformation behavior of the materials with high number of load cycles. This information when combined the results of submaximal test provided valuable information on both the compressive and tensile behavior of stabilized systems under repeated dynamic loads. After the completion of the 50,000 load cycles the specimen were subjected to the UCS test to explore the possibility of incurred damage in the materials.

- ***Free-Free Resonant Column (FFRC) Test:*** this test was incorporated in the experiment design as an indication of the small-strain stiffness properties of the laboratory specimen. The periodic measurement of the seismic modulus values during a 10-day period provided valuable information on the rate and the magnitude of strength gain with time and available moisture.

- ***Dielectric Value Measurements:*** the dielectric values at five points at the top of the specimen were measured in a course of a 10-day period for all permutations of the experiment design. This test was incorporated to study the affinity of the aggregates to transport and hold moisture. The information derived from this test when juxtaposed with the FFRC test provided valuable information on the favorable (or deleterious) effect of moisture on the mechanical performance of the stabilized systems.

Table 6.1 provides the total number of samples tested in this project. The laboratory research team preformed trend analysis of the laboratory results to ensure the validity of the data before inclusion in the aggregate database. The laboratory research team highlighted the outliers in the trend analysis for re-test or incorporation of additional replicates. Therefore, Table 6.1 provides the total number of specimens tested in each permutation in the experiment design.

Table 6.1 – Specimen Tested for each Material

Material	UCS	Static IDT	Dynamic IDT			Submaximal Modulus			Total
			20%	40%	60%	20%	40%	60%	
El Paso	26	24	30	32	25	14	16	16	183
San Antonio	17	16	20	20	24	18	19	19	153
Pharr	24	28	19	14	11	20	13	10	139
Paris	20	19	9	8	9	9	10	11	95
TOTAL	87	87	78	74	69	61	58	56	**570**

Monitoring the Moisture Susceptibility of the Stabilized Materials

Two different methods of conditioning/curing of the stabilized materials were incorporated in this research to study the influence of moisture ingress on the mechanical properties of the stabilized materials. The aforementioned methods were:

a. **7-Day Moist Cured:** Stabilized specimens were deposited in a temperature-controlled chamber with at least 95% relative humidity for seven days. Dielectric and seismic modulus values were determined after specimen preparation (first day) and after the 7th day prior to subjecting the samples to destructive laboratory tests.

b. **10-Day Capillary Soak:** Based on the procedure specification Tex-144-E (Draft), stabilized specimens were placed on porous stones in a tub of water at ambient temperature, and were subjected to capillary action for the ten days prior to laboratory testing. Dielectric and seismic modulus values were determined every day for ten consecutive days. The specimens were in turn subjected to destructive laboratory tests according to the experiment design.

The main motivation for the capillary soak procedure was to identify the sensitivity of the aggregates in the experiment matrix to hold and transport unbound moisture. The rationale is that unreacted moisture trapped in the pores can potentially degrade the stiffness properties of the stabilized layers. Additionally, the delayed pozzolanic reactions will result in volumetric instability of the stabilized pavement foundations.

The constant nature of the dielectric value plots presented in chapter five indicated that the moisture state close to the top of the specimen remained constant throughout the day measurements. This information, when combined with corresponding seismic modulus values, revealed that the provided moisture was consumed in the pozzolanic reaction which resulted in improvements in mechanical properties of the mixes. Therefore, the research team concluded that the virgin aggregates selected in this research were not moisture sensitive materials.

Development of New Laboratory Testing Protocol

The main objective of this research was to develop a practical laboratory test for the estimation of the tensile strength of the cement stabilized materials in the laboratory. The following parameters were considered for the development and refinement of traditional protocols:

a. **Practical Aspects:** the proposed test method should be of familiar form (similarity to traditional split tension test) so the laboratory personnel can easily perform this test in the laboratory. Additionally, the sample sizes should be of traditional dimensions to eliminate the necessity to acquire new molds, sample extruder, and etc.

b. **Theoretical Aspects:** the proposed test should conform to robust theoretical principals with the least amount of simplifying assumptions. The finite element analysis of the third point beam test and comparisons with traditional split tension test were performed to better understand the behavior of stabilized specimen in such tests. Figure 6.2 shows the side-by-side comparisons of stress distributions in cross section of the tensile tests. The nonlinear nature of the stresses in the third point beam test imposes a systematic error for the calculations of the modulus of rupture of the stabilized materials.

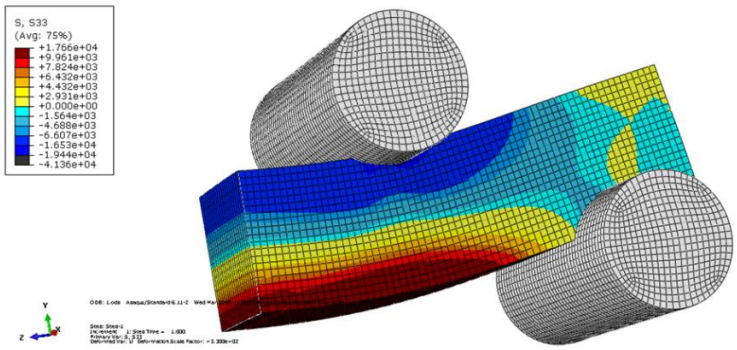

(a)

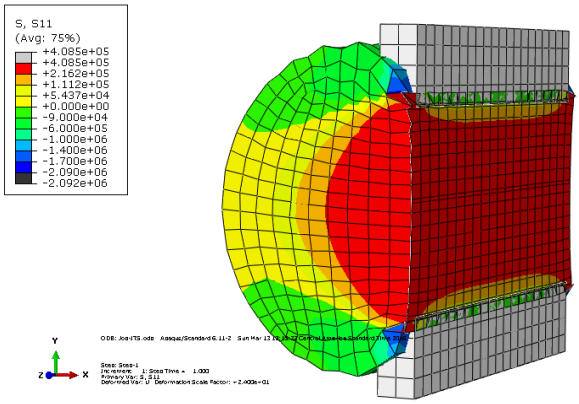

(b)

Figure 6.2 – Nature of Stress Distributions in (a) Third Pint Beam Test (B) Indirect Diametrical Tension Test

Based on the review of the literature, discussions with the technical advisory panel a new variation of the traditional split tension test was developed in the laboratory. The research team designed a new all-around bracket to allow for orthogonal measurements of strains developed during the dynamic loading of the stabilized specimen in the laboratory. The CAD drawing of the brackets and locations of the LVDTs were presented in chapter 4 of this report.

Refinement of the Laboratory Test

Preliminary analysis of the dynamic IDT results for the El Paso limestone materials revealed unexpected noises in the recorded data. Despite the fact that the general trends of the progression of plastic deformations with increasing number of load cycles were meaningful, our research team were concerned about the occasional "jumps" in the permanent deformation data. This was the motivation to adopt a trial and error approach to identify the sources of anomalies and to improve the cyclic IDT test data. Figure 6.2 presents an example of D-IDT results before implementing the modifications to the test setup.

Following adjustments and refinements were implemented to enhance the repeatability of the dynamic IDT test results:

- Experimenting with different types of glues with different chemical compositions and strength profiles.
- Increasing the curing time of the selected glue from two hours, as suggested by the manufacturer, to 24 hours. This proved to have significant influence on the resolution of the test data and the smoothness of [ε_p-N] curves.
- Changing the material type and structure of the brackets. The first prototype of the jig was made of plastic frames as shown in Figure 6.3. Later two generations of aluminum brackets with different stiffeners were designed to reduce the vibrations due to high amplitude of loads applied to stabilized specimen with high cement contents.

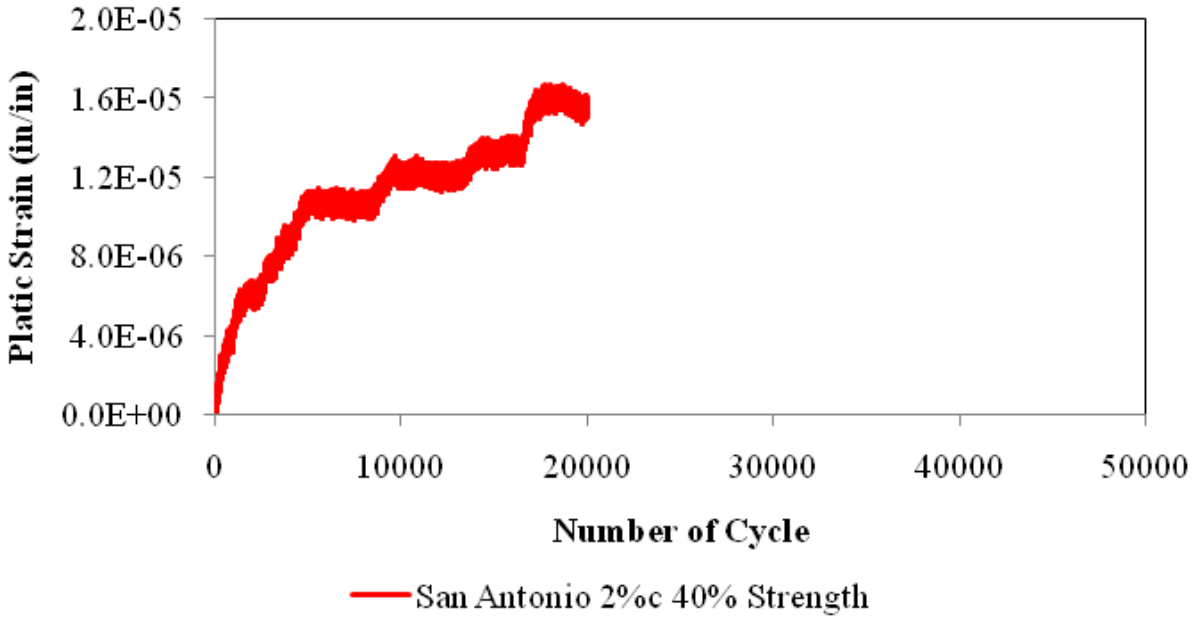

Figure 6.2 – Dynamic IDT Results before Modifications

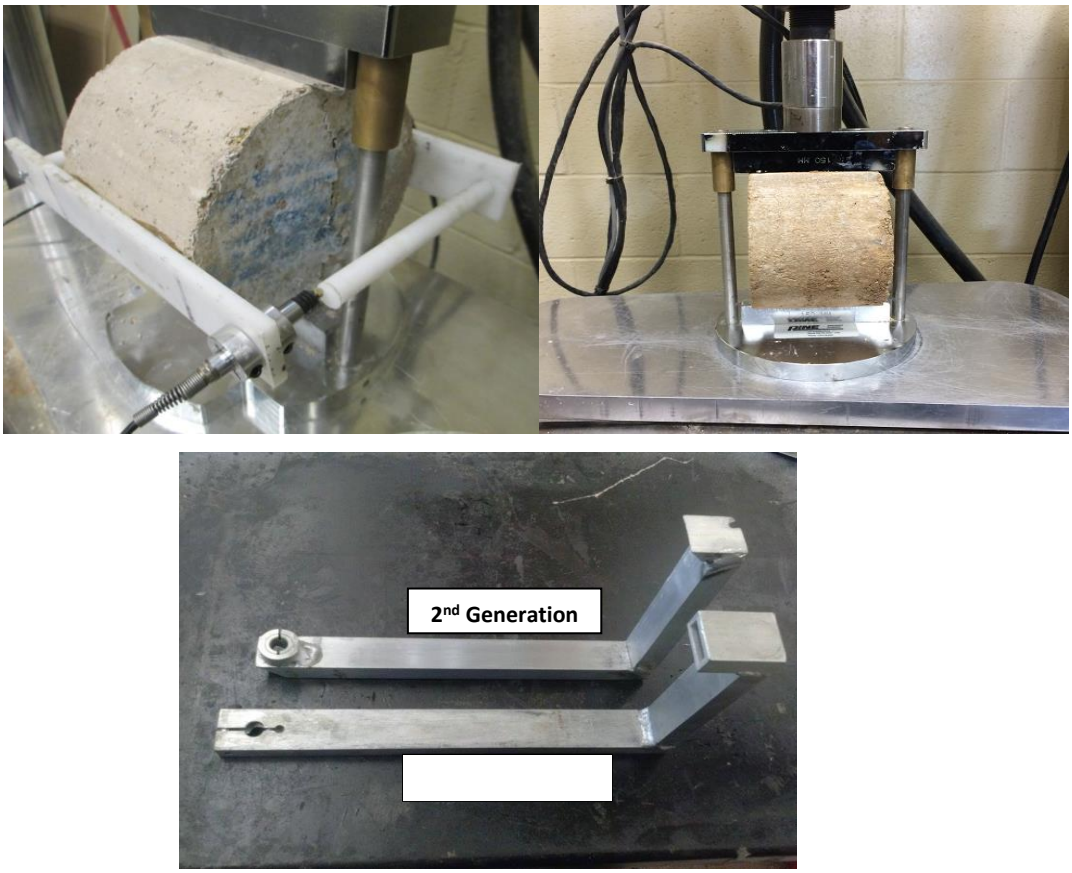

Figure 6.3 – Modifications of Brackets in the IDT Test

- Changing the LVDTs to new transducers with better resolution and range.
- Changing the sample preparation process. One of the noteworthy observations of our laboratory research team was the non-uniform distribution of cement in the specimen after breaking the samples. This was more pronounced when low levels of stabilizers, 2% cement, were added to the mixes. In order to ensure uniform distribution of the cement throughout the samples, we added the cement to the water and then proceeded with mixing and compaction of specimen. The "slurry process" proved to eliminate the pockets of un-hydrated cement after breaking the specimen.
- Changing the number of load cycles from 20,000 to 50,000. Initial analysis of the El Paso limestone materials revealed that for most of the permutations, the rates of the accumulation of the plastic deformations were still ascending at 20,000 load cycles. Since the objective of the project is to identify the fatigue performance of cement stabilized layers subjected to high number of load applications, we decided to increase the number of load repetitions to 50,000 cycles.

Figure 6.4 provides dynamic IDT test results after implementing the series of modifications previously discussed in this section.

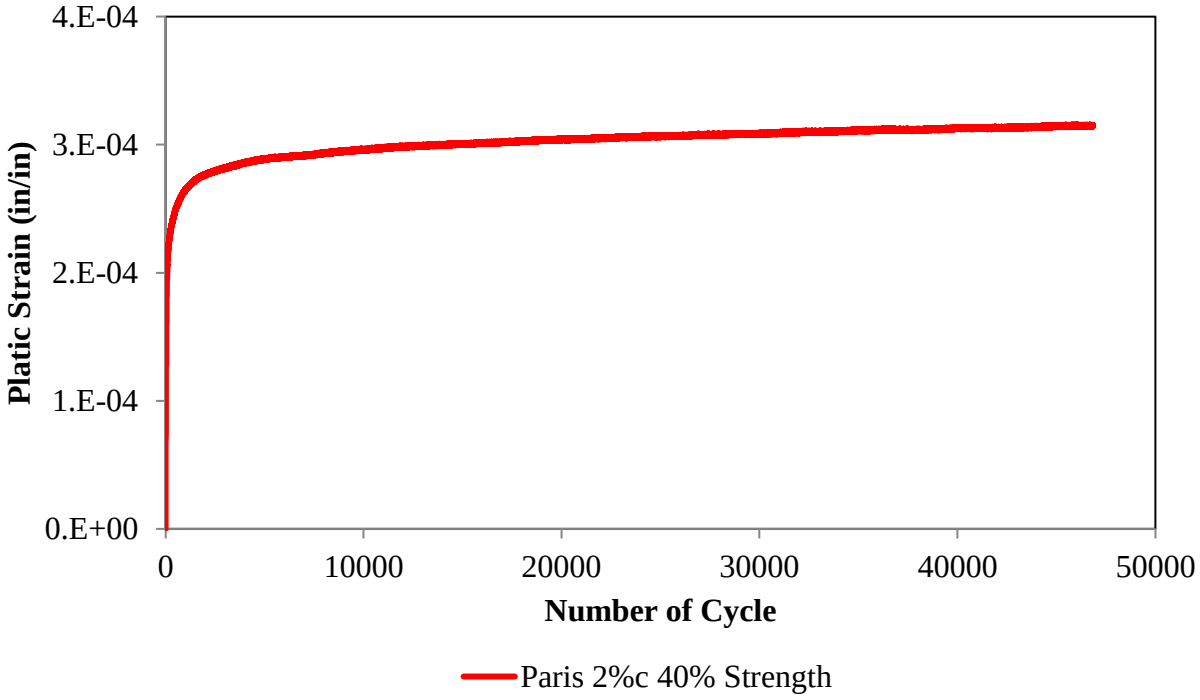

Figure 6.4 – Dynamic IDT Results after Modifications

The efforts pertaining to the development of a new laboratory testing method is summarized in the Appendix A of this report. The research team compiled the details of the testing equipment, CAD drawings, sample preparation, required measurements, and formulations for the calculation of the tensile strength of the cement stabilized materials in a TxDOT specification format. The specification is categorized in two distinct parts: part I pertains to the determination of the tensile strength of 7-day cured stabilized materials and part II is related to the 10-day capillary soak conditions.

The research team recommends the inclusion of dielectric measurement in capillary soak conditions to monitor the moisture susceptibility of stabilized materials in the laboratory. This is of great importance when recycled materials are also considered as an alternative aggregate source in the granular layers. The research team recommends monitoring the influence of moisture in marginal and local materials. Our previous experience underscored the significance of inclusion of moisture susceptibility tests in combination with mechanical tests to properly characterize the degradation of stiffness properties with moisture intrusion.

References

Ashtiani R., D. N. Little and E. Masad. Evaluation of Impact of Fines on the Performance of Lightly Cement Stabilized Aggregate Systems" Transportation Research Record (TRR): Journal of Transportation Research Board, No. 2026, Transportation Research Board of National Academics, Washington D.C. ,2007, pp.81-88.

Arnold, G., and Morkel, C. (2012). "Development of tensile fatigue criteria for bound materials." NZ Transport Agency research report 463.

Burns, S. and Tillman, A. K. (2006). "Evaluation of the Strength of Cement-Treated Aggregate for Pavement Bases" Virginia Transportation Research Council VTRC 06-CR7

Flintsch, G. W., Diefenderfer, B. K., and Nunez, O. (2008). "Composite pavement systems: Synthesis of design and construction practices." Virginia Transportation Research Council, Report No. FHWA/VTRC 09-CR2, Charlottesville, Virginia.

Gaspard, J. K. (2000) "Evaluation of Cement Treated Base Courses." Louisiana Transportation Research Center, Technical Assistance Report Number 00-1TA.

Gnanendran, C. T., and Piratheepan, J. (2008) "Indirect diametrical tensile testing with internal displacement measurement and stiffness determination." Geotechnical Testing Journal, 32(1), 1-10.

Gnanendran, C. T., and Piratheepan, J. (2008) "Dynamic Modulus and Fatigue Testing of Lightly Cementitiously Stabilized Granular Pavement Materials." ASCE Airfield and Highway Pavements.

Gnanendran, C. T., and Piratheepan, J. (2010) "Determination of fatigue life of a granular base material lightly stabilized with slag lime from indirect diametral tensile testing." Journal of Transportation Engineering (ASCE), 136(8), 736-745.

Gupta, S., Ranaivoson, A., Edil, T., Benson, C., Sawangsuriya, A. (2007). "Pavement design using unsaturated soil technology." Final Research Report submitted to Minnesota Department of Transportation, Report No. MN/RC-2007-11, University of Minnesota, Minneapolis.

Khalid, A. H. (2000). "A comparison between bending and diametral fatigue test fo bituminous material." Materials and Structures Vol. 33 457-465.

Khoury, N. N., and Zaman, M. M. (2007). "Environmental effects on durability of aggregates stabilized with cementitious materials." Journal of Materials in Civil Engineering (ASCE), 19(1), 41-48.

Li, Y., Metcalf, I. J. B., Romanoschi, S. A., and Rasoulian, M. (1999). "Performance and failure modes of Louisiana asphalt pavements with soil-cement bases under full-scale accelerated loading." Transportation Research Record 1673, 600, 9-15.

Mahasantipiya, S. (2000). "Performance analysis of bases for flexible pavement." Dissertation submitted for award of Doctor of Philosophy, College of Engineering and Technology, Ohio University.

Majumder, B. K., Das, A., and Pandey, B. B. (1999). "Cement treated marginal aggregates for roads." Journal of Materials in Civil Engineering (ASCE), 11(3), 257-265.

Mbaraga, N. A., Jenkins, J. K., and Van de Ven, M., (2013). "Influence of beam geometry and aggregate size on the flexural strength and elastic moduli of cement stabilized materials." TRB 2014 Annual

Meeting. University of Stellenbosh Institute of Integrated Engineering and Technology, Stellenbosh, Western Cape, South Africa.

Midgley, L., and Yeo, R. (2008). "The development and evaluation of protocols for the laboratory characterisation of cemented materials." AUSTROADS TECHNICAL REPORT APT-T101-08.

Molenaar, A.A.A., and Pu, B. (????) "Prediction of Fatigue Cracking in Cement Treated Base Courses" Delft University of Technology, the Netherlands.

Nazarian S., Yuan D., and Williams R. R. (2003). "A simple method for determining modulus of base and subgrade materials." ASTM STP 1437, ASTM, West Conshohocken, PA, 152-164.

Paul, D. K., and Gnanendran, C. T. (2012). "Characterization of Lightly Stabilized Granular Base Materials by Flexural Beam Testing and Effects of Loading Rate." Geotechnical Testing Journal, Vol. 35, No. 5.

Papacostas, A. (2010). "Prediction of Flexural Strength and Breaking Strain of Cemented Materials: Laboratory Study." AUSTROADS TECHNICAL REPORT AP-T251-13

Paul, D. K., and Gnanendran, C. T. (2013) "Stress–strain behaviour and stiffness of lightly stabilised granular materials from UCS testing and their predictability." International Journal of Pavement Engineering, 14:3, 291-308

Paul, D. K., and Gnanendran, C. T. (2012) "Characterisation of Lightly Stabilised Granular Base Materials by Flexural Beam Testing and Effects of Loading Rate" Geotechnical Testing Journal, Vol. 35, No. 5.

Puppala, A. J., Hoyos, L. R., and Potturi, A. K. (2011). "Resilient moduli response of moderately cement-treated reclaimed asphalt pavement aggregates." Journal of Materials in Civil Engineering (ASCE), 23(7), 990-998.

Scullion, T., Uzan, J., Hilbrich, S., and Chen, P. (2008). "Thickness Design Systems for Pavements Containing Soil-Cement Bases." SN2863, Portland Cement Association, Skokie, Illinois.

Scullion, T., Sebesta, S., Estakhri, C., Harris, P., Shon, C., Harvey O., and Rose-Harvey, K. (2012) "Full-Depth Reclamation: New Test Procedures and Recommended Updates to Specifications" Texas Transportation Institute FHWA/TX-11/0-6271-2

Sobhan, K., and Das, B. M. (2007). "Durability of soil–cements against fatigue fracture." Journal of Materials in Civil Engineering (ASCE), 19(1), 26-32.

Yan, W., Weihong, X., and Xiaotong, F. (2011). "Studies on fatigue behaviors of cement stabilized macadam mixture." Emerging Technologies for Material, Design, Rehabilitation, and Inspection of Roadway Pavements, Geotechnical Special Publication No. 218 ASCE.

Zhou, F., Fernado E., and Sculion T. (2010) "Development, Calibration, and Validation of Performance Prediction Models for the Texas M-E Flexible Pavement Design System." Texas Transportation Institute FHWA/TX-10/0-5798-2

APPENDIX A. Draft Specification

Test Procedure for

STATIC INDIRECT DIAMETRICAL TEST (S-IDT) FOR THE LABORATORY DETERMINATION OF THE MODULUS OF RUPTURE OF CEMENT STABILIZED SPECIMENS

Texas Department of Transportation

TxDOT Designation: Tex-XXX-E

Effective Date: January 201X

SCOPE

This procedure consists of two different methods.

Part I determines the tensile strength of compacted soil-cement specimens after seven days of curing in a moisture chamber (7-day-moist-cured tensile strength).

Part II determines the tensile strength of compacted soil-cement specimens after ten days of subjecting the specimen to capillary soak (TST-Tube Suction Test tensile strength).

Both methods require the compaction of the specimens with the following parameters: 10 lb. hammer, 18-inch drop, 50 blows/layer using 6 x 4.5 in. mold.

APPARATUS

As outlined in test methods:

Tex-101-E

Tex-113-E

Tex-117-E

Tex-114-E

Tex-226-F

Compression testing machine, with nominal capacity of 270 MN (60,000 lb), meeting the requirements of ASTM D-1633.

Triaxial screw jack press (Tex-117-E), used when anticipated strengths are not in excess of 2.8 MPa (400 psi).

Metal Jigs, used for indirect diametrical strength test.

MATERIALS

Hydraulic (Portland) cement.

Tap water.

PREPARING SAMPLE

Prepare approximately 90 kg (200 lb) of material in accordance with Tex-101-E part II.

Mix 12 lb of dry material following the graduation requirements outlined in Item 247 to prepare 6 x 4.5 in. specimens.

PART I—INDIRECT DIAMETRICAL TEST METHOD FOR 7 DAY MOIST CURED SPECIMEN

PROCEDURE

Determine the optimum moisture content and maximum density for a soil-cement mixture in accordance with Tex-113-E. The amount of cement added is a percentage based on the dry mass of the soil. To calculate the amount of cement added to the mixture, multiply the percentage of cement by total weight of the dry soil.

—In calculating the actual dry density of the laboratory mixed soil-cement specimens, the dry mass of the material is the total mass of the oven dry soil in the specimen plus the mass of the cement.

Calculate the amount of water in accordance with the optimum moisture content of the mixture. Incrementally adjust the molding water content with the increasing (or decreasing) the percentage of cement in the mix. The slight modification is envisioned to compact the soil-cement mix near the optimum moisture content, and to avoid performing a new moisture-density (M/D) curve for each percentage of cement.

Referring to Tex-120-E, use the following guideline to adjust for the molding water content:

*% molding water = % optimum moisture content from M/D curve + 0.25 * (% cement increase),*

Where:

% cement increase = difference in cement content between curve and other cement contents.

Place the predetermined amount of cement in a medium bowl. Add half of the molding water and mix thoroughly. Use spatula to mix cement and water. Mix uniformly while adding the remainder of the molding water to eliminate possible cement clumps.

Add cement and water mixture to the dry soil. Mix thoroughly.

Compact the specimen in three layers using Tex-113-E compaction effort. Compact three identical specimens for each percentage of cement. Cure and test for indirect diametrical test.

Set aside approximately 0.7 to 1.0 kg (1.5 to 2.0 lb) of each mix to for the determination of the moisture content after compaction.

Place a card on the lateral side of each specimen showing the laboratory identification name and the percent of cement used.

Store the specimens in the moisture chamber immediately after recording the height, diameter, and weight measurements. Ensure the chamber temperature is set at 27°C (80°F) and maintains at least 95% relative humidity. Monitor the relative humidity and the temperature of the chamber periodically during the seven-day curing period of the specimen.

Remove the specimens after the seven-days of curing in the moisture chamber, and dry any free moisture on their surfaces with a dry cloth.

Transfer the specimens to the automated loading frame and proceed with the set up as shown in Figure 1.

Apply 10 lb (4.5 kg) to lower the load frame to place the specimen in contact with the load frame. Make sure that the load frame is in contact along the specimen surface and clean of debris in accordance with Tex-117-E, Section 5.19.

Offset the load cell readings to zero.

Apply strain rate of 0.04 in/min (0.1 mm/min) until the specimen fails in accordance with Tex-226-F.

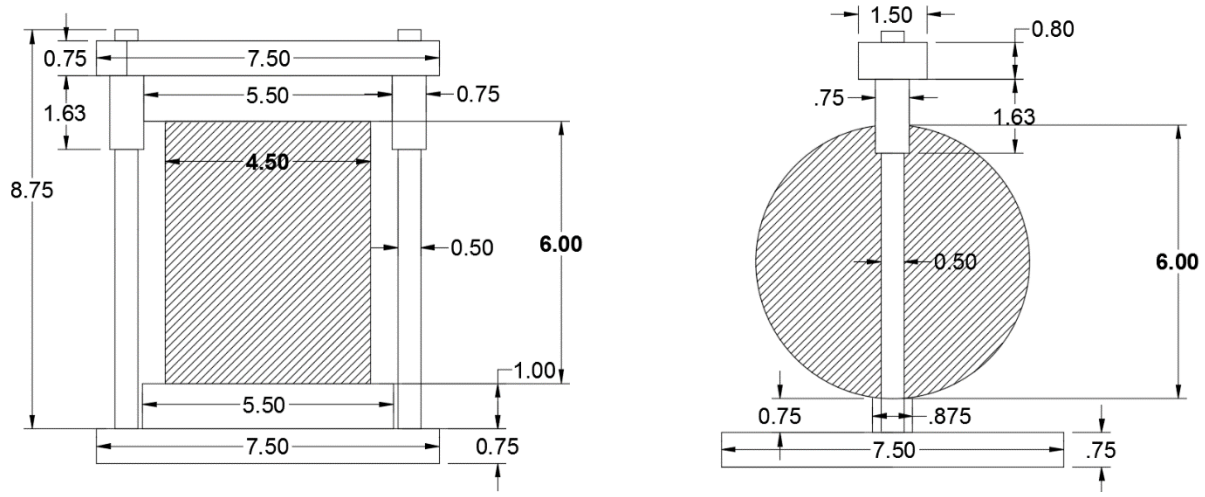

Figure 1— Specimen Set Up and Dimensions of the Static IDT.

CALCULATIONS

Use the electronics data sheets provided with Tex-117-E to calculate and record the following.

Calculate vertical stress (σ) in lb/in^2 (psi)

$$\sigma = \frac{2p}{\pi DL}$$

Where:

p = Maximum vertical load applied to the specimen, lb (N)

D = Specimen diameter, in. (m)

L= Specimen length, in. (m)

Calculate vertical strain (ε) in in. /in., (mm/mm)

$$\varepsilon = \frac{D_f - D_i}{D}$$

Where:

D_f= Final deformation, in. (mm)

D_i =Initial deformation, in. (mm)

D = Specimen diameter, in. (mm)

GRAPHS AND DIAGRAMS

Use the electronics data sheets in form Tex-113-E to plot the following

Moisture-density curves.

Use the electronics data sheets in form Tex-117-E to plot the following

Stress-strain-diagram.

Determine the stress at failure as the tensile strength of the material

---

TEST REPORT

Molding moisture to the nearest 0.1%.

Specimen height permissible to ± 6.35 mm considering 114.3 mm as optimum height. (± 0.25 in., optimum height 4.5 in)

Dry density to the nearest 1 kg/m^3 (0.1 pcf).

Indirect diametrical strength to the nearest whole kPa (psi) for each cement content tested.

Recommended cement content to the nearest 0.5 percent.

—Store cement in airtight container.

PART II—TENSILE STRENGTH TEST METHOD-TUBE SUCTION TEST

PROCEDURE

Follow 5.1 to 5.4.

After recording the weight, diameter and height of the specimen, extrude the specimen from the mold and immediately cover the specimen using a rubber membrane. Make sure the membrane is free of porous holes.

Place the specimen at room temperature on the top of a porous stone in a water supply pan.

Make sure the porous stone is clean and unclogged to be able to transport water through micro-pores to the specimen through capillary action. The water surface must be 0.25 in. away from the top of the porous stone.

Subject three identical specimens prepared for each cement content to capillary action for ten days.

Place a card on each specimen showing the laboratory identification name and the percent of cement used.

Carefully remove the rubber membrane upon completion of 10 days of capillary soak at ambient temperature. Use a cloth to dry any free water from the top and the bottom of the specimen. Transport the specimen to the automated loading frame.

Follow 5.7-5.8.2

CALCULATIONS

Follow 6.1-6.3

GRAPHS AND DIAGRAMS

Follow 7.1-7.3

TEST REPORT

Follow 8.1-8.5

APPENDIX B. Survey Questionnaire

Survey for TxDOT Research Project 0-6812

District: _____Contact Person: _____

Telephone number and e-mail: _____

1. Do you use Portland cement to stabilize the base layers in your district?
☐ Often ☐ Sometimes ☐ Never

2. If often or sometimes, in your judgment how many such projects have been completed in the last 5 years or are scheduled to be constructed in the near future in your district?
_____Project(s).

3. Please indicate the percentage of cement content that you typically use for the stabilization of the aggregate base layers (check all that applies).
☐ 2% ☐ 3% ☐ 4%
☐ 5% ☐ 6% ☐ Other (please specify in %) _____

4. The cement content is usually estimated based on
☐ Local experience ☐ Laboratory testing ☐ District/Area office preference
☐ Other (please specify) _____.

5. Are there any strength requirements for cement stabilized base in your district? If so, what are the typical requirements?
☐ Yes ☐ No

6. Are there any other requirements for cement stabilized base in your district? If so, what are they?
☐ Yes ☐ No

7. Please indicate the most common aggregate type(s) and the quarries you used to obtain aggregates for cement stabilized base layers.
☐ Limestone from _Hanson Perch Hill_____ ☐ Granite from _____
☐ Gravel from _____ ☐ Other (please specify)_____

8. As per Item 275, please indicate the Grade that you most frequently use for cement stabilized base layers.
☐ Grade 1 ☐ Grade 2 ☐ Grade 3 ☐ Grade 4

9. Could you please comment on any area that this research should address to help you?
_____

10. Do you mind if we contact you for more information?
☐ Yes ☐ No

APPENDIX C. Submaximal Test Results

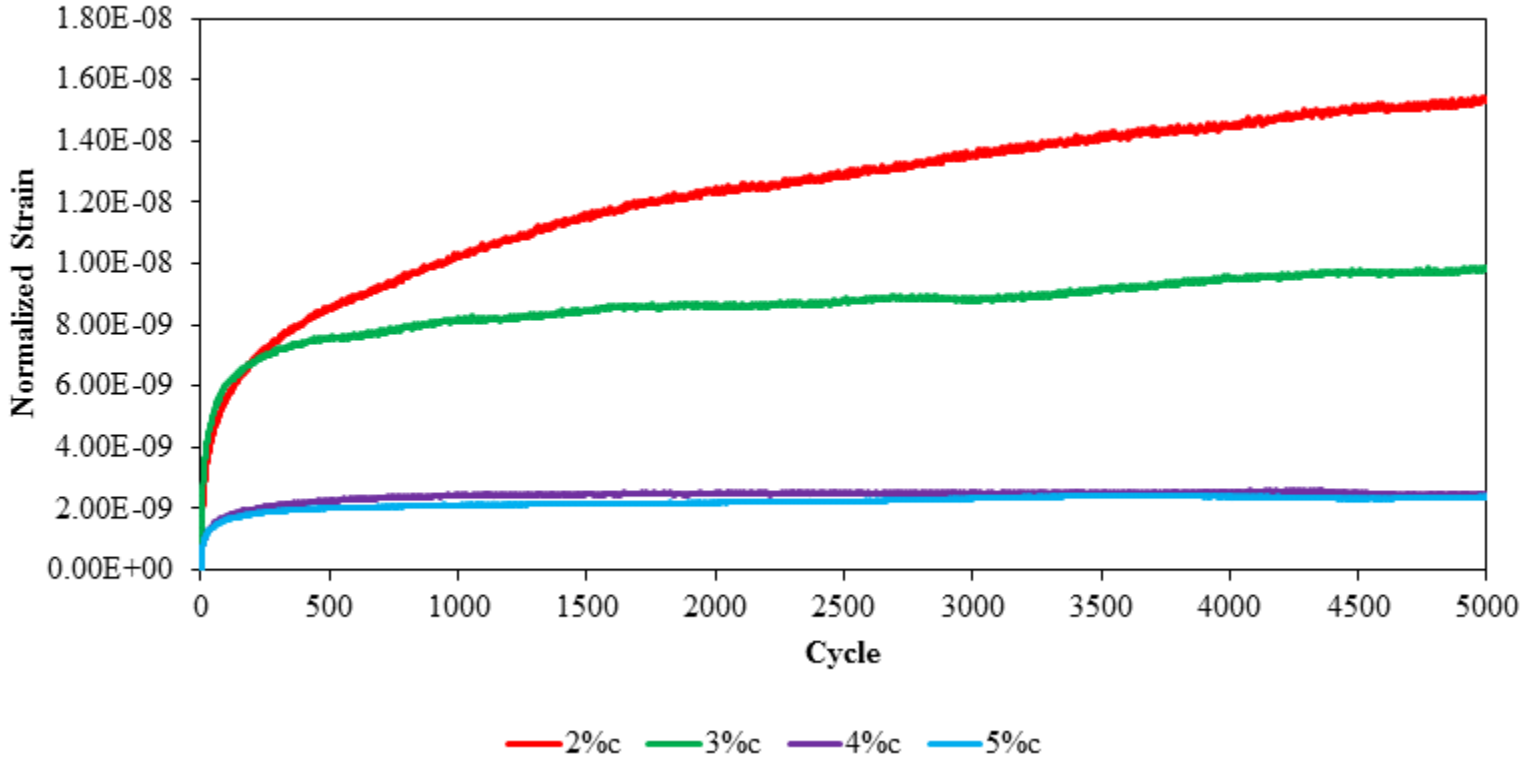

Figure C.1 – Permanent Deformation for El Paso Material @20% UCS Strength for 7-day Moist Cured Samples

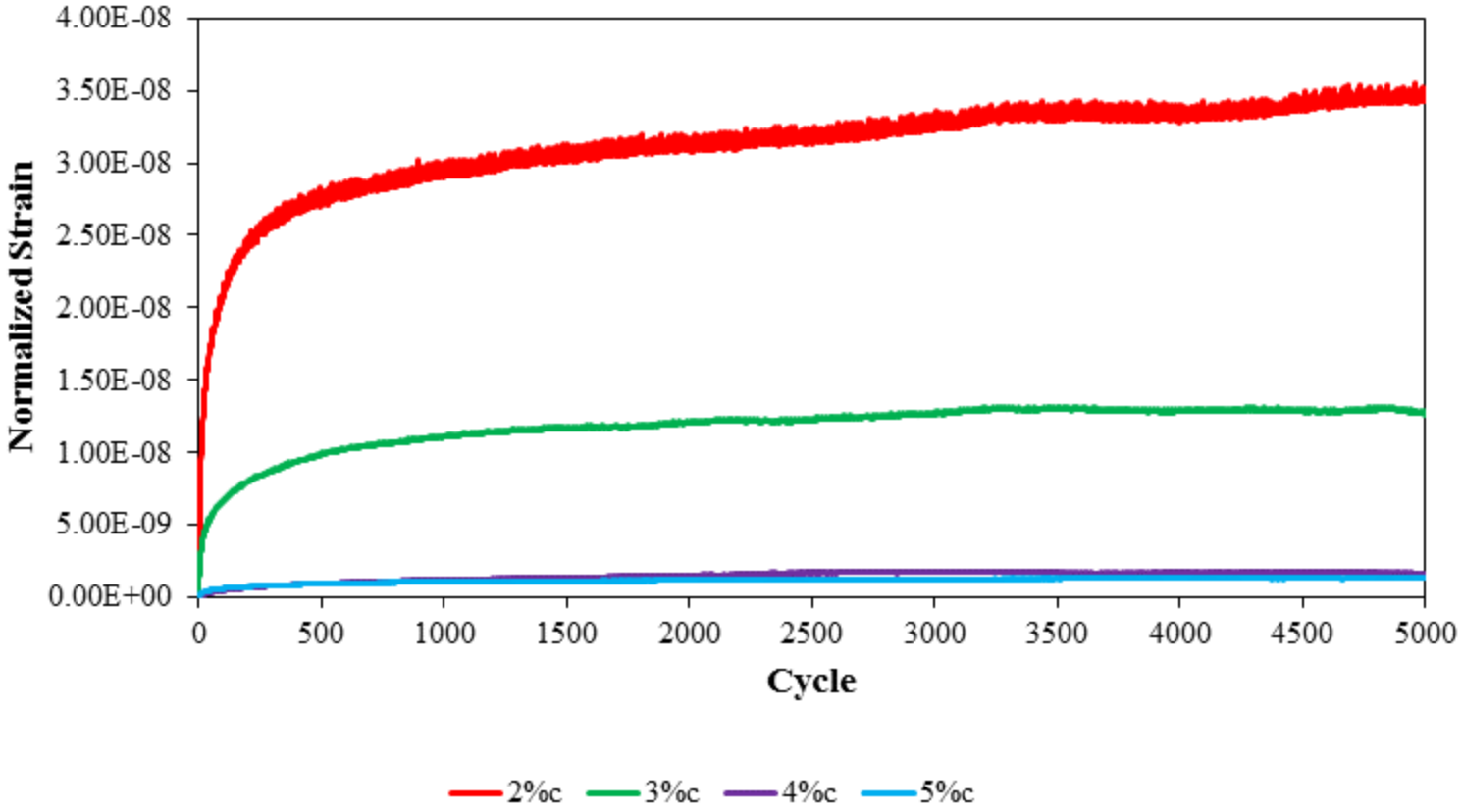

Figure C.2 – Permanent Deformation for El Paso Material @20% UCS Strength for 10-day Capillary Soak Samples

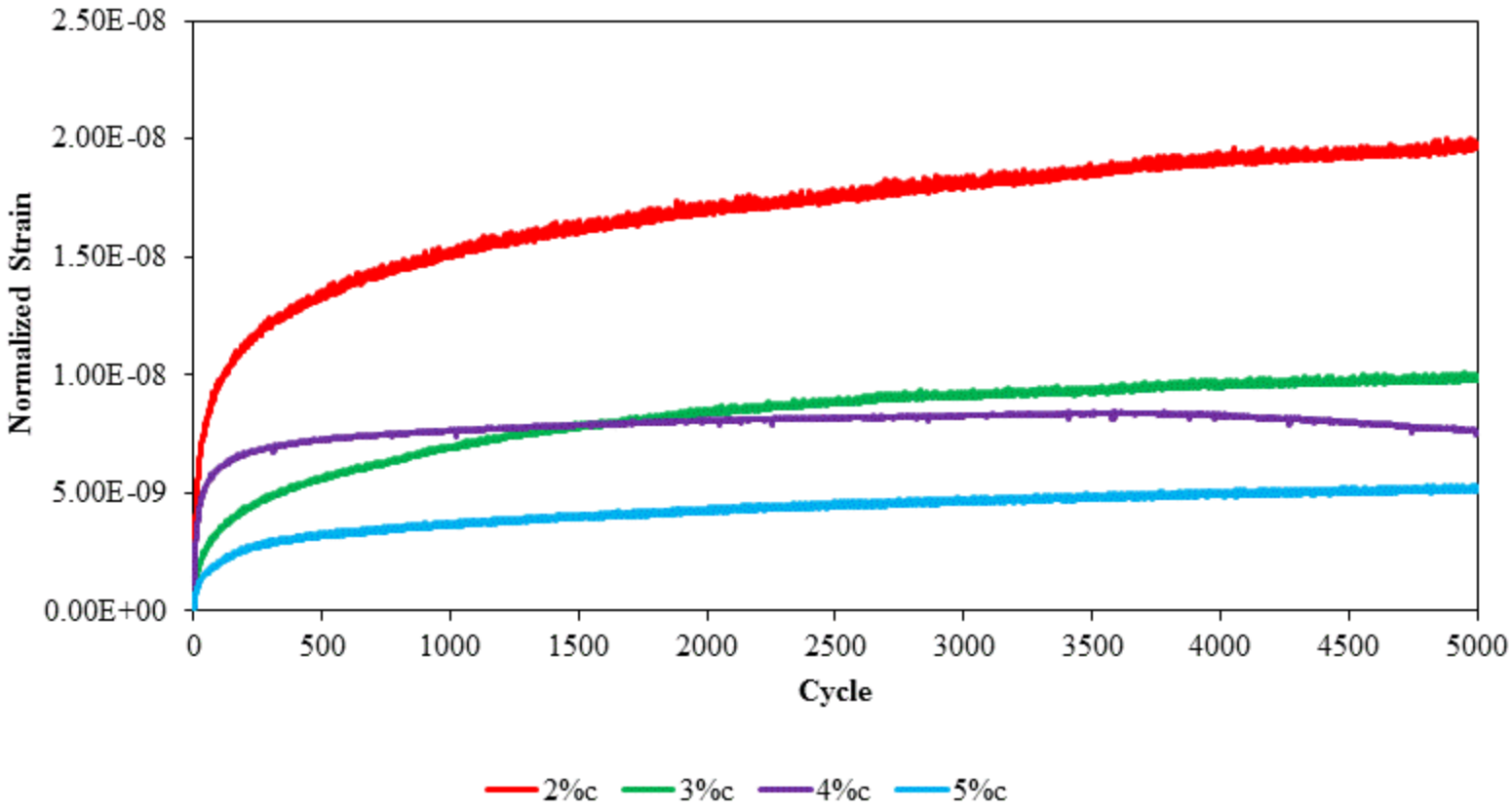

Figure C.3 – Permanent Deformation for San Antonio Material @20% UCS Strength for 7-day Moist Cured Samples

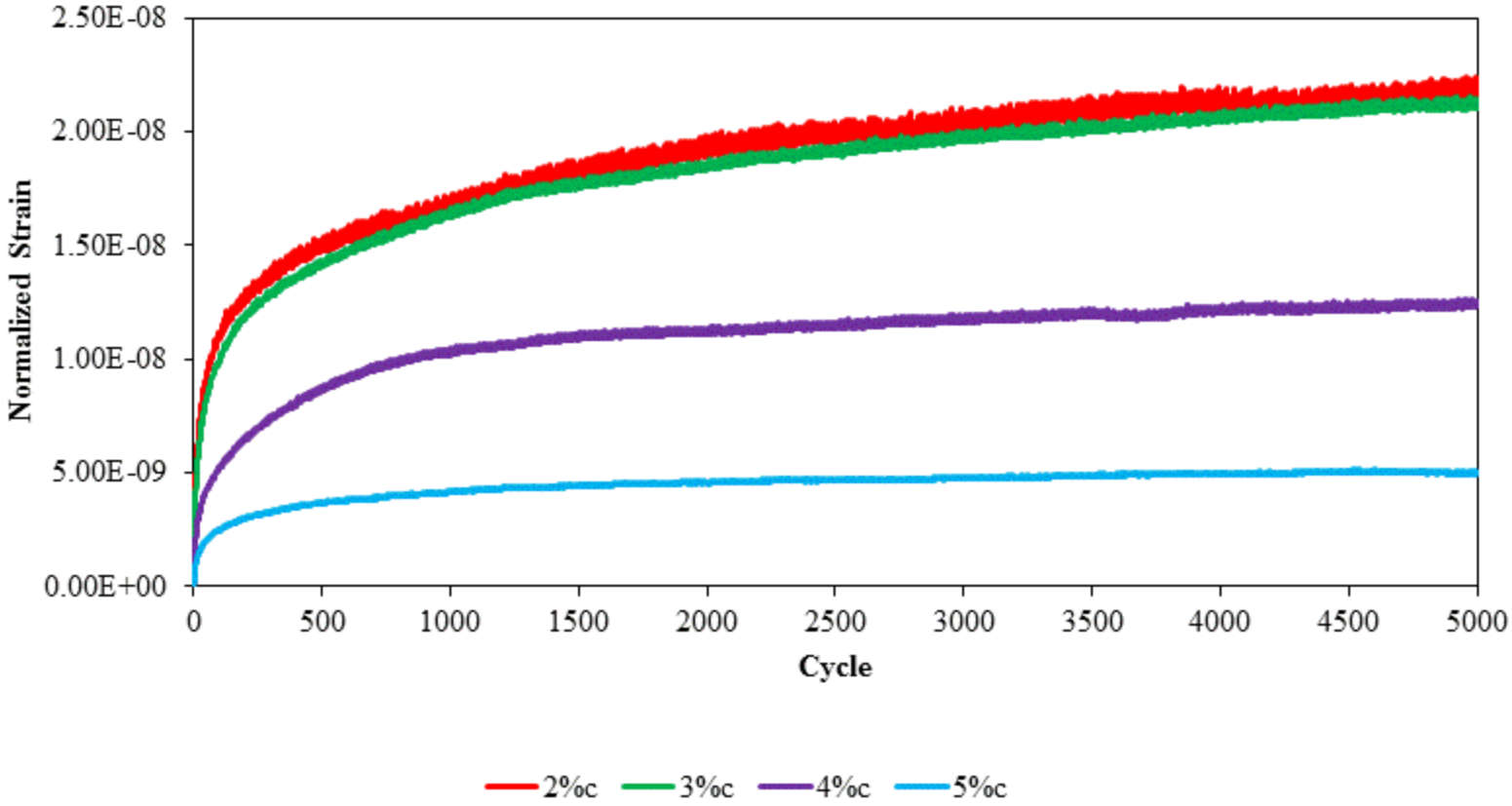

Figure C.4 – Permanent Deformation for San Antonio Material @20% UCS Strength for 10-day Capillary Soak Samples

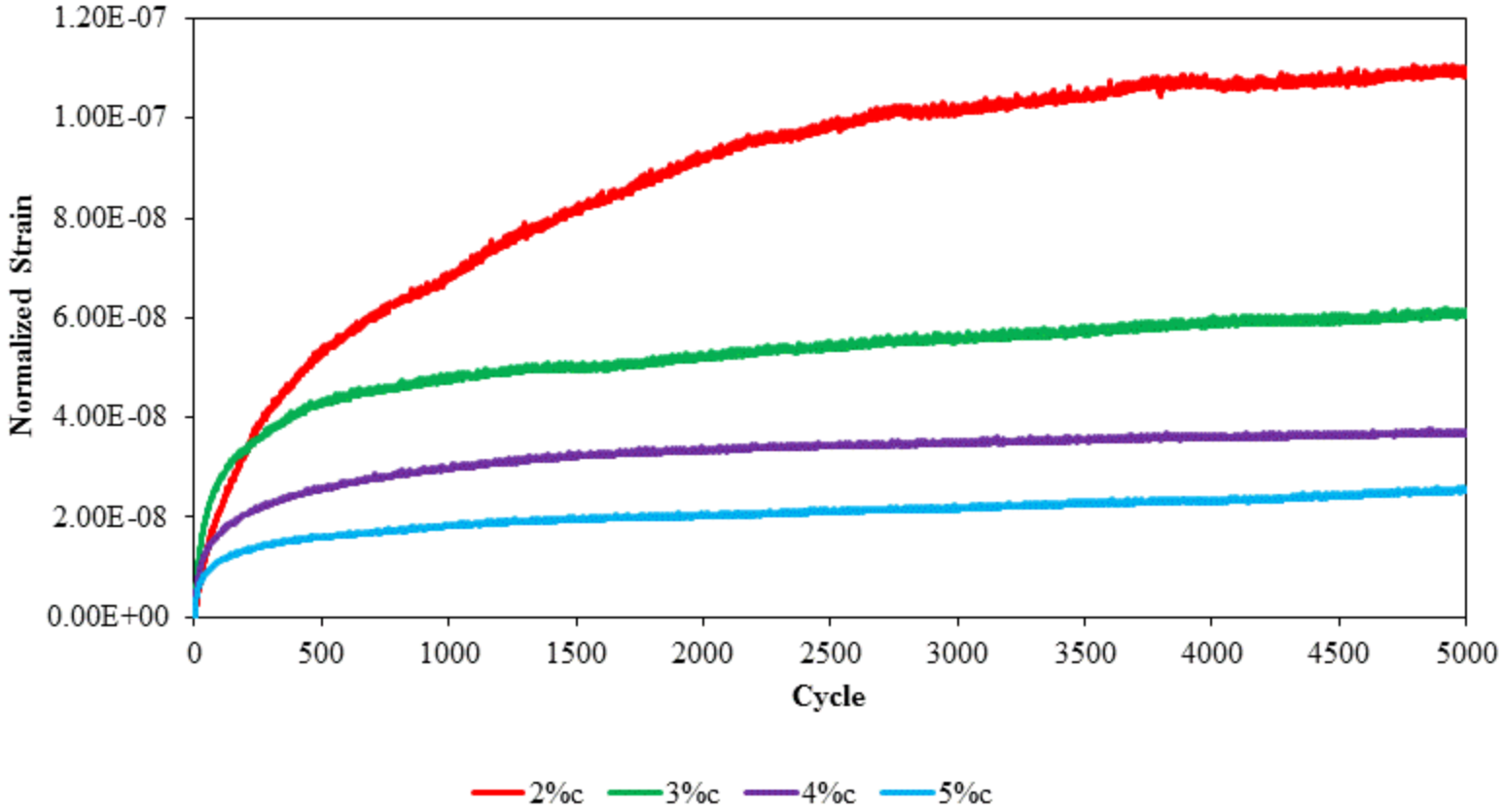

Figure C.5 – Permanent Deformation for Pharr Material @20% UCS Strength for 7-day Moist Cured Samples

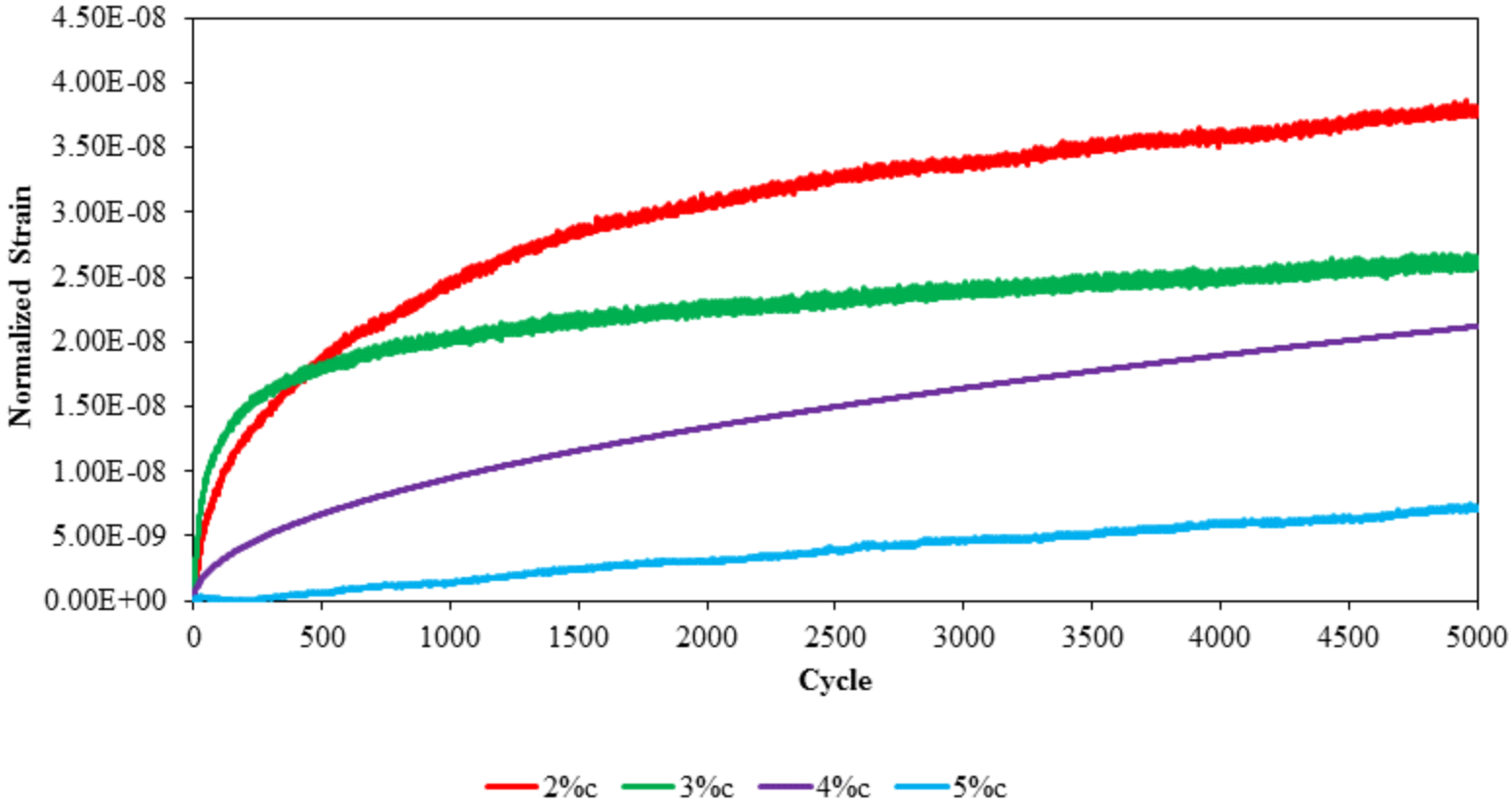

Figure C.6 – Permanent Deformation for Pharr Material @20% UCS Strength for 10-day Capillary Soak Samples

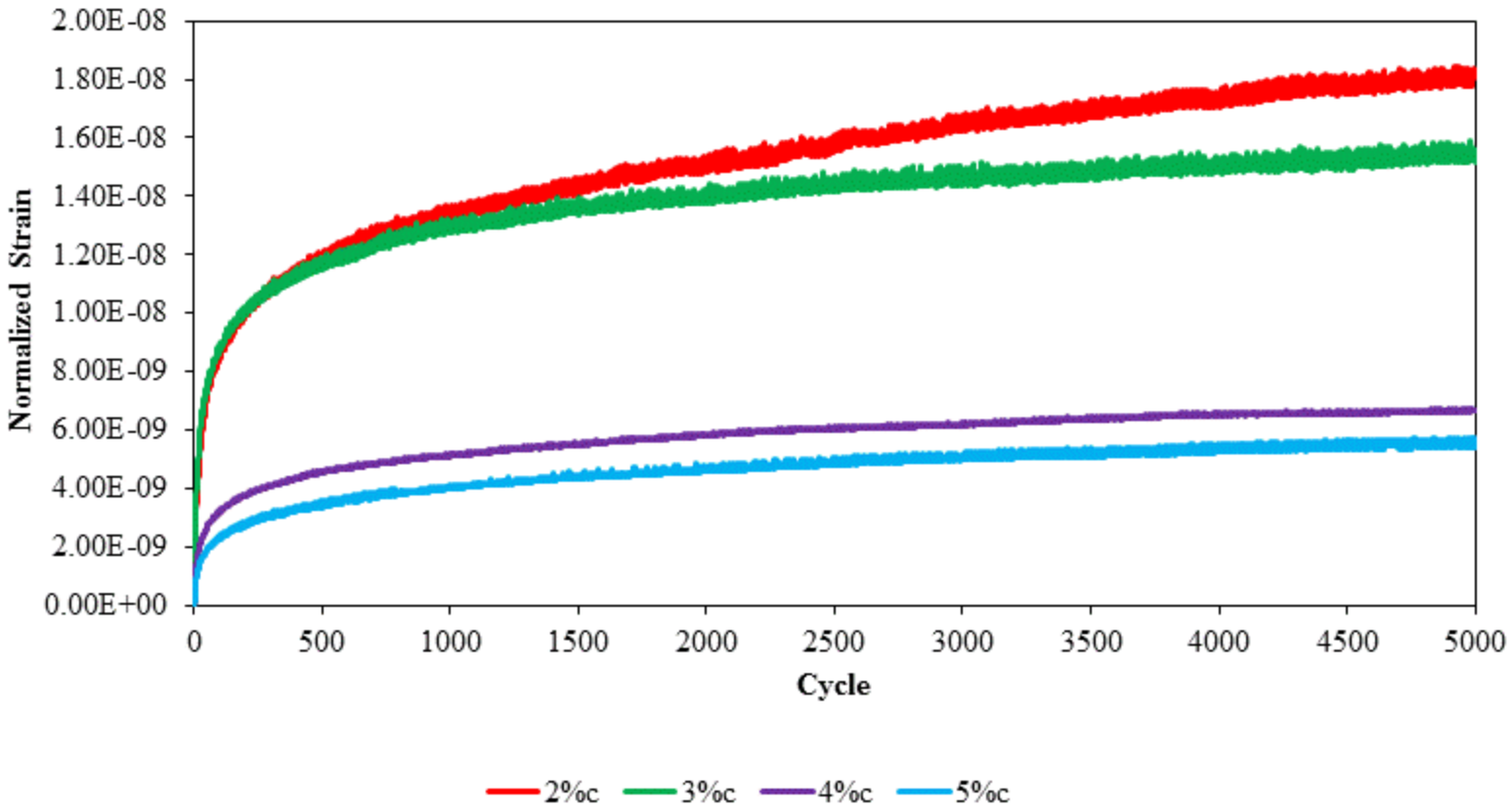

Figure C.7 – Permanent Deformation for Paris Material @20% UCS Strength for 7-day Moist Cured Samples

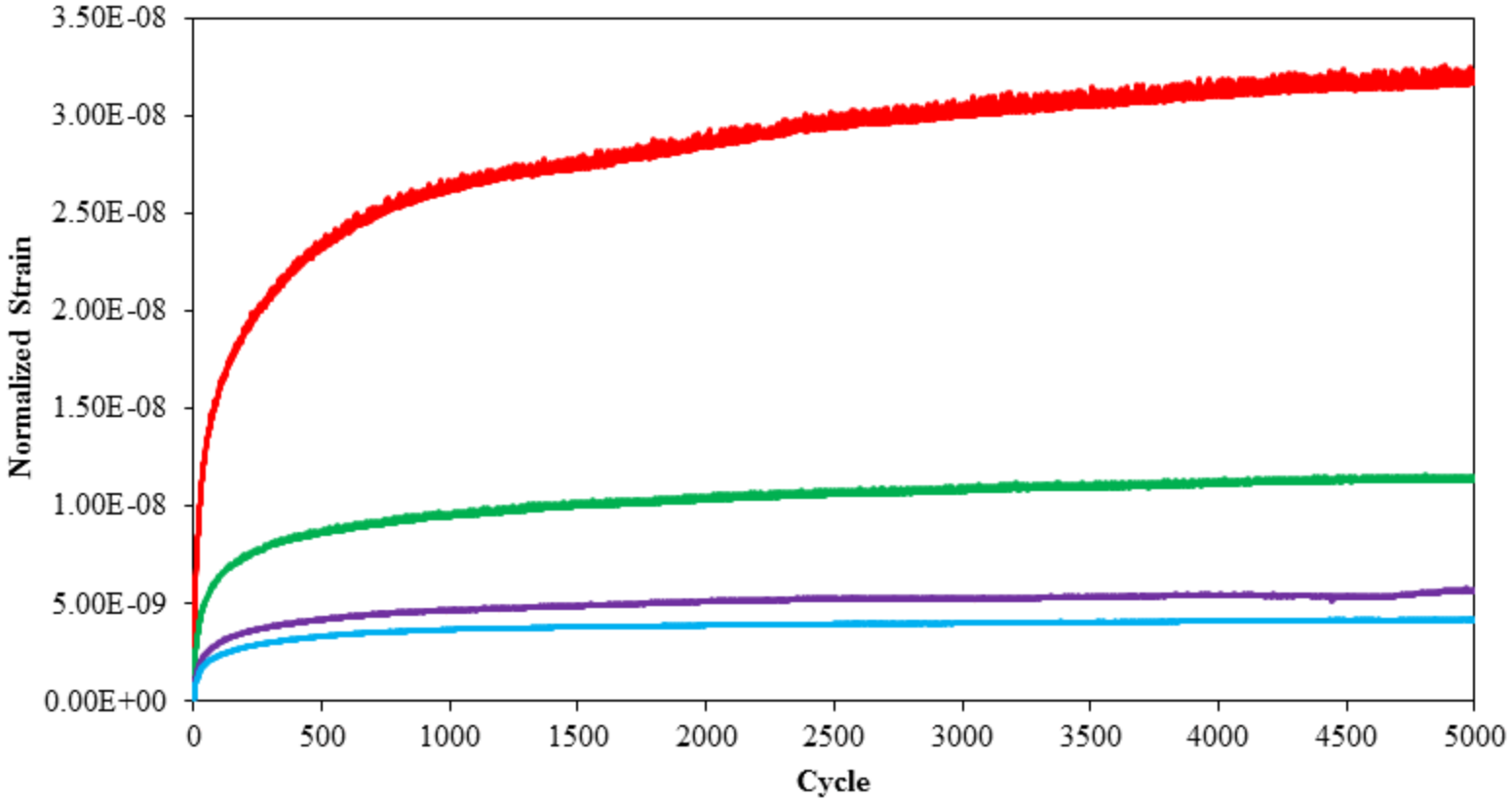

Figure C.8 – Permanent Deformation for Paris Material @20% UCS Strength for 10-day Capillary Soak Samples

APPENDIX D. Dynamic IDT Test Results

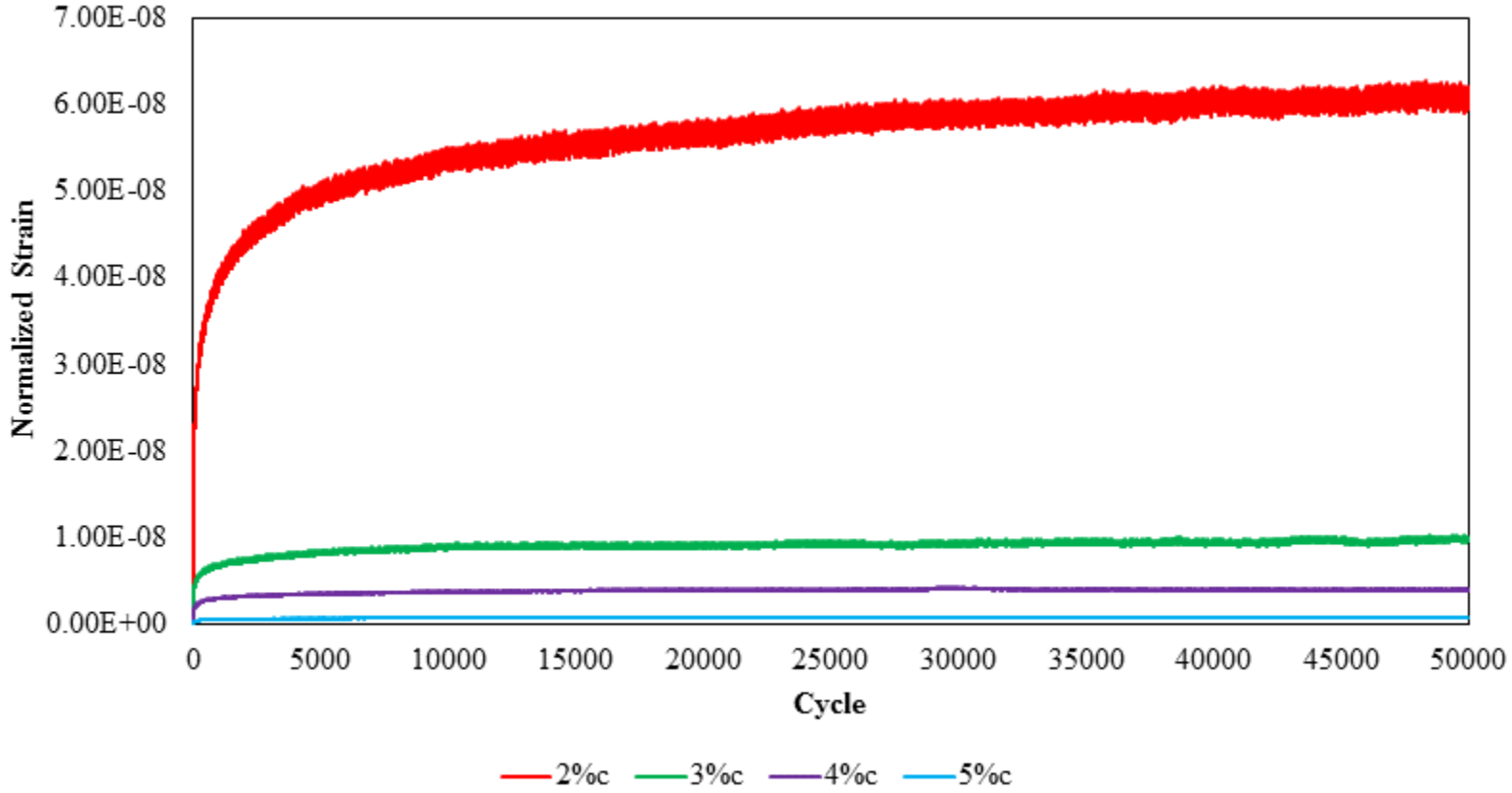

Figure D.1 – Permanent Deformation for El Paso Material @20% IDT Strength for 7-day Moist Cured Samples

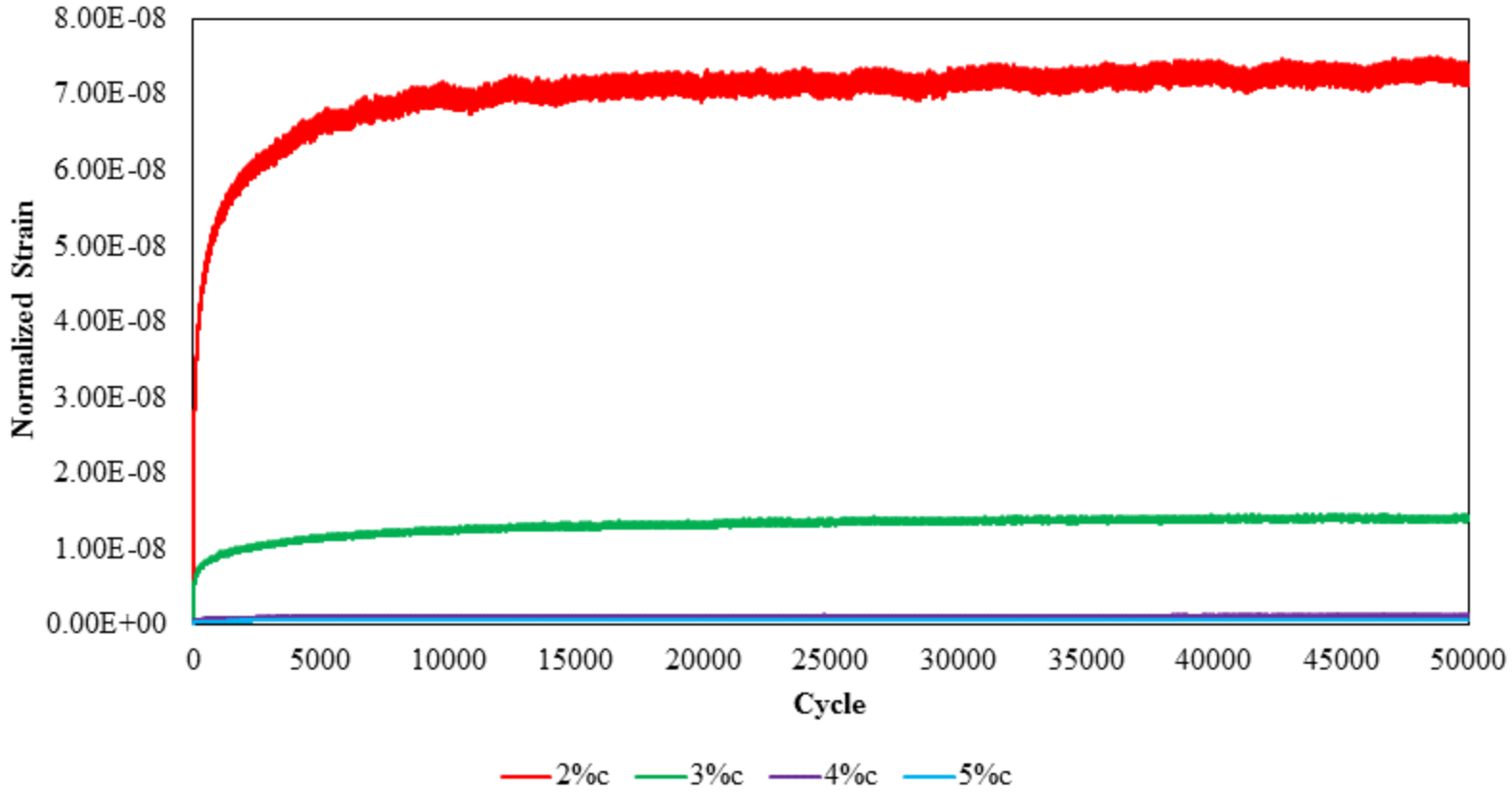

Figure D.2 – Permanent Deformation for El Paso Material @20% IDT Strength for 10-day Capillary Soak Samples

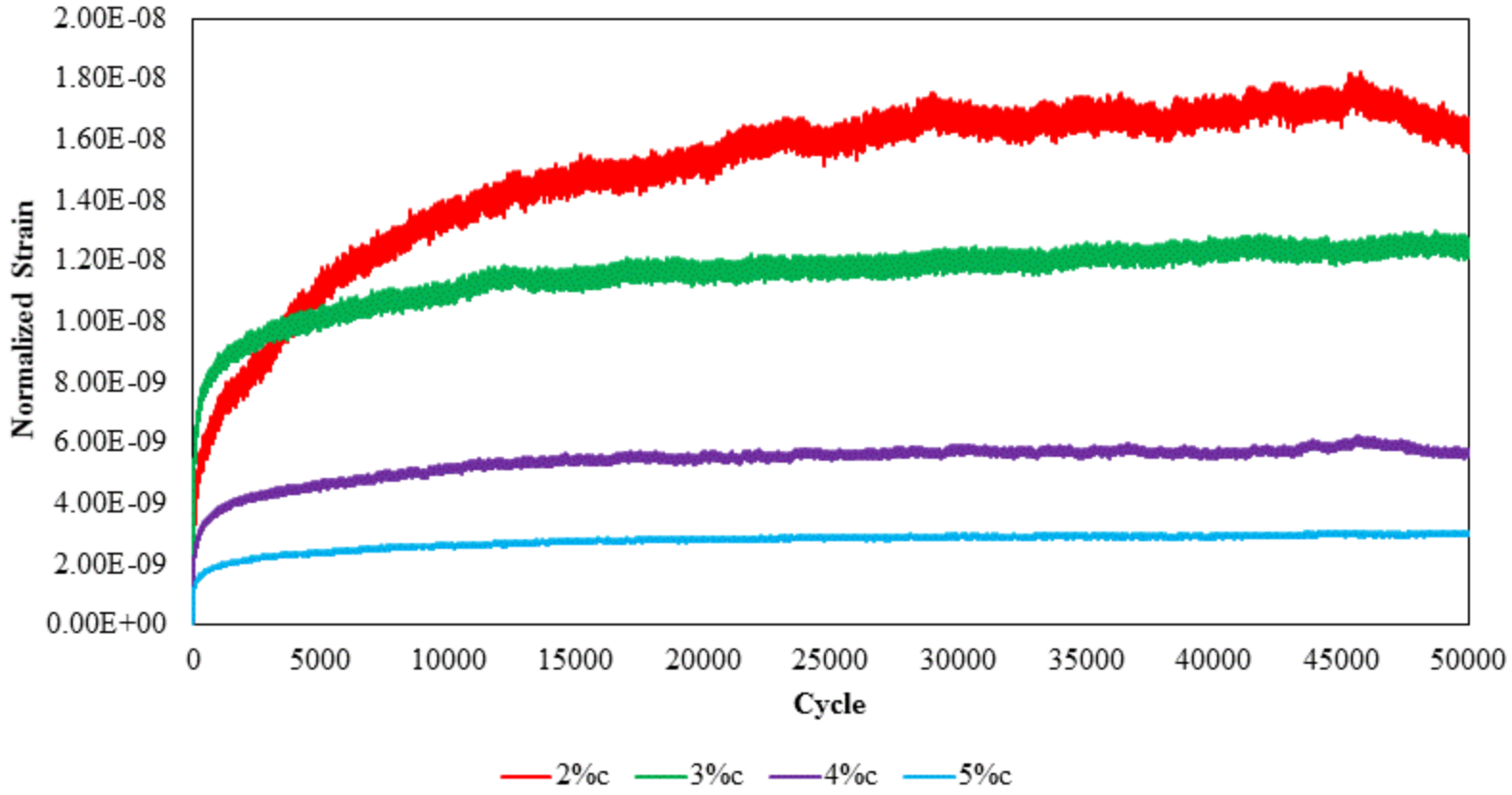

Figure D.3 – Permanent Deformation for San Antonio Material @20% IDT Strength for 7-day Moist Cured Samples

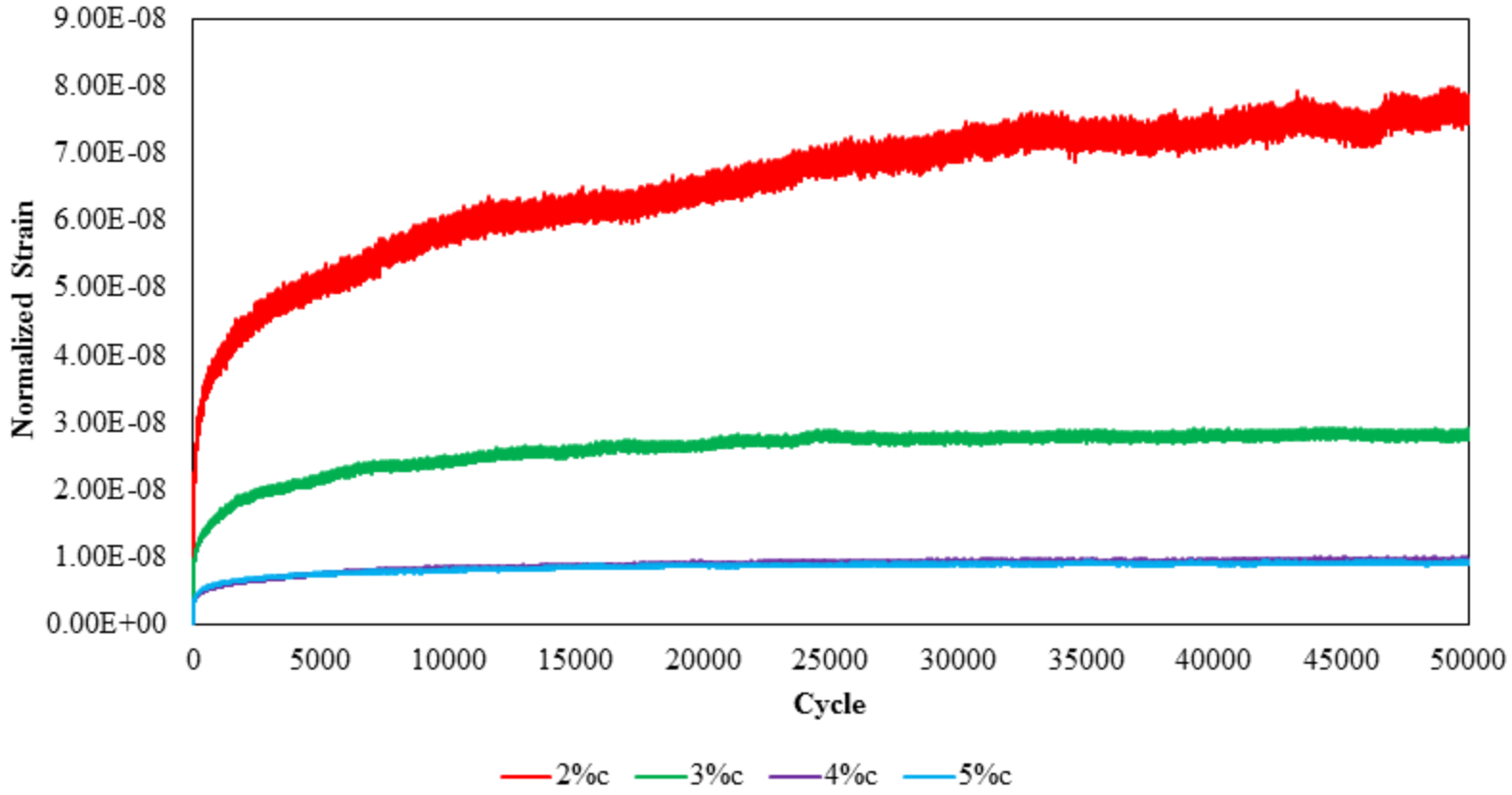

Figure D.4 – Permanent Deformation for San Antonio Material @20% IDT Strength for 10-day Capillary Soak Samples

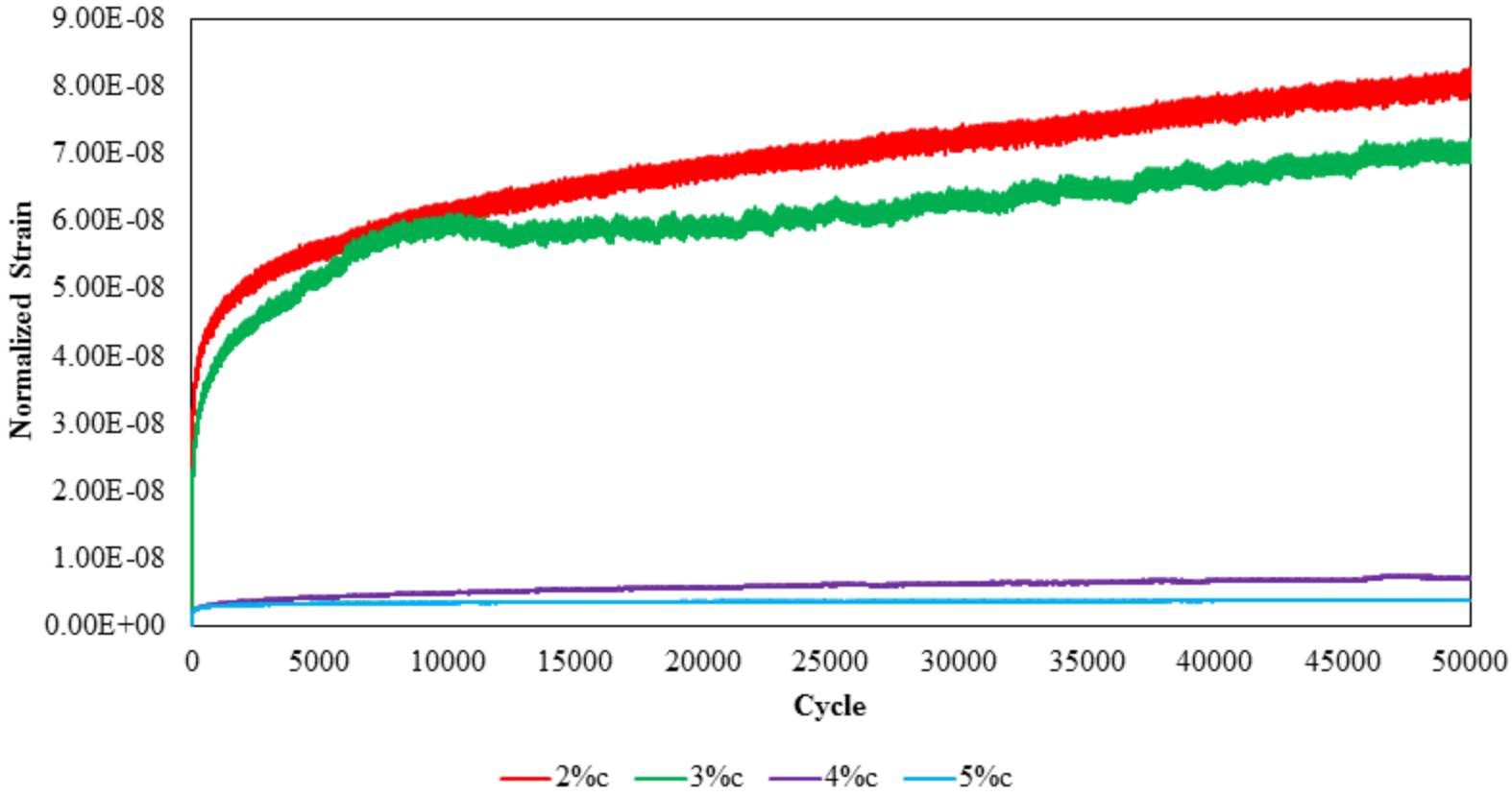

Figure D.5 – Permanent Deformation for Pharr Material @20% IDT Strength for 7-day Moist Cured Samples

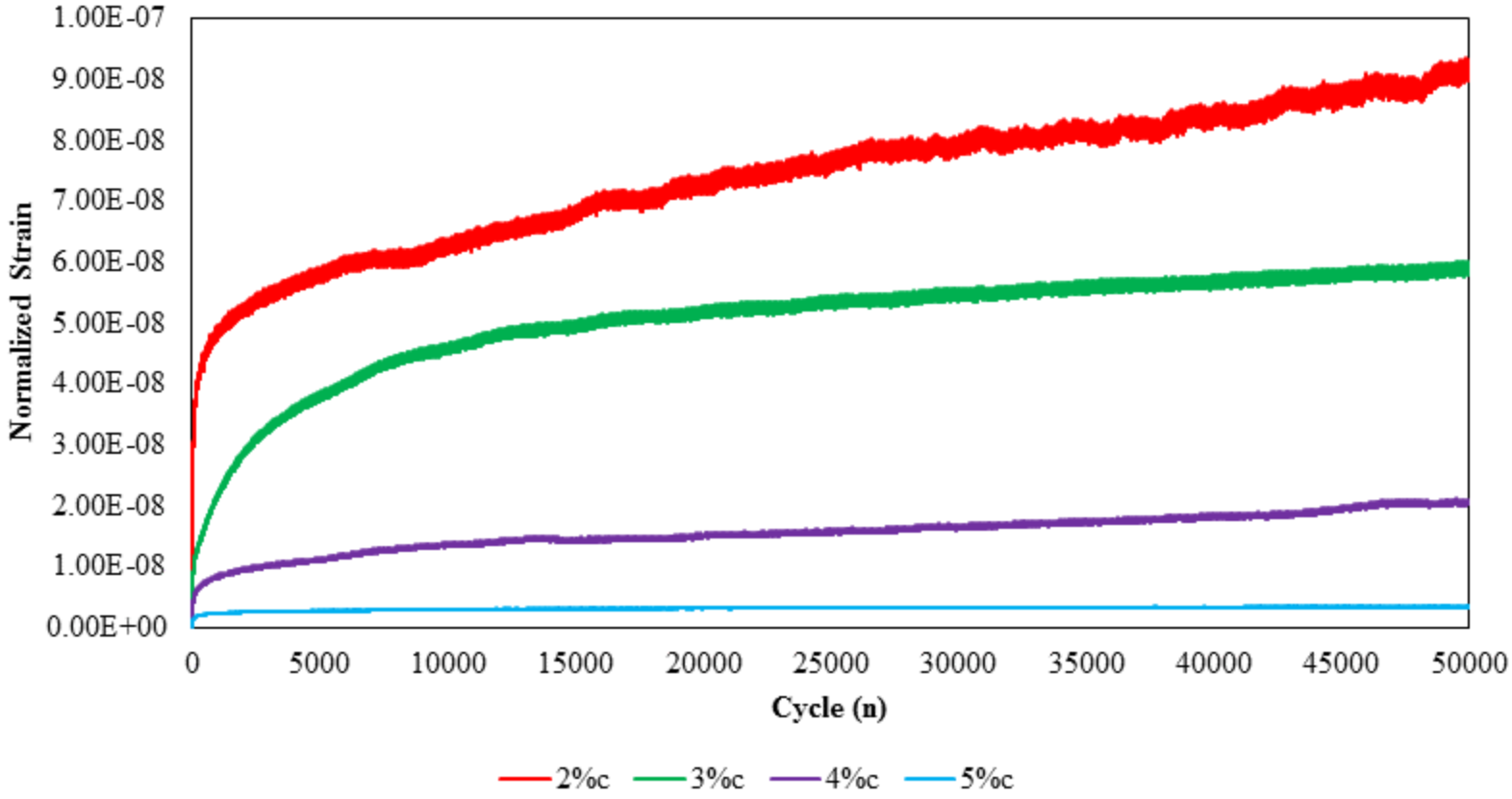

Figure D.6 – Permanent Deformation for Pharr Material @20% IDT Strength for 10-day Capillary Soak Samples

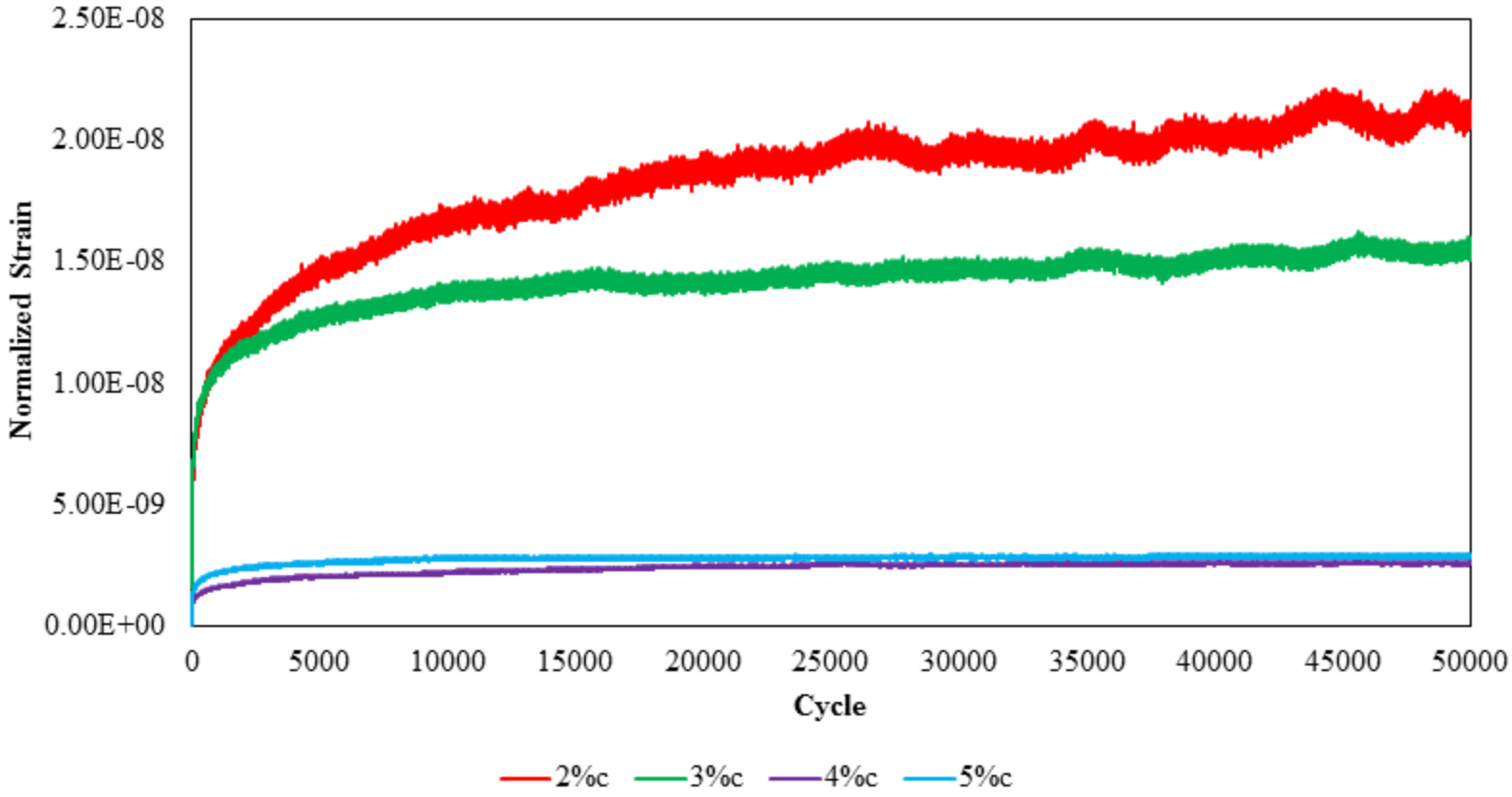

Figure D.7 – Permanent Deformation for Paris Material @20% IDT Strength for 7-day Moist Cured Samples

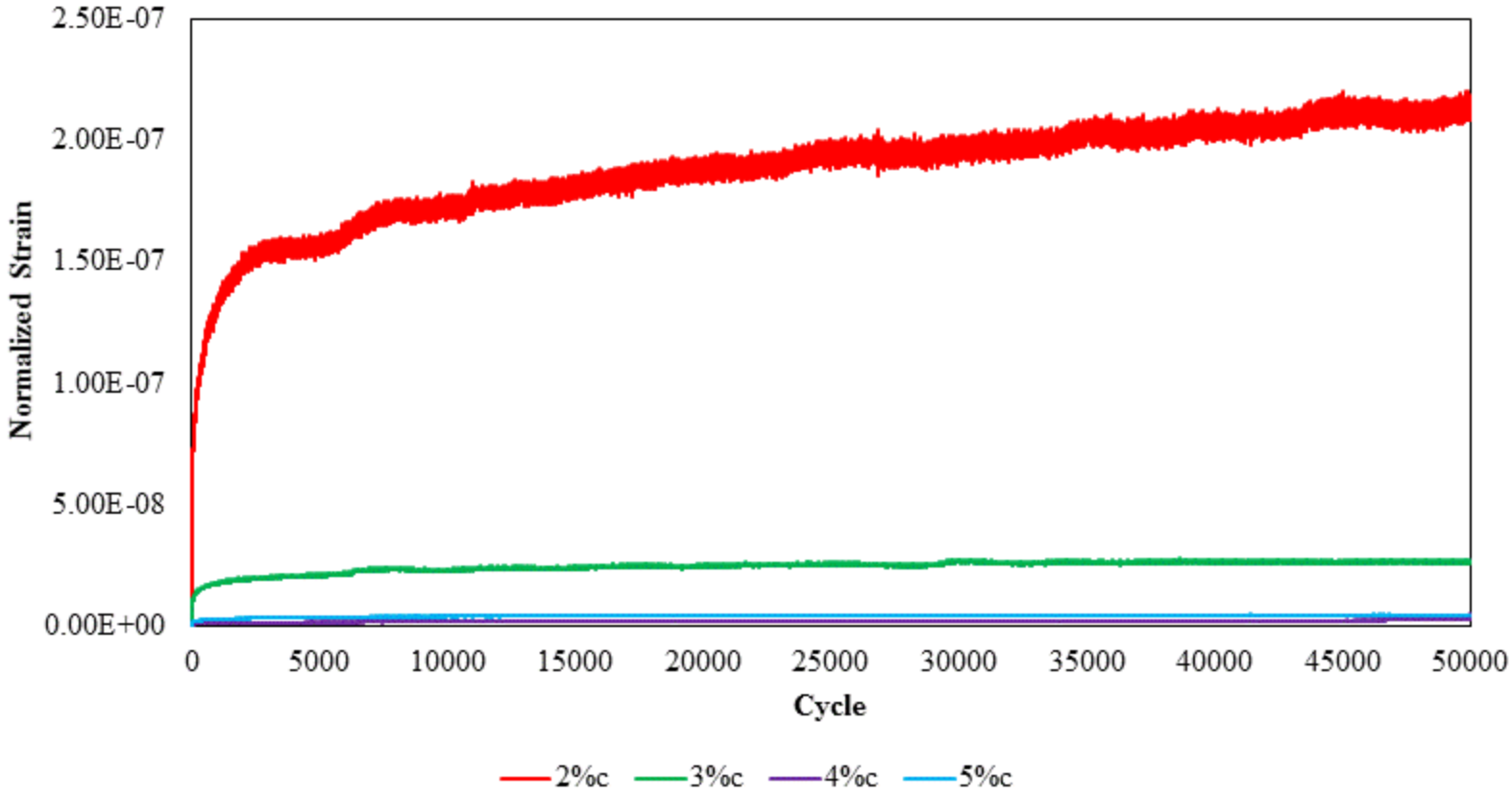

Figure D.8 – Permanent Deformation for Paris Material @20% IDT Strength for 10-day Capillary Soak Samples

APPENDIX E. Pre-processed Laboratory Data

Table E.1 – Unconfined Compressive Strength Data

Test	Material	Curing Condition	Cement Content (%)	Max Load (lb)	
				Set 1	Set 2
Unconfined Compressive Strength	El Paso	7 Day Moist Cured	2	8674	7579
			3	11697	12729
			4	17914	19043
			5	23755	27617
		10-Day TST	2	5082	8021
			3	11710	12577
			4	19077	18635
			5	25509	20130
	San Antonio	7 Day Moist Cured	2	6300	9973
			3	10962	10459
			4	13394	13345
			5	16800	18860
		10-Day TST	2	6642	8209
			3	10713	10426
			4	12283	11634
			5	14806	12007
	Pharr	7 Day Moist Cured	2	3205	3818
			3	5212	5033
			4	6705	7103
			5	6914	7553
		10-Day TST	2	3995	4090
			3	5212	5108
			4	7893	6567
			5	9250	8372
	Paris	7 Day Moist Cured	2	7800	10041
			3	13857	14780
			4	20725	19850
			5	27413	23420
		10-Day TST	2	7913	9874
			3	17207	15324
			4	22884	18555
			5	27280	29411

Table E.2 – Static Indirect Diametrical Test Data

Test	Material	Curing Condition	Cement Content (%)	Max Load (lb)	
				Set 1	Set 2
Static Indirect Diametrical Test	El Paso	7 Day Moist Cured	2	1796	1478
			3	2191	2634
			4	3698	4047
			5	4568	4008
		10-Day TST	2	1791	806
			3	2338	1851
			4	3622	3679
			5	5144	4024
	San Antonio	7 Day Moist Cured	2	1731	2168
			3	2829	1807
			4	3084	3407
			5	3508	3894
		10-Day TST	2	1064	1111
			3	1421	2335
			4	2905	2604
			5	3618	3370
	Pharr	7 Day Moist Cured	2	1822	2083
			3	2445	2579
			4	2496	2670
			5	2963	3197
		10-Day TST	2	1657	1697
			3	1814	2069
			4	2042	2240
			5	2665	2406
	Paris	7 Day Moist Cured	2	1292	1254
			3	1952	1614
			4	3551	2590
			5	4542	4663
		10-Day TST	2	699	971
			3	2094	1428
			4	2985	2322
			5	4058	4246

Table E.3 – Normalized Strain @5,000 cycles from Submaximal Test Data

Material	Curing Condition	Strength Applied (%)	Cement Content (%)			
			2	3	4	5
El Paso	7 day	20	1.53E-08	9.80E-09	2.48E-09	2.39E-09
		40	4.38E-09	1.41E-08	4.79E-09	1.65E-09
		60	1.52E-08	5.14E-09	2.56E-09	1.01E-09
	TST	20	3.43E-08	1.27E-08	1.66E-09	1.34E-09
		40	5.09E-08	7.88E-09	2.09E-09	5.35E-10
		60	NA	NA	NA	NA
San Antonio	7 day	20	1.96E-08	9.78E-09	7.54E-09	5.16E-09
		40	2.86E-08	2.27E-08	1.40E-08	8.93E-09
		60	7.73E-08	1.29E-08	1.97E-08	7.00E-09
	TST	20	2.13E-08	2.11E-08	1.25E-08	5.03E-09
		40	1.52E-07	3.85E-08	1.71E-08	1.04E-08
		60	9.38E-08	5.15E-08	1.51E-08	4.34E-09
Pharr	7 day	20	1.09E-07	6.16E-08	3.65E-08	2.52E-08
		40	4.85E-08	2.46E-08	1.35E-08	4.11E-09
		60	6.81E-08	2.85E-08	1.74E-08	7.17E-09
	TST	20	3.40E-08	2.49E-08	1.01E-08	8.00E-09
		40	4.85E-08	2.46E-08	1.35E-08	4.11E-09
		60	6.81E-08	2.85E-08	1.74E-08	7.17E-09
Paris	7 day	20	1.82E-08	1.52E-08	6.67E-09	5.56E-09
		40	2.75E-08	1.14E-08	6.57E-09	4.06E-09
		60	4.98E-08	3.19E-08	6.36E-09	2.60E-09
	TST	20	3.16E-08	1.14E-08	5.68E-09	4.21E-09
		40	1.87E-08	6.48E-09	3.56E-09	1.25E-09
		60	5.37E-08	1.33E-08	3.99E-09	2.89E-09

Table E.4 – Normalized Strain @ 50,000 cycles from Dynamic IDT Test Data

Material	Curing Condition	Strength Applied	Cement Content (%)			
			2	3	4	5
El Paso	7 day	20	6.04E-08	9.00E-09	4.00E-09	7.97E-10
		40	2.26E-08	1.51E-08	8.78E-09	2.87E-09
		60	NA	NA	NA	NA
	TST	20	7.33E-08	1.41E-08	1.31E-09	7.29E-10
		40	NA	1.15E-08	4.30E-09	6.69E-10
		60	NA	NA	1.84E-09	1.59E-09
San Antonio	7 day	20	1.64E-08	1.25E-08	5.60E-09	3.04E-09
		40	4.88E-08	2.19E-08	1.27E-08	3.21E-09
		60	1.64E-08	1.14E-08	4.34E-09	3.38E-09
	TST	20	7.62E-08	2.86E-08	9.59E-09	9.19E-09
		40	3.25E-08	5.83E-09	1.27E-09	9.06E-11
		60	NA	NA	NA	7.60E-10
Pharr	7 day	20	8.08E-08	6.96E-08	7.18E-09	3.84E-09
		40	1.82E-08	6.53E-09	5.80E-09	6.03E-09
		60	NA	NA	NA	NA
	TST	20	9.24E-08	5.87E-08	2.04E-08	3.40E-09
		40	NA	2.01E-07	5.46E-08	9.18E-09
		60	NA	NA	NA	NA
Paris	7 day	20	2.07E-08	1.57E-08	2.58E-09	2.84E-09
		40	4.02E-08	9.18E-09	2.63E-09	3.43E-09
		60	2.41E-08	1.12E-08	6.14E-09	1.18E-09
	TST	20	1.20E-07	2.65E-08	5.33E-09	4.69E-09
		40	3.83E-08	5.81E-09	2.19E-09	2.61E-10
		60	8.40E-09	2.03E-10	2.22E-09	1.56E-09